ISSN 2413-5577

№ 1 Январь – Март 2024

Экологическая безопасность прибрежной и шельфовой зон моря

Ecological Safety of Coastal and Shelf Zones of Sea

No. 1 January – March 2024

ecological-safety.ru

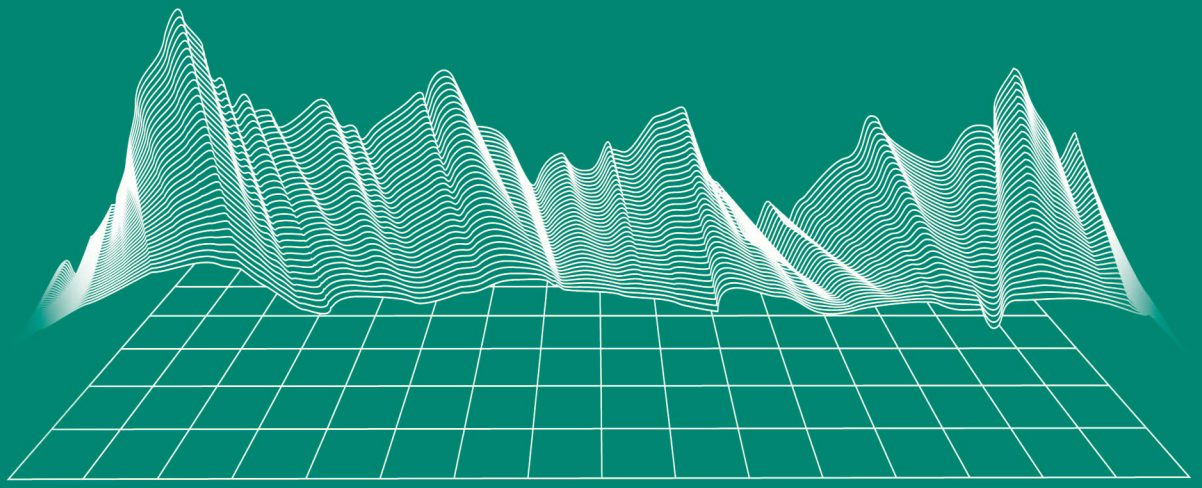

No. 1, 2024
January – March

Publication frequency:
Quarterly

16+

ECOLOGICAL SAFETY OF COASTAL AND SHELF ZONES OF SEA

Scientific and theoretical journal

FOUNDER AND PUBLISHER:
Federal State Budget Scientific Institution
Federal Research Centre
"Marine Hydrophysical Institute of RAS"

Journal is on the list of peer reviewed academic journals of the Higher Attestation Commission of the Russian Federation, where one may publish main research results of a Ph.D. thesis in the following field:

1.6.14 – Geomorphology and paleography (geographical sciences),
1.6.17 – Oceanology (geographical sciences, physical and mathematical sciences, technical sciences),
1.6.18 – Atmosphere and Climate ((geographical sciences, physical and mathematical sciences),
1.6.20 – Geoinformatics, cartography (geographical sciences),
1.6.21 – Geoecology (geographical sciences),
1.5.16 – Hydrobiology (biological sciences).

Journal is under the scientific and methodological guidance of the Earth Sciences Department of the Russian Academy of Sciences.

Journal is registered by the Federal Service for Supervision of Communications, Information Technology, and Mass Media (registration number ПИ № ФС77-73714 of 21 September 2018 and Эл № ФС77-82679 of 21 January 2022).)

Journal coverage: The Russian Federation, other countries.

The Journal is indexed in and reposited at Russian Science Citation Index (RSCI), International Interactive Information and Bibliography System EBSCO, Scopus.

Journal is in the catalog of scientific periodicals of the RSCI on the platform of the scientific electronic library eLibrary.ru, Cyberleninka.

There is no fee for publishing articles.

e-mail: ecology-safety@mhi-ras.ru

website: http://ecological-safety.ru

Founder, Publisher and Editorial Office address:

2, Kapitanskaya St.,
Sevastopol, 299011, Russia

Phone, fax: + 7 (8692) 54-57-16

РЕДАКЦИОННАЯ КОЛЛЕГИЯ

CONTENTS

No. 1. 2024 January – March, 2024

СОДЕРЖАНИЕ

№ 1. 2024 Январь – Март, 2024

Original article

Features of the Stokes Drift in the Northeastern Coastal Zone of the Black Sea from Modelling Results

B. V. Divinsky *, S. B. Kuklev, V. V. Ocherednik, O. N. Kukleva

Shirshov Institute of Oceanology, Russian Academy of Sciences, Moscow, Russia
** e-mail divin@ocean.ru*

Abstract
The Stokes drift generated by surface waves affects many physical processes occurring in the coastal zone of the sea, including heat and salt transport, as well as transport of pollutants. Taking into account the parameters of sea currents caused by the Stokes drift is important for a more correct description of the general hydrodynamic structure of coastal waters. Moreover, sea currents generated by surface waves make a significant contribution to the processes of accumulation and redistribution of pollutants in the coastal zone of the sea. The article presents the results of the study of the Stokes drift on the northeastern shelf of the Black Sea near Gelendzhik for the period from 2003 to 2022. Seasonal and interannual features of variability of Stokes current velocities and directions have been identified. It has been shown that from December to April, excluding February, the Stokes transport has comparable repeatability in directions towards the coast, away from the coast, and towards the northwest. In February, the main flow tends to the open sea. In May and June, the repeatability of currents towards the coastline increases significantly, with the contribution of currents to the southeast increasing at the beginning of summer. In July, the currents directed to the southeast and away from the coast become almost identical in terms of repeatability. From August to November, the proportion of currents directed away from the coast increases with a gradual decrease in the repeatability of currents towards the southeast. In multi-year terms, the flow directed away from the coast to the open sea prevails (repeatability of 34.3%). The same flow has the highest mean velocity (0.053 m/s). Repeatability of the long-shore currents directed towards the southeast and northwest is almost the same, but the currents towards the northwest are much more intense.

Keywords: wind waves, Stokes drift, coastal zone, spread of pollutants, anthropogenic pollution

Acknowledgements: The work was performed under agreement 075-15-2021-941 “Comprehensive studies of the ecological state of the waters of the coastal zone of the northeastern shelf of the Black Sea in the framework of participation in the international project DOORS” of the Ministry of Science and Higher Education of the Russian Federation .

For citation: Divinsky, B.V., Kuklev, S.B., Ocherednik, V.V. and Kukleva, O.N., 2024. Features of the Stokes Drift in the Northeastern Coastal Zone of the Black Sea from Modelling Results. *Ecological Safety of Coastal and Shelf Zones of Sea*, (1), pp. 6–19.

Особенности дрейфа Стокса в прибрежной зоне северо-восточного побережья Черного моря по результатам моделирования

Б. В. Дивинский *, С. Б. Куклев, В. В. Очередник, О. Н. Куклева

Институт океанологии им. П.П. Ширшова РАН, Москва, Россия
* *e-mail: divin@ocean.ru*

Аннотация
Стоксов дрейф, генерируемый поверхностным волнением, влияет на множество физических процессов, проистекающих в береговой зоне моря, в том числе на перенос тепла и соли, а также транспорт загрязняющих веществ. Учет параметров морских течений, вызываемых дрейфом Стокса, важен для более корректного описания общей гидродинамической структуры прибрежных вод. Кроме того, морские течения, генерируемые поверхностным волнением, могут вносить существенный вклад в процессы накопления и перераспределения загрязняющих веществ в прибрежной зоне моря. Представлены результаты исследований стоксова дрейфа на северо-восточном шельфе Черного моря в районе г. Геленджика за климатический отрезок времени с 2003 по 2022 г. Выявлены сезонные и межгодовые особенности изменчивости скоростей и направлений течений Стокса. Показано, что с декабря по апрель, за исключением февраля, стоксов перенос обладает сопоставимыми повторяемостями по направлениям к берегу, от берега и на северо-запад. В феврале основной поток стремится в открытое море. В мае и июне значительно увеличивается повторяемость течений в сторону береговой линии, при этом в начале лета растет доля потоков, направленных на юго-восток. В июле течения с направлением на юго-восток и от берега становятся почти одинаковыми по повторяемости. С августа по ноябрь вырастает доля течений, направленных от берега, при постепенном уменьшении повторяемости потоков на юго-восток. В многолетнем выражении преобладает поток, направленный от берега в открытое море (повторяемость 34.3 %). Этот же поток обладает и наибольшей средней скоростью (0.053 м/с). Повторяемости вдольбереговых потоков, направленных на юго-восток и северо-запад, почти одинаковы, но при этом течения на северо-запад гораздо интенсивнее. Основной вывод: морские течения, генерируемые поверхностным волнением, вносят существенный вклад в процессы накопления и перераспределения загрязняющих веществ в прибрежной зоне моря.

Ключевые слова: ветровое волнение, Стоксов дрейф, прибрежная зона, распространение примеси, антропогенные загрязнения

Благодарности: работа выполнена по соглашению 075-15-2021-941 Минобрнауки РФ «Комплексные исследования экологического состояния вод прибрежной зоны северо-восточного шельфа Черного моря в рамках участия в международном проекте DOORS».

Для цитирования: Особенности дрейфа Стокса в прибрежной зоне северо-восточного побережья Черного моря по результатам моделирования / Б. В. Дивинский [и др.] // Экологическая безопасность прибрежной и шельфовой зон моря. 2024. № 1. С. 6–19. EDN CAVUNO.

Introduction

Open condition of wave orbital trajectories causes an additional resulting fluid flow in the upper few meters of the water column (with the highest value at the surface) corresponding to the general direction of wave propagation. This phenomenon was first described by the English scientist D. Stokes [1)] and subsequently received his name.

Stokes drift affects directly many physical processes occurring in the coastal zone of the sea [1–4]. Work [5] shows that the trajectories of surface drifters under conditions of arisen sea with significant wave heights exceeding 1 m are determined precisely by the Stokes drift and only at relatively low heights (less than 0.6 m) they are determined by the local wind and main currents. Together with wind currents, density gradients and tides, the Stokes drift makes a significant contribution to heat and salt transport, as well as transport of pollutants including micro- and macroplastics, and oil spills [6–8]. Taking into account the Stokes drift, it is possible to improve significantly numerical models of the spread of passive pollutants [9] in order to understand better the environmental consequences of human economic activity.

Current velocities caused by the Stokes transport can reach 2% of the local wind velocity [8] and the contribution of the Stokes transport to the total flow caused by wind load can be up to 40% [10]. The Stokes drift parameters also depend significantly on the season and geographical features of the sea area [11]. It should also be noted according to [12] that currents caused by the Stokes transport have mean velocities of 0.08–0.10 m/s and maximum velocities of ~0.6 m/s in the Baltic Sea.

Thus, the Stokes drift can influence both hydrodynamic regime and ecological state of a water body significantly.

Hence, the main purpose of this study is to analyze the basic parameters of the Stokes drift (velocities and directions) including their seasonal and interannual variability on the northeastern shelf of the Black Sea near Gelendzhik for a climatic period from 2003 to 2022. Such estimates have not been previously carried out for the Black Sea conditions. Additionally, seasonal and interannual patterns of distributions of wind wave and surface wind parameters were studied over the same period.

Materials and methods

The study uses such tools as the DHI MIKE SW modern spectral wave model of Danish Hydraulic Institute and the ERA5 global reanalysis database provided by the European Center for Medium-Range Weather Forecasts (ECMWF).

The DHI MIKE SW model takes into account basic physical mechanisms of wave field transformation including wave generation under the influence of surface wind, nonlinear three- and four-wave interactions, wave energy dissipation resulted from bottom friction and breaking, as well as diffraction and refraction [13].

[1)] *Stokes G. G.* On the numerical calculation of a class of definite integrals and infinite series // Transactions of the Cambridge Philosophical Society. Cambridge, 1847. Vol. IX, part 1. P. 166–187.

Non-stationary fully spectral model is used when calculating the Black Sea wave fields. Spectral frequencies are included in the range of wave periods from 1.6 to 16.5 s. The model resolution in the directions of wave propagation is 15°. The model is configured to separate the wave field into two components (pure wind waves and swell waves) and verified based on numerous *in situ* experiments and satellite data [14].

The calculation grid with condensation in the coastal zone covers the Black Sea and the Sea of Azov and consists of 20,000 calculation elements (Fig. 1). The calculation point indicated in the inset to Fig. 1 is located 4 km seaward of Gelendzhik at a depth of 40 m.

The performed modeling made it possible to obtain a data array consisting of the main parameters of pure wind waves and swell waves covering a period of 20 years (from 2003 to 2022). The array includes significant heights of wind waves and swell waves, as well as the directions of their propagation. The time step is 1 h.

The meridional and zonal components of surface wind velocities and the Stokes drift were extracted from the ERA5 global atmospheric reanalysis array for the same period and with the similar time step. The Stokes drift is calculated based on the analysis of two-dimensional wave energy spectra [15].

Thus, we further study the climatic features of the variability of the following parameters:

– significant heights, as well as directions of propagation of wind waves and swell waves;
– wind direction and velocity;
– direction and velocity of the Stokes drift at the sea surface.

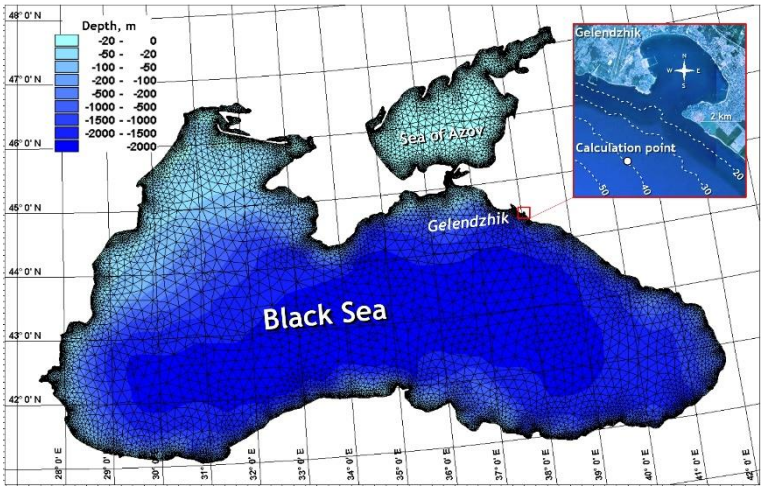

Fig. 1. Calculation grid of the Black Sea and the Sea of Azov. The inset shows the position of the calculation point near Gelendzhik

Results and discussion

Figs. 2–4 show seasonal features of the distribution of significant heights of wind waves, swell waves and wind velocities, respectively.

Pursuant to Fig. 2, wind waves of sea directions (from the southeast to the northwest) dominate from late autumn to mid-spring. November and February with their strong storms in the northeast directions are the exceptions. Wind waves in the west and northwest directions predominate in May, June and July. The wave disturbance from the northeast increases significantly from August to October. At the same time, the open sea brings little risk of storms in August and September.

Long swell waves experience significant refraction with the restructuring of the wave front normal to the coast on a relatively narrow shelf with almost parallel isobaths near Gelendzhik (see the inset to Fig. 1). As a result, all seasons are characterized by the absolute predominance of swell waves in the southwest and west-southwest directions (Fig. 3).

The region under consideration is under the influence of surface winds in all directions, with the exception of the southeast ones, in December, January and March (Fig. 4). The contribution of the northeast wind increases sharply in February. Two main wind directions in April–May are the southwest and the northeast. Weak winds of the northern sectors with a predominance of the northeast prevail from June to September. The northeast winds become dominant in October and November.

Fig. 5 shows generalizing climatic roses for wind waves, swell waves and surface wind constructed over 20 years from 2003 to 2022.

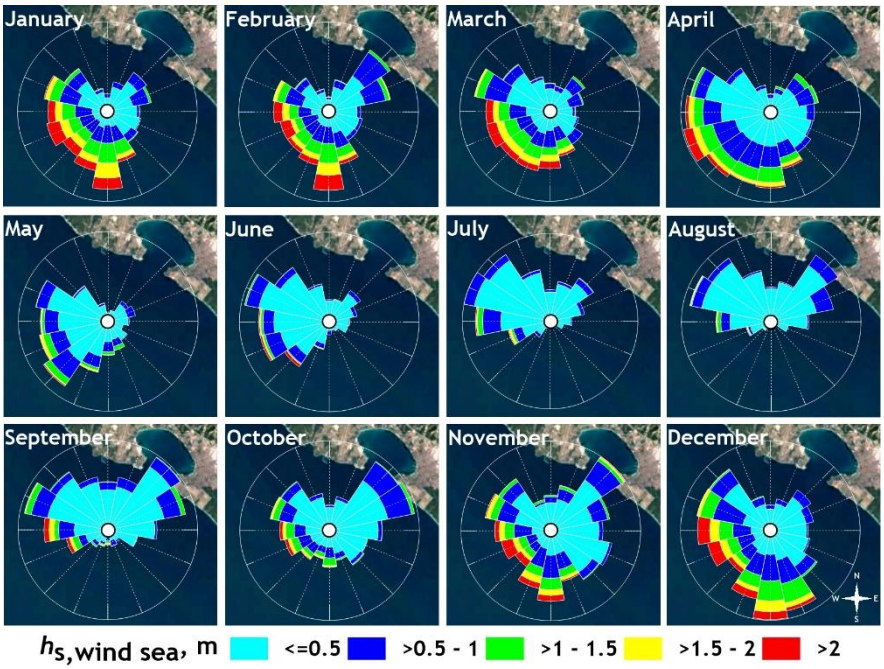

Fig. 2. Monthly wind wave roses near Gelendzhik

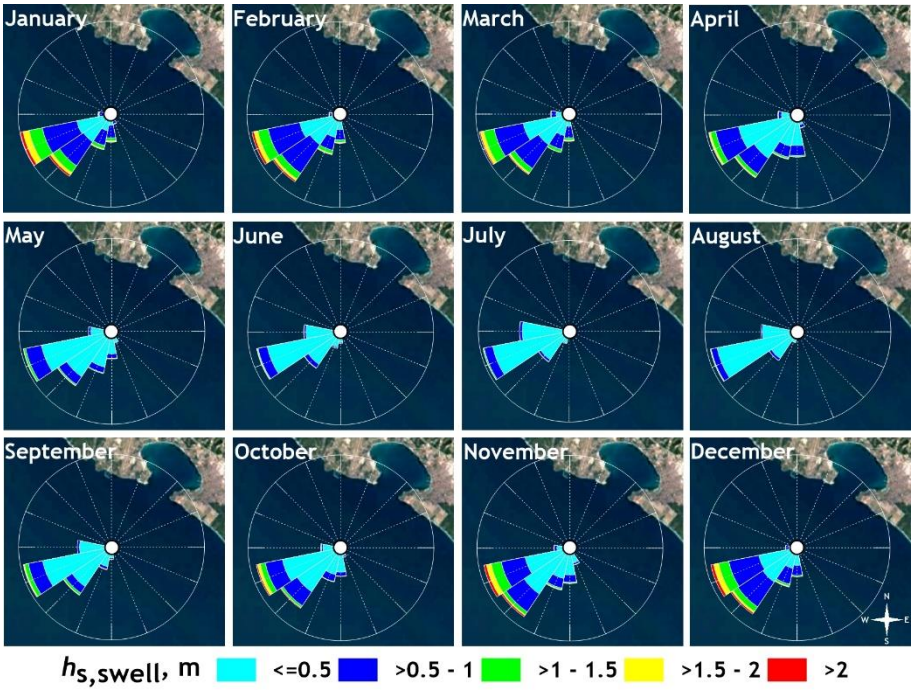

F i g . 3 . Monthly swell wave roses near Gelendzhik

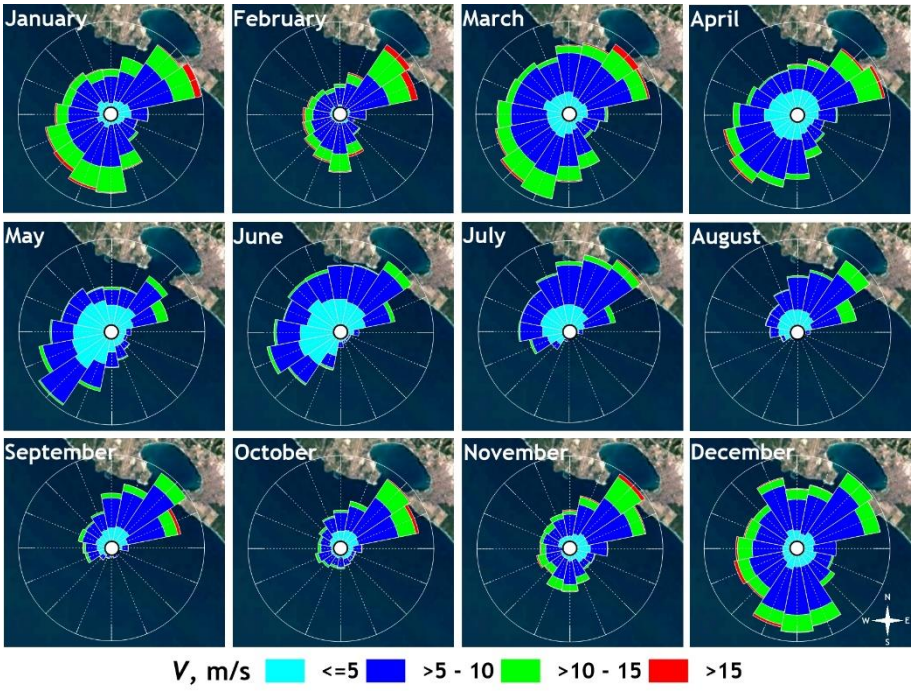

F i g . 4 . Monthly surface wind roses near Gelendzhik

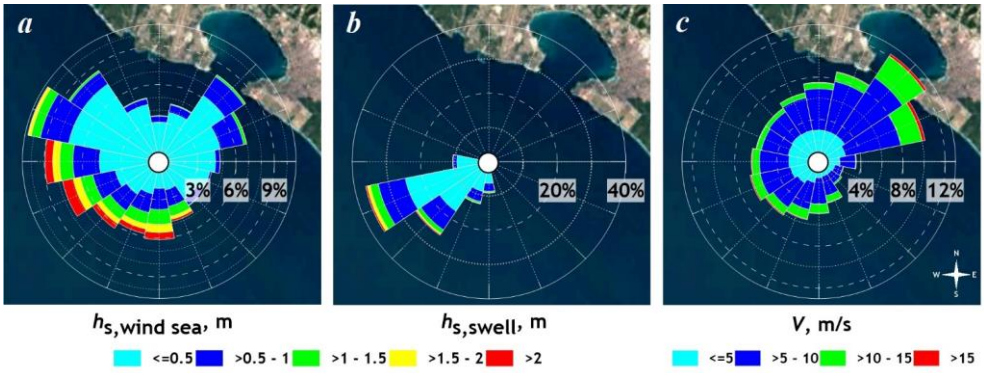

Fig. 5. Climatic roses: for wind waves (*a*), for swell waves (*b*), for the surface wind (*c*)

Pursuant to Fig. 5, wind waves in the west-southwest and northeast directions have the greatest repeatability while the strongest waves develop in the south-southeast-west sector. As in all seasons separately, the swell waves of the west-southwest and southwest directions dominate in the interannual sense. The prevailing wind is in the northeast directions, the least repeated wind is in the southeast directions.

Fig. 6 shows the so-called whisker boxes giving a visual graphical representation of certain statistical characteristics (mean distribution, 1st and 3rd quartiles

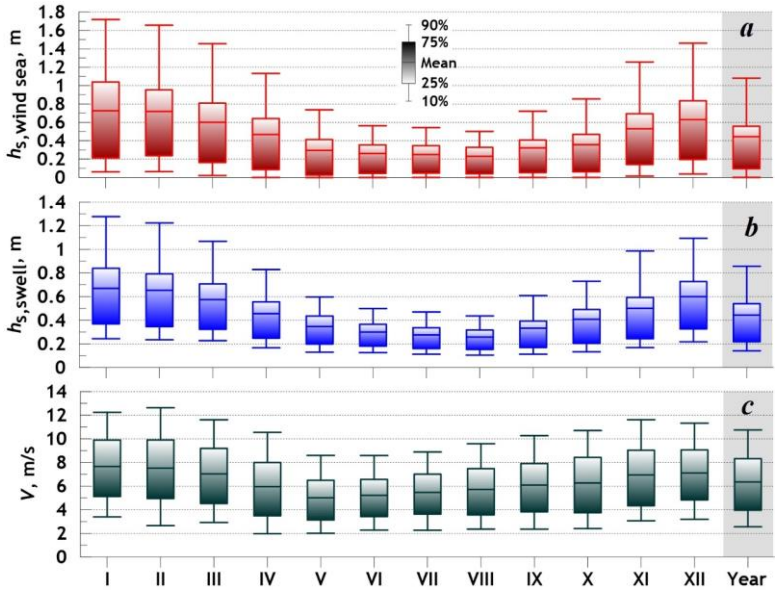

Fig. 6. Statistical characteristics of the distributions of: significant wind wave heights (*a*), significant swell waves heights (*b*), surface wind speeds (*c*)

(or 25th and 75th percentiles), 10th and 90th percentiles) of wave height and wind velocity values separately by month and overall for the year.

The data (Fig. 6) show that wave height distributions are characterized by strong intraseasonal variability. The strongest wind waves are observed in the winter months with mean wave heights of ~0.7 m, and weakest ones – in summer ($h_{s,wind\ sea}$ ~0.3 m). The same picture is observed for the swell waves with mean heights slightly exceeding 0.6 m in winter and 0.2 m in summer. August is the quietest month. The differences among seasons in wind velocities are not as obvious as in wave parameters. Mean wind velocities are ~7 m/s in winter, as well as in early spring and late autumn, and 5 m/s in summer. The weakest wind is observed in May.

Fig. 7 shows seasonal features of the Stokes drift velocities and directions. Note that in accordance with well-established oceanographic traditions, the direction of the Stokes currents is determined relative to the side of the world towards which they are headed (the direction of waves and wind – from the side). For convenience of consideration and taking into account the general orientation of the coastline, the repeatability of the Stokes drift is calculated for four 90° sectors conditionally defining the following directions of currents: towards the coast, along the coast towards the southeast, away from the coast, along the coast towards the northwest.

Pursuant to Fig. 7, surface currents caused by wind waves formed both by large-scale processes throughout the entire Black Sea water area and by local wind have well-defined seasonal differences. From December to April, excluding February, the Stokes transport has comparable repeatability in directions towards the coast, away from the coast and towards the northwest. In February, the main flow tends to the open sea under the influence of strong northeast winds. In May and June, the repeatability of currents towards the coastline increases significantly with the contribution of currents towards the southeast increasing at the beginning of summer. In July, the currents directed towards the southeast and away from the coast become almost identical in terms of repeatability. From August to November, the proportion of currents directed away from the coast increases with a gradual decrease in the repeatability of currents towards the southeast.

Fig. 8 shows the generalized pattern of sea currents caused by the Stokes transport.

Pursuant to Fig. 8, the long-term repeatability of the Stokes currents in directions is as follows: towards the coast – 27.4%, towards the southeast – 20.9%, away from the coast – 34.3%, towards the northwest – 17.4%. In general, the flow directed to the open sea predominates climatically. The repeatability of alongshore flows directed towards the southeast and northwest is almost the same.

Statistical characteristics of flow velocities also show intraseasonal differences (Fig. 9). The currents directed towards the coast are the strongest ones in December–January (mean velocities ~ 0.07 m/s), away from the coast – in winter and autumn, especially in February (more than 0.08 m/s), towards the northwest – from November to February. The weakest currents are directed towards the southeast with mean values of 0.04 m/s in winter. The extremely insignificant transport (mean velocities less than 0.02 m/s) towards the coast and towards the northwest

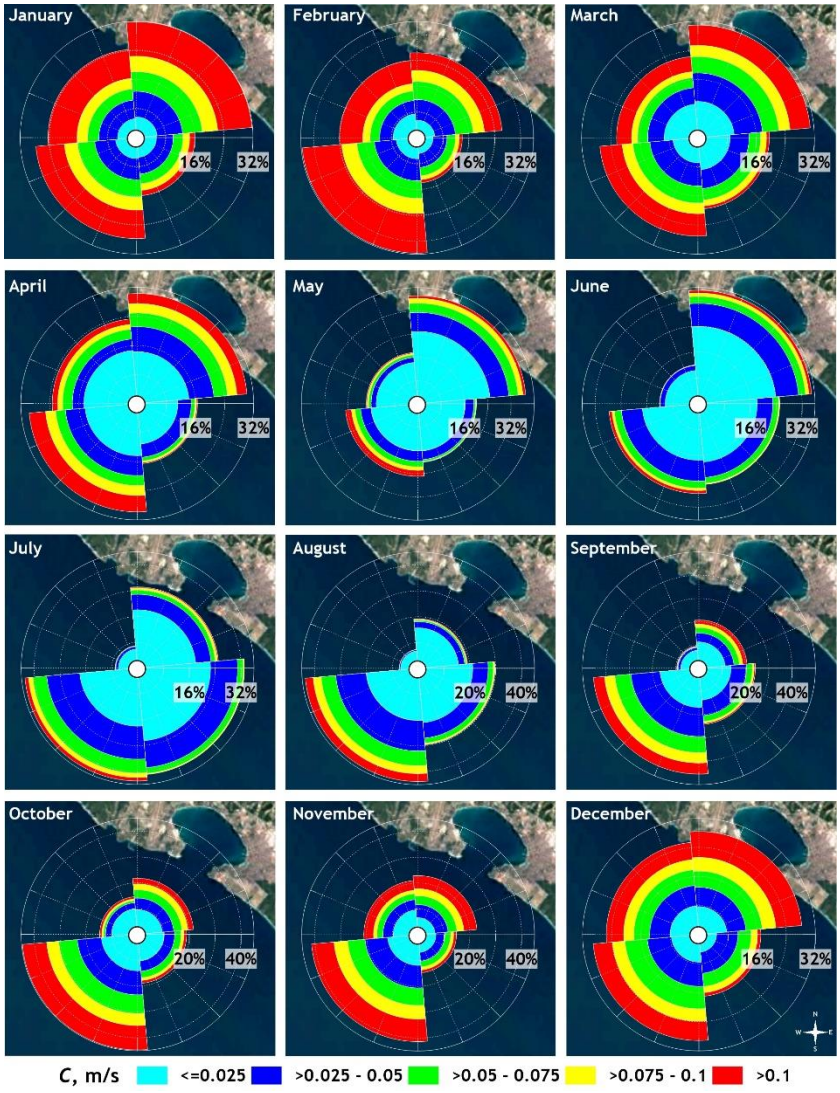

F i g . 7 . Monthly roses of the Stokes drift near Gelendzhik

is observed in August, in May – towards the southeast, in July – towards the sea. In general, currents towards the sea have the highest mean annual velocities (almost 0.06 m/s). They are followed by currents towards the coast and towards the northwest (~ 0.05 m/s) and alongshore currents towards the southeast (~ 0.03 m/s).

Fig. 10 shows interannual variability of the Stokes drift velocities. According to the data, despite the climatic dominance of flows directed towards the sea, currents towards the coast can prevail in some years (e.g., in 2004 and 2021). The mean annual repeatability of the Stokes drift by 90° sectors is as follows: towards the coast – 23.4–34.7%, towards the southeast – 16.1–25.5%, away from the coast – 24.8–44.1%, towards the northwest – 12.6–23.3%. The mean annual current velocities vary as follows: towards the coast – 0.037–0.054 m/s,

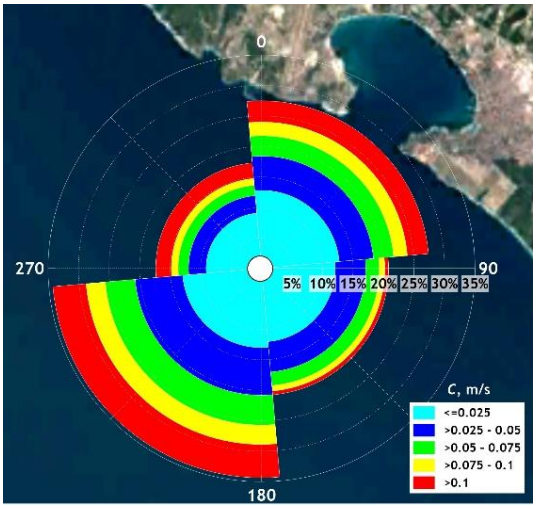

Fig. 8. Climatic roses of currents caused by the Stokes drift

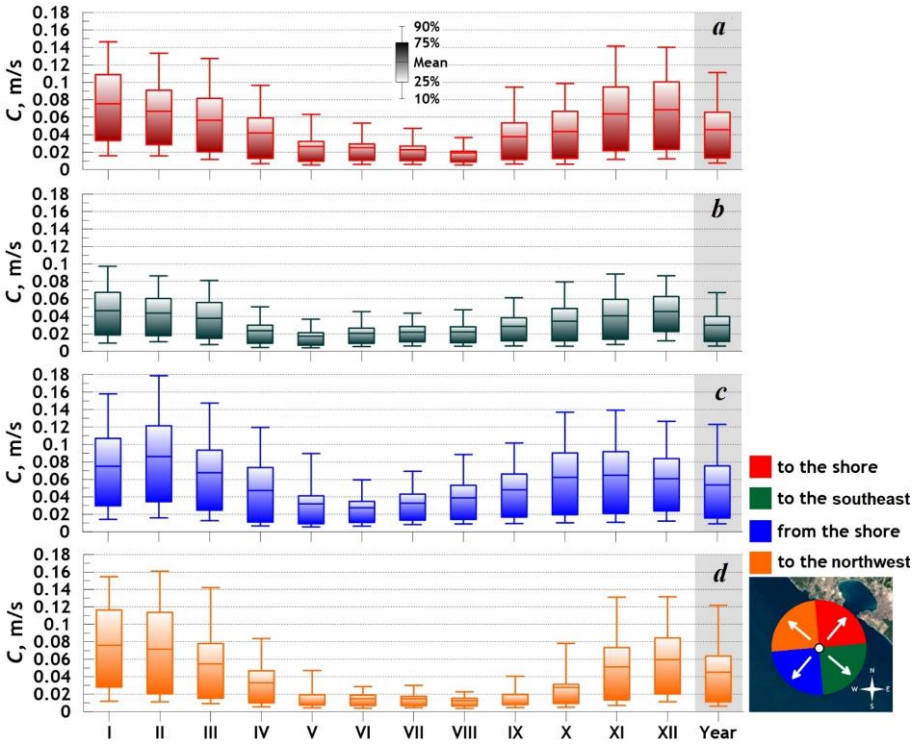

Fig. 9. Statistical characteristics of Stokes drift velocities by distribution sectors: *a* – towards the coast; *b* – to the south-east; *c* – away from the coast; *d* – towards the northwest

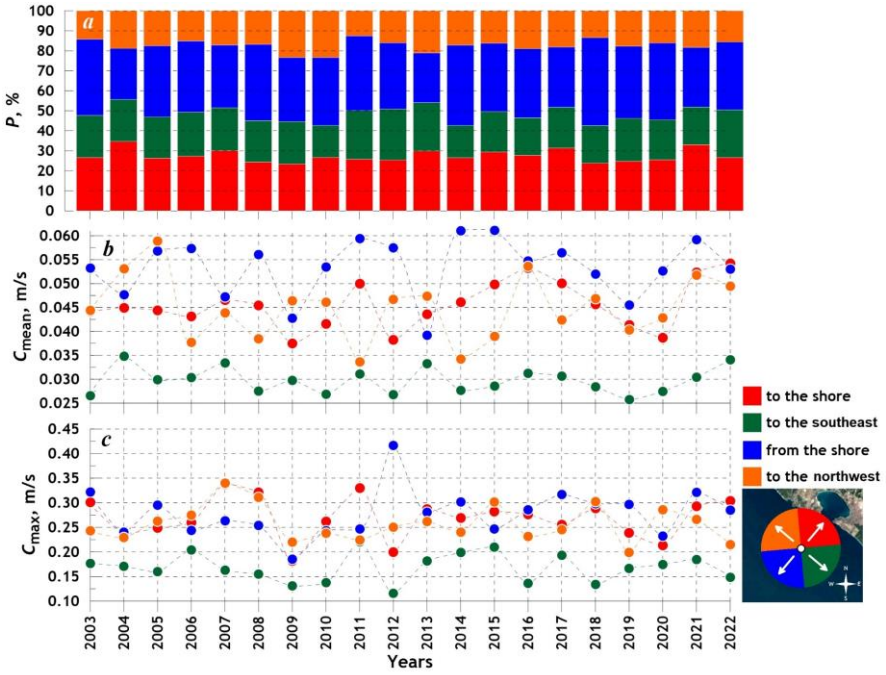

Fig. 10. Repeatability (*a*), mean (*b*) and maximum (*c*) Stokes drift velocities by distribution sectors

towards the southeast – 0.025–0.035 m/s, away from the coast – 0.039–0.061 m/s, towards the northwest – 0.033–0.059 m/s. The maximum velocities are an order of magnitude higher than the mean values. Intraannual maximum velocities also vary widely: towards the coast – 0.18–0.34 m/s, towards the southeast – 0.12–0.22 m/s, away from the coast – 0.19–0.42 m/s, towards the northwest – 0.20–0.34 m/s. The maximum Stokes drift velocity amounting to 0.42 m/s was observed in 2012 with the currents directed towards the open sea.

Conclusion

The performed research results in the analysis of the Stokes drift main parameters (velocities and directions) on the northeastern shelf of the Black Sea near Gelendzhik over a long period of time from 2003 to 2022 and the study of the seasonal and interannual patterns of distribution of wind wave and surface wind parameters.

Main results.

Wind waves. Wind waves of sea directions (from the southeast to the northwest) dominate from late autumn to mid-spring. November and February with their strong storms in the northeast directions represent some exceptions. Wind waves in the west and northwest directions predominate in May, June and July. The wave disturbance from the northeast increases significantly from August to October. At the same time, the open sea brings little risk of storms in August and September.

The strongest wind waves are observed in the winter months with mean wave heights of ~ 0.7 m, and weakest ones – in summer (0.3 m).

Swell waves. All seasons are characterized by the absolute predominance of swell waves in the southwest and west-southwest directions. The swell waves with mean heights slightly exceed 0.6 m in winter and 0.2 m in summer.

Wind. The region under consideration is under the influence of surface winds in all directions, with the exception of the southeast ones, in December, January and March. The contribution of the northeast wind increases sharply in February. Two main wind directions in April–May are the southwest and the northeast. Weak winds of the northern sectors with a predominance of the northeast prevail from June to September. The northeast winds become dominant in October and November. Mean wind velocities are ~ 7 m/s in winter, as well as in early spring and late autumn, and 5 m/s in summer. The weakest wind is observed in May.

The Stokes drift. From December to April, excluding February, the Stokes transport has comparable repeatability in directions towards the coast, away from the coast and towards the northwest. In February, the main flow tends to the open sea. In May and June, the repeatability of currents towards the coastline increases significantly with the contribution of currents towards the southeast increasing at the beginning of summer. In July, the currents directed towards the southeast and away from the coast become almost identical in terms of repeatability. From August to November, the proportion of currents directed away from the coast increases with a gradual decrease in the repeatability of currents towards the southeast.

The table shows the interannual characteristics of the Stokes currents.

In multi-year terms, the flow directed away from the coast to the open sea prevails. The same flow has the highest mean velocity. Repeatability of the longshore currents directed towards the southeast and northwest is almost the same, but the currents towards the northwest are much more intense.

Long-term characteristics of the Stokes drift by wave directions

Flow direction	Repeatability, %	Mean velocity, m/s	Mean maximum velocity, m/s
Towards the coast	27.4	0.046	0.27
Towards the southeast	20.9	0.030	0.17
Away from the coast	34.3	0.053	0.28
Towards the northwest	17.4	0.045	0.26

Note that the Stokes drift is only part of the complex hydrodynamic picture characteristic of coastal waters. Experimental observations and numerical modeling carried out by A. Isobe et al. made it possible to establish that under the influence of the Stokes transport, large plastics were mostly transported and accumulated in the coastal zone of the sea, processed into smaller forms (microplastics) and subsequently transported into the open sea. Thus, we can conclude that sea currents generated by surface waves make a significant contribution to the processes of accumulation and redistribution of pollutants in the shelf zone of the sea and determine largely the ecological state of coastal waters.

Final remark. Average currents can be generated in the field of groups of waves at the ocean surface. Such currents differ in their pure form from the Stokes drift induced directly by the waves. Naturally, this results in certain errors in the estimates of the Stokes transport values. Nevertheless, we believe that the indicated inaccuracies are, let's say, a kind of a systematic error and do not affect the climatic features of variations in the Stokes drift greatly.

REFERENCES

1. Clarke, A. and Van Gorder, S., 2018. The Relationship of Near-Surface Flow, Stokes Drift and the Wind Stress. *Journal of Geophysical Research: Oceans*, 123(7), pp. 4680–4692. https://doi.org/10.1029/2018JC014102
2. Lentz, S., Fewings, M., Howd, P., Fredericks, J. and Hathaway, K., 2008. Observations and a Model of Undertow over the Inner Continental Shelf. *Journal of Physical Oceanography*, 38(11), pp. 2341–2357. https://doi.org/10.1175/2008JPO3986.1
3. Lentz, S. and Fewings, M., 2012. The Wind- and Wave-Driven Inner-Shelf Circulation. *Annual Review of Marine Science*, 4, pp. 317–343. https://doi.org/10.1146/annurev-marine-120709-142745
4. Sullivan, P. and McWilliams, J., 2010. Dynamics of Winds and Currents Coupled to Surface Waves. *Annual Review of Fluid Mechanics*, 42, pp. 19–42. https://doi.org/10.1146/annurev-fluid-121108-145541
5. Pärn, O., Davulien, L., Macías, D.M., Vahter, K., Stips, A. and Torsvik, T., 2023. Effects of Eulerian Current, Stokes Drift and Wind While Simulating Surface Drifter Trajectories in the Baltic Sea. *Oceanologia*, 65(3), pp. 453–465. https://doi.org/10.1016/j.oceano.2023.02.001
6. Isobe, A., Kubo, K., Tamura, Y., Kako, S., Nakashima, E. and Fujii, N., 2014. Selective Transport of Microplastics and Mesoplastics by Drifting in Coastal Waters. *Marine Pollution Bulletin*, 89(1–2), pp. 324–330. https://doi.org/10.1016/j.marpolbul.2014.09.041
7. Iwasaki, S., Isobe, A., Kako, S., Uchida, K. and Tokai, T., 2017. Fate of Microplastics and Mesoplastics Carried by Surface Currents and Wind Waves: A Numerical Model Approach in the Sea of Japan. *Marine Pollution Bulletin*, 121(1–2), pp. 85–96. http://dx.doi.org/10.1016/j.marpolbul.2017.05.057
8. Yang, Y., Li, Y., Li, J., Liu, J., Gao, Z., Guo, K. and Yu, H., 2021. The Influence of Stokes Drift on Oil Spills: Sanchi Oil Spill Case. *Acta Oceanologica Sinica*, 40(10), pp. 30–37. https://doi.org/10.1007/s13131-021-1889-9
9. Bosi, S., Broström, G. and Roquet, F. 2021. The Role of Stokes Drift in the Dispersal of North Atlantic Surface Marine Debris. *Frontiers in Marine Science*, 8, 697430. doi:10.3389/fmars.2021.697430

10. McWilliams, J. and Restrepo, J., 1999. The Wave-Driven Ocean Circulation. *Journal of Physical Oceanography*, 29(10), pp. 2523–2540. doi:10.1175/1520-0485(1999)029<2523:TWDOC>2.0.CO;2
11. Markova, N.V. and Bagaev, A.V., 2016. The Black Sea Deep Current Velocities Estimated from the Data of Argo Profiling Floats. *Physical Oceanography*, (3), pp. 23–35. doi:10.22449/1573-160X-2016-3-23-35
12. Tuomi, L., Vähä-Piikkiö, O., Alenius, P., Björkqvist, J. and Kahma, K., 2017. Surface Stokes Drift in the Baltic Sea Based on Modelled Wave Spectra. *Ocean Dynamics*, 68(1), pp. 17–33. https://link.springer.com/article/10.1007/s10236-017-1115-7
13. Sørensen, O.R., Kofoed-Hansen, H., Rugbjerg, M. and Sørensen, L.S., 2005. A Third-Generation Spectral Wave Model Using an Unstructured Finite Volume Technique. In: J. M. Smith, ed., 2005. *Coastal Engineering 2004 – Proceedings of the 29th International Conference*. World Scientific, pp. 894–906. https://doi.org/10.1142/9789812701916_0071
14. Divinsky, B.V. and Kosyan, R.D., 2017. Spatiotemporal Variability of the Black Sea Wave Climate in the Last 37 Years. *Continental Shelf Research*, 136, pp. 1–19. http://dx.doi.org/10.1016/j.csr.2017.01.008
15. Breivik, Ø. and Christensen, K., 2020. A Combined Stokes Drift Profile under Swell and Wind Sea. *Journal of Physical Oceanography*, 50(10), pp. 2819–2833. doi:10.1175/JPO-D-20-0087.1

Submitted 28.06.2023; accepted after review 15.07.2023;
revised 27.12.2023; published 25.03.2024

About the authors:

Boris V. Divinsky, Leading Research Associate, Laboratory of Geology and Lithodynamics, P.P. Shirshov Institute of Oceanology, RAS (36 Nakhimovskiy Ave., Moscow, 117997, Russian Federation), PhD (Geogr.), **ORCID ID: 0000-0002-2452-1922**, **ResearcherID: C-7262-2014**, *divin@ocean.ru*

Sergey B. Kuklev, Head of Laboratory of Hydrophysics and Modelling, P.P. Shirshov Institute of Oceanology, RAS (36 Nakhimovskiy Ave., Moscow, 117997, Russian Federation), PhD (Geogr.), **ORCID ID: 0000-0003-4494-9878**, **ResearcherID: G-5656-2017**, *kuklev@ocean.ru*

Vladimir V. Ocherednik, Research Associate, Laboratory of Hydrophysics and Modelling, P.P. Shirshov Institute of Oceanology, RAS (36 Nakhimovskiy Ave., Moscow, 117997, Russian Federation), **ORCID ID: 0000-0002-3593-7114**, **ResearcherID: G-2850-2017**, *poekperementarium@gmail.com*

Olga N. Kukleva, Research Associate, Laboratory of Hydrophysics and Modelling, P.P. Shirshov Institute of Oceanology, RAS (36 Nakhimovskiy Ave., Moscow, 117997, Russian Federation), **ResearcherID: J-7126-2018**, *kukleva-ola@mail.ru*

Contribution of the authors:

Boris V. Divinsky – numerical modelling, analysis of the results

Sergey B. Kuklev – problem statement

Vladimir V. Ocherednik – analysis and presentation of the results

Olga N. Kukleva – source data preparation, presentation of the article text

All the authors have read and approved the final manuscript.

Original article

Distribution of Sea Surface Elevations in the Form of a Two-Component Gaussian Mixture

A. S. Zapevalov *, A. S. Knyazkov

Marine Hydrophysical Institute of RAS, Sevastopol, Russia
** e-mail: sevzepter@mail.ru*

Abstract

The approximation of the probability density function of sea surface elevations by a two-component Gaussian mixture has been verified. For verification, the data of direct wave measurements obtained on a stationary oceanographic platform, installed in the Black Sea, were used. The approximation correctness criterion is the relative error ε of deviation of the model of probability densities function from the experimental function calculated from the measurement data. The average error $\langle\varepsilon\rangle$ over the ensemble of situations is small if $|\xi| < 3$. The standard deviation δ is minimal if $|\xi| \approx 0$ and is equal to 0.12, if $|\xi| = 3$ then $\delta \approx 0.5$. It is shown that the error $\langle\varepsilon\rangle$ has a systematic component, which depends on the deviations of the third and fourth statistical moments from the values corresponding to the Gaussian distribution. A semi-empirical relationship has been constructed to take this component into account. It is noted that the approximation accuracy can be increased by 2–3 times by eliminating the systematic component.

Keywords: Gaussian mixture, sea waves, surface elevation, nonlinear waves, statistical moment, Black Sea

Acknowledgements: The work was performed under state assignment of Marine Hydrophysical Institute of RAS on topic FNNN-2021-0004 “Fundamental studies of oceanological processes which determine the state and evolution of the marine environment influenced by natural and anthropogenic factors, based on observation and modeling methods”.

For citation: Zapevalov, A.S. and Knyazkov, A.S., 2024. Distribution of Sea Surface Elevations in the Form of a Two-Component Gaussian Mixture. *Ecological Safety of Coastal and Shelf Zones of Sea*, (1), pp. 20–30.

Распределение возвышений морской поверхности в форме двухкомпонентной гауссовой смеси

А. С. Запевалов *, А. С. Князьков

Морской гидрофизический институт РАН, Севастополь, Россия
** e-mail: sevzepter@mail.ru*

Аннотация
Верифицирована аппроксимация функции плотности вероятностей возвышений морской поверхности двухкомпонентной гауссовой смесью. Для верификации использованы данные прямых волновых измерений, полученные на стационарной океанографической платформе, установленной в Черном море. Критерием корректности аппроксимации выбрана относительная ошибка ε отклонения модельной функции плотности вероятности от экспериментальной функции, рассчитанной по данным волновых измерений. Средняя по ансамблю ситуаций относительная ошибка ⟨ε⟩ мала, если значения нормированного на среднеквадратическую величину возвышения поверхности лежат в области $|\xi| < 3$. Среднеквадратическое отклонение относительной ошибки минимально при $|\xi| \approx 0$ и равняется 0.12, при $|\xi| = 3$ возрастает до ~ 0.5. Показано, что ошибка ⟨ε⟩ имеет систематическую составляющую, которая зависит от отклонений третьего и четвертого статистических моментов от значений, соответствующих распределению Гаусса. Построена полуэмпирическая зависимость, позволяющая учесть эту составляющую. Отмечено, что точность аппроксимации можно повысить в 2–3 раза, исключив систематическую составляющую.

Ключевые слова: гауссова смесь, морская поверхность, нелинейные волны, статистический момент, Черное море

Благодарности: работа выполнена в рамках госзадания ФГБУН ФИЦ МГИ по теме FNNN-2021-0004 «Фундаментальные исследования океанологических процессов, определяющих состояние и эволюцию морской среды под влиянием естественных и антропогенных факторов, на основе методов наблюдения и моделирования».

Для цитирования: *Запевалов А. С., Князьков А. С*. Распределение возвышений морской поверхности в форме двухкомпонентной гауссовой смеси // Экологическая безопасность прибрежной и шельфовой зон моря. 2024. № 1. С. 20–30. EDN EHKUET.

Introduction

Sea surface waves are a weakly nonlinear process, and the statistical distributions of sea surface elevations and slopes are close to the Gaussian distribution [1]. Although deviations from the Gaussian distribution are small, they play an important role in applications related to ocean remote sensing [2, 3], as well as when forecasting the occurrence of anomalous waves [4].

As a rule, distributions based on truncated Gram–Charlier or Edgeworth series are used for the sea surface statistical description [5, 6]. The distributions are the expansion of the desired probability density function in Chebyshev–Hermite orthogonal polynomials. The use of truncated series leads to distortions in the desired probability density function due to the appearance of negative values in it, as well as several local maxima [7–9].

The relevance of the search for new approaches to the statistical description of the sea surface is determined by the fact that existing models do not make it possible to construct a probability density function of sea surface elevations over the entire

range of their changes. One possible solution to this problem is to approximate the distribution of a quasi-Gaussian process by a two-component Gaussian mixture. Distributions of this type have not yet found wide application in oceanology, which may be due to the complex procedure for calculating their parameters [10]. For the first time, the use of such a model to describe the sea surface was independently proposed in [11, 12], in which probability density functions were constructed for the sea surface slopes. Recently, a two-component Gaussian mixture has been proposed to describe the distributions of sea surface elevations [13]. Unknown parameters for the desired Gaussian mixture are calculated based on the known statistical moments as in the construction of the Gram–Charlier and Edgeworth distributions.

This work aims at analyzing the possibility and limits of a two-component Gaussian mixture in order to describe the distribution of sea surface elevations. The analysis is based on direct measurements of sea waves carried out in the Black Sea.

Two-component Gaussian mixture

Finite Gaussian mixtures are widely used in various fields to approximate unknown probability density functions [9, 14]. The two-component Gaussian mixture of random variable ξ is as follows [15]

$$P_S(\xi) = \sum_i \frac{\alpha_i}{\sqrt{2\pi}\sigma_i} \exp\left(-\frac{(\xi - m_i)^2}{2\sigma_i^2} \right), \quad (1)$$

where α_i – weight of the i-th component (i = 1, 2), $\alpha_i \in (1, 2)$; m_i – expected value; σ_i^2 – variance. Weighting coefficients satisfy the condition

$$\alpha_1 + \alpha_2 = 1. \quad (2)$$

Taking into account condition (2), it is necessary to find five parameters: m_1, m_2, σ_1, σ_2 and α_1 to construct $P_S(\xi)$. In [13], it was proposed to calculate them based on the first five statistical moments of sea surface elevations. The disadvantage of this approach is that according to wave measurements under marine conditions, as a rule, statistical moments are determined only up to the fourth order inclusive [16–18]. Therefore, we will use the first four statistical moments to calculate the model parameters (m_1, m_2, σ_1, σ_2) leaving the fifth parameter (α_1) free [11]. Parameter α_1 will be varied to satisfy the condition of distribution unimodality.

The procedure for calculating model parameters (1) is described in [10]. It amounts to solving the system of equations

$$\alpha_1 m_1 + (1 - \alpha_1) m_2 = \mu_1, \quad (3)$$

$$\alpha_1 \left(m_1^2 + \sigma_1^2 \right) + (1 - \alpha_1) \left(m_2^2 + \sigma_2^2 \right) = \mu_2, \quad (4)$$

$$\alpha_1 \left(m_1^3 + 3 m_1 \sigma_1^2 \right) + (1 - \alpha_1) \left(m_2^3 + 3 m_2 \sigma_2^2 \right) = \mu_3, \quad (5)$$

$$\alpha_1 \left(m_1^4 + 6 m_1^2 \sigma_1^2 + 3\sigma_1^4 \right) + (1 - \alpha_1) \left(m_2^4 + 6 m_2^2 \sigma_2^2 + 3\sigma_2^4 \right) = \mu_4, \quad (6)$$

where μ_i – statistical moment of order i :

$$\mu_j = \int \xi^j P_S(\xi) d\xi ,$$

Let us assume that the average level of the surface is zero ($\mu_1 = 0$), and the variance of the analyzed random variable is equal to 1 ($\mu_2 = 1$). Parameters μ_3 and $\mu_4 - 3$ are the skewness and excess kurtosis, respectively. System of equations (3)–(6) is symmetric with respect to triples of parameters (m_1, σ_1^2, α_1) and (m_2, σ_2^2, α_2).

Verification

To verify the model probability density function of sea surface elevations (1), the data of wave measurements obtained on a stationary oceanographic platform of Marine Hydrophysical Institute of RAS were used [19]. The measurements were carried out during December 2018. The platform was located in the Black Sea 600 m from the coast at a depth of about 30 m. The waves were measured with a string wave recorder [20].

The measurements were carried out under wind conditions that varied from calm to wind speed of 25 m/s. Significant wave heights (the average height of 1/3 of the highest waves) varied from 0.23 m to 2.26 m, the maximum wave height reached 4.9 m. The wavelengths corresponding to the peak of the wave spectrum ranged from 10 to 120 m.

The verification took place as follows. Continuous wave measurements were divided into wave records lasting 20 min. The total volume of data for analysis was more than 2200 wave records. Each wave record was centered and normalized so that its variance was equal to one, then experimental probability density function $P_E(\xi)$ was calculated for each wave record. Statistical moments $\mu_3 = \langle \xi^3 \rangle$ and $\mu_4 = \langle \xi^4 \rangle$ were also determined so that to calculate the parameters of two-component Gaussian mixture $P_S(\xi)$. Here and below, symbol $\langle\ \rangle$ means averaging.

According to wave measurements previously carried out in the Black Sea, the values of statistical moments μ_3 and μ_4 can be found mainly in the following ranges [19]

$$-0.2 < \mu_3 < 0.3 \quad \text{и} \quad 2.6 < \mu_4 < 3.4 . \tag{7}$$

The same ranges were determined from measurements in the North Sea [18]. As a rule, exceeding the specified ranges occurs in situations where abnormally high waves (rogue waves) are observed. [17]. In this work, we will limit ourselves to the analysis of situations when μ_3 and μ_4 satisfy condition (7).

The experimental probability density function is calculated based on the analysis of the histogram of sea surface elevations. Width of intervals $\Delta\xi$ was taken equal to 0.45. Function $P_E(\xi)$ was obtained from the histogram by normalizing it to the total number of points in the wave record and to the width of the interval.

The verification procedure for a two-component Gaussian mixture model consists of comparing functions $P_E(\xi)$ and $P_S(\xi)$. The criterion for the correspondence of model (1) to wave measurement data is relative error

$$\varepsilon(\xi) = \frac{P_S(\xi) - P_E(\xi)}{P_E(\xi)},$$

for which average value $\langle\varepsilon(\xi)\rangle$ and standard deviation $\delta(\xi) = \langle(\varepsilon(\xi) - \langle\varepsilon(\xi)\rangle)^2\rangle^{0.5}$ are calculated.

To calculate Gaussian mixture $P_S(\xi)$, the procedure described in [10] was chosen. Taking into account condition (2), system of equations (3)–(6) was reduced to one sixth degree polynomial equation in m_1

$$\begin{aligned} &2\alpha_1^2(\alpha_1 - \alpha_1^2 - 1)m_1^6 - 4\mu_3\alpha_1(2\alpha_1 - 1)(\alpha_1 - 1)^2 m_1^3 + \\ &+3(\mu_4 - 3)\alpha_1(\alpha_1 - 1)^3 m_1^2 + \mu_3^2(\alpha_1 - 1)^4 = 0, \end{aligned} \tag{8}$$

the solutions of which for given values μ_3 and μ_4 were found numerically by Newton's method by varying α_1 The coefficients included in equation (8) were analyzed in [10], where it was shown that, except for the rare case when $\mu_3 = 0$ and $\mu_4 > 3$, it could always be solved and the construction of a probability density function was possible. From several solutions obtained for various possible α_1, the one was chosen that corresponded to the physical condition of unimodality of the resulting distribution and the positivity of values σ_1^2 и σ_2^2, which were recalculated, like m_2, from value m_1 according to the method discussed in [3]. Values μ_3 and μ_4 calculated for model Gaussian mixture $P_S(\xi)$ obtained as a result of solving equation (8) were compared with the values calculated from the wave record and used in original equations (3)–(6). The accuracy of agreement between values μ_3 and μ_4 calculated from the Gaussian mixture and from the wave record is achieved no worse than 10^{-3}.

Figure 1 shows functions $\langle\varepsilon(\xi)\rangle$ and $\delta(\xi)$. Here, $N(\xi)$ is number of points from which statistical characteristics were calculated in given interval $\Delta\xi$. Functions $\langle\varepsilon(\xi)\rangle$ and $\delta(\xi)$ are average over the ensemble of situations in which measurements were carried out, with μ_3 and μ_4 satisfying condition (7). Parameters $\mu_3 = 0$ and $\mu_4 > 3$ in 11 wave records led to their exclusion from consideration for the reason stated above.

Analysis of deviations of model function $P_S(\xi)$ from experimental one $P_E(\xi)$ given in Fig. 1 indicates their smallness in the vicinity of point $\xi = 0$ and increase with $|\xi|$. As for range $|\xi| < 3$, the parameters characterizing this deviation satisfy conditions

$$\left|\langle\varepsilon(\xi)\rangle\right| < 0.05, \quad \delta(\xi) < 0.3.$$

For further analysis, all data were divided into groups corresponding to four ranges of the third statistical moment: group 1 – $-0.2 < \mu_3 \le 0$, group 2 – $0 < \mu_3 \le 0.1$, group 3 – $0.1 < \mu_3 \le 0.2$, group 4 – $0.2 < \mu_3 \le 0.3$. Figure 2 shows variables $\langle\varepsilon(\xi, \mu_3)\rangle$ and $\delta_i(\xi, \mu_3)$ calculated for each group. Here, index i taking values from one to four corresponds to the group number. Parameter $N_i(\xi, \mu_3)$ shows the number of

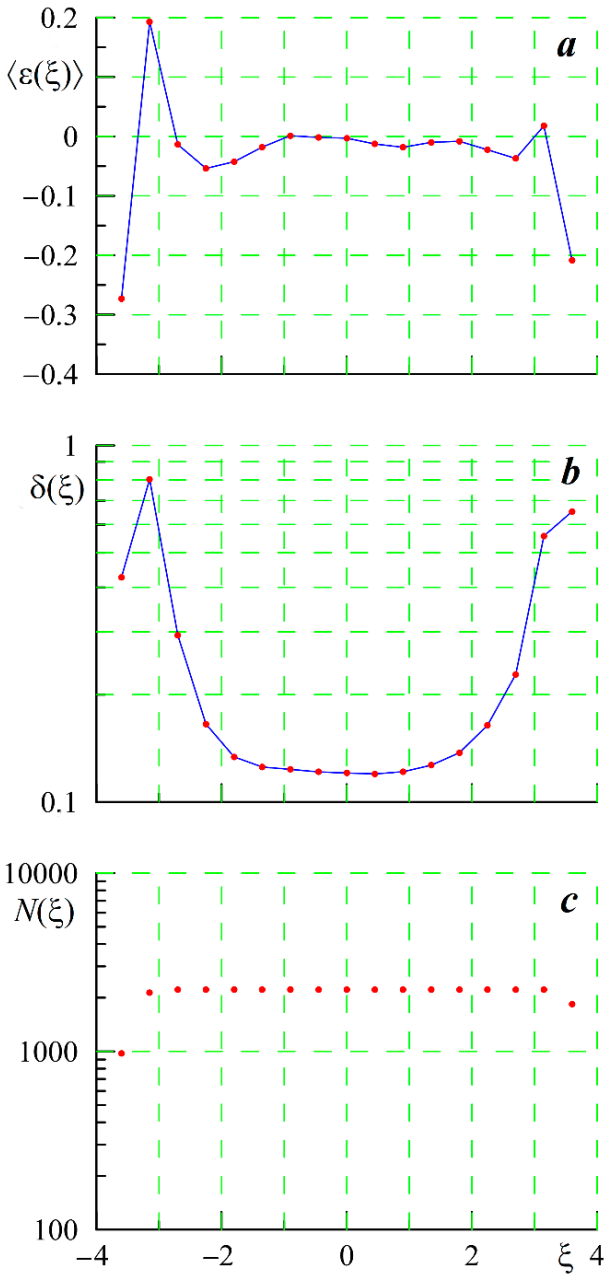

Fig. 1. Relative error ε(ξ) (*a*) and standard deviation δ(ξ) (*b*) calculated for an ensemble of situations, the number of points $N(\xi)$ from which statistical characteristics were calculated in a given interval Δξ (*c*)

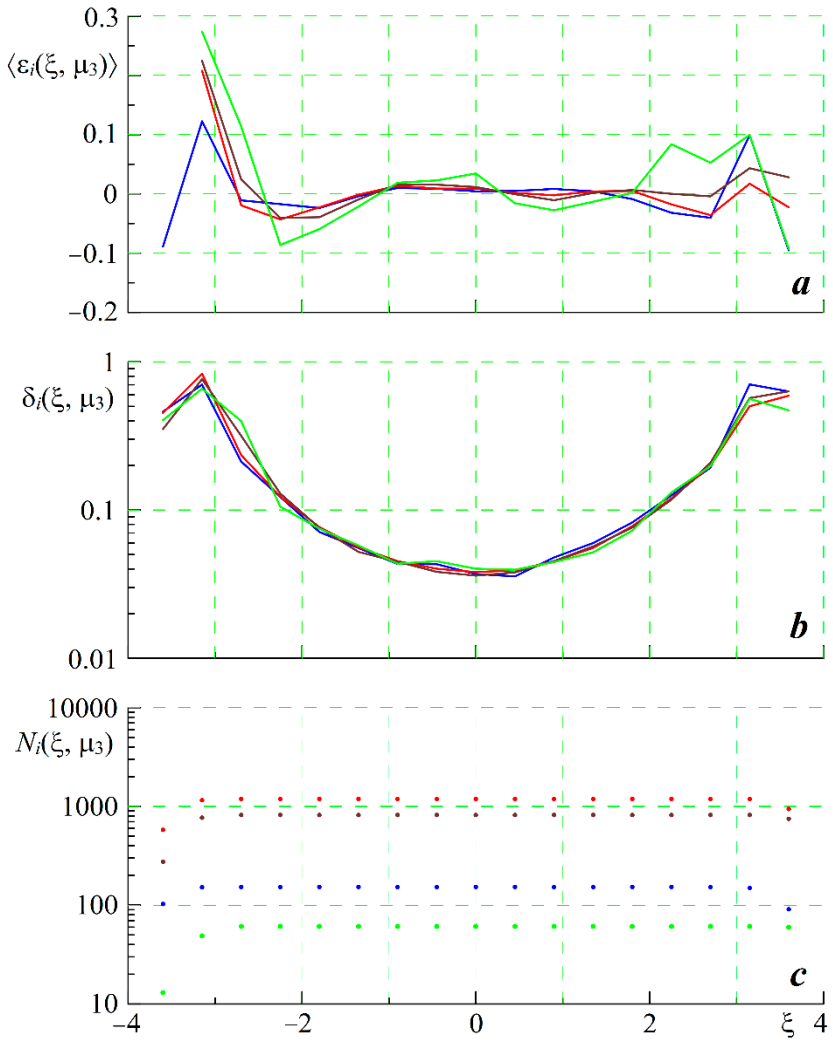

F i g . 2 . Variables ε(ξ) (*a*), δ(ξ) (*b*), *N*(ξ) (*c*) calculated for four ranges μ_3: $-0.2 < \mu_3 \le 0$ (blue), $0 < \mu_3 \le 0.1$ (red), $0.1 < \mu_3 \le 0.2$ (brown), $0.2 < \mu_3 \le 0.3$ (green)

points from which the values $\langle \varepsilon_i(\xi, \mu_3) \rangle$ and $\delta_i(\xi, \mu_3)$ were calculated. Average value of relative error $\langle \varepsilon_i(\xi, \mu_3) \rangle$ depends significantly on the group for which it was calculated. At the same time, standard deviation $\delta_i(\xi, \mu_3)$ is almost the same for all groups. The discrepancy between $P_S(\xi)$ and $P_E(\xi)$ depends on how much statistical moment μ_3 deviates from the zero value corresponding to the Gaussian distribution. The greatest discrepancies are observed for group 4.

We use a similar approach to analyze the approximation of the probability density of sea surface elevations for different values of the fourth statistical moment. Let us divide the data into groups corresponding to four ranges μ_4: group 1 – $2.6 < \mu_4 \le 2.8$, group 2 – $2.8 < \mu_4 \le 3.0$, group 3 – $3.0 < \mu_4 \le 3.2$, group 4 – $3.2 < \mu_4 \le 3.4$. Figure 3 shows variables $\langle \varepsilon_i(\xi, \mu_4) \rangle$ and $\delta_i(\xi, \mu_4)$ calculated for the specified groups.

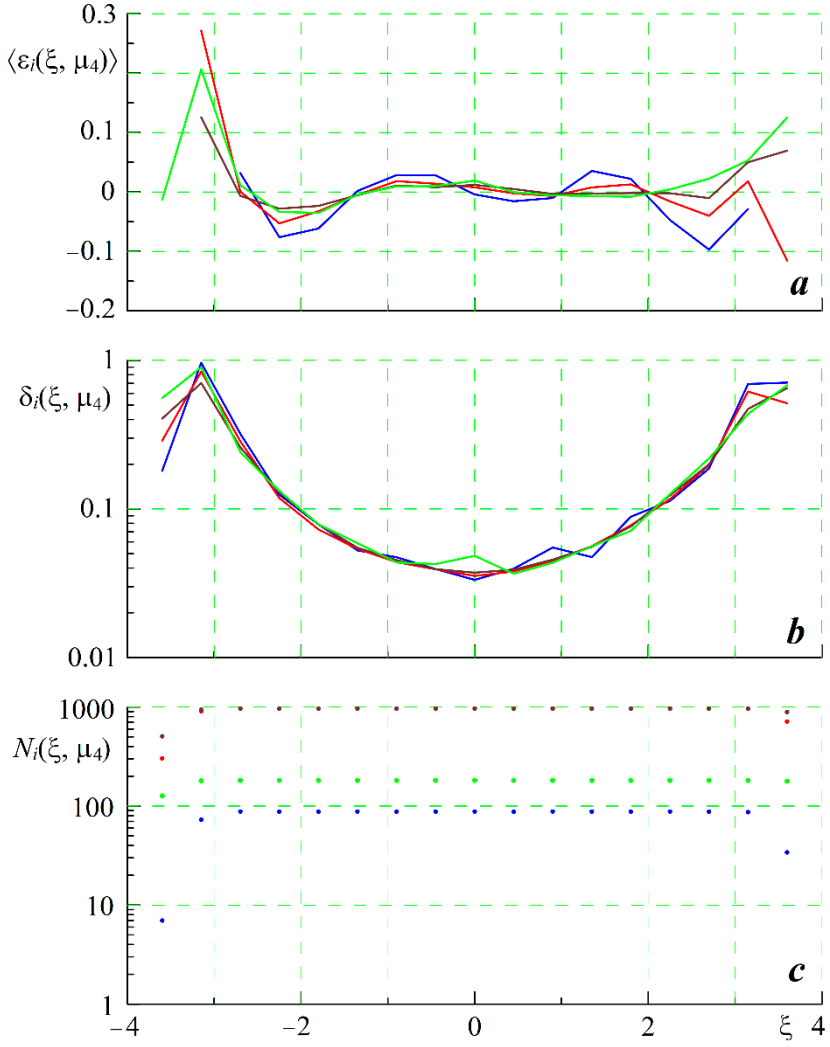

F i g . 3 . Variables $\varepsilon(\xi)$ (*a*), $\delta(\xi)$ (*b*), $N(\xi)$ (*c*) calculated for four ranges μ_4: $2.6 < \mu_4 \le 2.8$ (blue), $2.8 < \mu_4 \le 3.0$ (red), $3.0 < \mu_4 \le 3.2$ (brown), $3.2 < \mu_4 \le 3.4$ (green)

Division into groups according to the range of changes in statistical moments μ_3 and μ_4 results in a significant change in the relative error in the approximation of the probability density of sea surface elevations. In range $|\xi| < 2$, values $\delta_i(\xi, \mu_3)$ and $\delta_i(\xi, \mu_4)$ are 2–3 times lower than values $\delta(\xi)$ calculated for the entire ensemble of situations. This makes it possible to describe the probability density function by the semi-empirical relationship

$$P_\xi(\xi) = P_S(\xi)\left(1 + \langle \varepsilon_E(\xi) \rangle\right),$$

where $\langle \varepsilon_E(\xi) \rangle$ is average relative error calculated for corresponding ranges μ_3 and μ_4.

Conclusion

The approximation of the probability density function of sea surface elevations by a two-component Gaussian mixture was verified for the values of the third and fourth statistical moments which vary within $-0.2 < \mu_3 < 0.3$ and $2.6 < \mu_4 < 3.4$ and are characteristic of the Black Sea coastal zone. The criterion for the correctness of the approximation is the deviation of the model probability density function from that one calculated from wave measurement data, which is characterized by relative error.

In range $|\xi| < 3$, values of average relative error $\langle \varepsilon(\xi) \rangle$ and its standard deviation $\delta(\xi)$ are small and satisfy condition $|\langle \varepsilon(\xi) \rangle| < 0.05$, $\delta(\xi) < 0.3$. Approximation error $\langle \varepsilon(\xi) \rangle$ has a systematic component which depends on the deviations of the third and fourth statistical moments from the values corresponding to the Gaussian distribution. A semi-empirical relationship has been constructed to take this component into account. The elimination of the systematic component will reduce $\delta(\xi)$, and the approximation accuracy can accordingly be increased by 2–3 times.

REFERENCES

1. Longuet-Higgins, M.S., 1963. The Effect of Non-Linearities on Statistical Distributions in the Theory of Sea Waves. *Journal of Fluid Mechanic*s, 17(3), pp. 459–480. https://doi.org/10.1017/S0022112063001452
2. Hayne, G.S., 1980. Radar Altimeter Mean Return Waveforms from Near-Normal-Incidence Ocean Surface Scattering. *IEEE Transactions on Antennas and Propagation*, 28(5), pp. 687–692. https://doi.org/10.1109/TAP.1980.1142398
3. Kay, S., Hedley, J.D. and Lavender, S., 2009. Sun Glint Correction of High and Low Spatial Resolution Images of Aquatic Scenes: A Review of Methods for Visible and Near-Infrared Wavelengths. *Remote Sensing*, 1(4), pp. 697–730. https://doi.org/10.3390/rs1040697
4. Annenkov, S.Y. and Shrira, V.I., 2014. Evaluation of skewness and kurtosis of wind waves parameterized by JONSWAP spectra. *Journal of Physical Oceanography*, 44(6), pp. 1582–1594. https://doi.org/10.1175/JPO-D-13-0218.1
5. Bréon, F.M. and Henriot, N., 2006. Spaceborne observations of ocean glint reflectance and modeling of wave slope distributions. *Journal of Geophysical Research: Oceans*, 111(C6), C06005. https://doi.org/10.1029/2005JC003343
6. Callahan, P.S. and Rodriguez, E., 2004. Retracking of Jason-1 Data. *Marine Geodesy*, 27(3–4), pp. 391–407. https://doi.org/10.1080/01490410490902098

7. Kwon, O.K., 2022. Analytic Expressions for the Positive Definite and Unimodal Regions of Gram-Charlier Series. *Communications in Statistics – Theory and Methods*, 51(15), pp. 5064–5084. https://doi.org/10.1080/03610926.2020.1833219
8. Lin, W. and Zhang, J.E., 2022. The Valid Regions of Gram–Charlier Densities with High-Order Cumulants. *Journal of Computational and Applied Mathematics*, 407, 113945. https://doi.org/10.1016/j.cam.2021.113945
9. Blinnikov, S. and Moessner, R., 1998. Expansions for nearly Gaussian Distributions. *Astronomy and Astrophysics Supplement Series*, 130(1), pp. 193–205. https://doi.org/10.1051/aas:1998221
10. Zapevalov, A.S. and Knyazkov, A.S., 2022. Statistical Description of the Sea Surface by Two-Component Gaussian Mixture. *Physical Oceanography*, 29(4), pp. 395–403.
11. Zapevalov, A.S. and Ratner, Y.B., 2003. Analytic Model of the Probability Density of Slopes of the Sea Surface. *Physical Oceanography*, 13(1), pp. 1–13. https://doi.org/10.1023/A:1022444703787
12. Tatarskii, V.I., 2003. Multi-Gaussian Representation of the Cox–Munk Distribution for Slopes of Wind-Driven Waves. *Journal of Atmospheric and Oceanic Technology*, 20(11), pp. 1697–1705. https://doi.org/10.1175/1520-0426(2003)020<1697:MROTCD>2.0.CO;2
13. Gao, Z. and Sun Z. Liang, S., 2020. Probability Density Function for Wave Elevation Based on Gaussian Mixture Models. *Ocean Engineering*, 213, 107815. https://doi.org/10.1016/j.oceaneng.2020.107815
14. Carreira-Perpinan, M.A., 2000. Mode-Finding for Mixtures of Gaussian Distributions. *IEEE Transactions on Pattern Analysis and Machine Intelligence*, 22(11), pp. 1318–1323. https://doi.org/10.1109/34.888716
15. Aprausheva, N.N. and Sorokin, S.V., 2013. Exact Equation of The Boundary of Unimodal and Bimodal Domains of a Two-Component Gaussian Mixture. *Pattern Recognition and Image Analysis*, 23(3), pp. 341–347. https://doi.org/10.1134/S1054661813030024
16. Babanin, A.V. and Polnikov, V.G., 1995. On the Non-Gaussian Nature of Wind Waves. *Physical Oceanography*, 6(3), pp. 241–245. https://doi.org/10.1007/BF02197522
17. Guedes Soares, C., Cherneva, Z. and Antão, E.M., 2003. Characteristics of Abnormal Waves in North Sea Storm Sea States. *Applied Ocean Research*., 25(6), pp. 337–344. https://doi.org/10.1016/j.apor.2004.02.005
18. Jha, A.K. and Winterstein, S.R., 2000. Nonlinear Random Ocean Waves: Prediction and Comparison with Data. In: ASME, 2000. *Proceedings of the 19th International Offshore Mechanics and Arctic Engineering Symposium*. New Orleans, USA. Paper No. 00-6125.
19. Zapevalov, A.S. and Garmashov, A.V., 2021. Skewness and Kurtosis of the Surface Wave in the Coastal Zone of the Black Sea. *Physical Oceanography*, 28(4), pp. 414–425. https://doi.org/10.22449/1573-160X-2021-4-414-425
20. Toloknov, Yu.N. and Korovushkin, A.I., 2010. The System of Collecting Hydrometeorological Information. In: MHI, 2010. *Monitoring Systems of Environment*. Sevastopol: ECOSI-Gidrofizika. Iss. 13, pp. 50–53 (in Russian).

Submitted 06.07.2023; accepted after review 03.09.2023;
revised 27.12.2023; published 25.03.2024

About the authors:

Aleksandr S. Zapevalov, Chief Research Associate, Marine Hydrophysical Institute of RAS (2 Kapitanskaya St., Sevastopol, 299011, Russian Federation), Dr.Sci. (Phys.-Math.), **Scopus Author ID: 7004433476**, **ResearcherID: V-7880-2017**, **ORCID ID: 0000-0001-9942-2796**, *sevzepter@mail.ru*

Aleksandr S. Knyazkov, Leading Engineer, Marine Hydrophysical Institute of RAS (2 Kapitanskaya St., Sevastopol, 299011, Russian Federation), **ORCID ID: 0000-0003-1119-1757**, *fizfak83@yandex.ru*

Contribution of the authors:

Aleksandr S. Zapevalov – task statement, review of literature on the study topic, article preparation

Aleksandr S. Knyazkov – algorithm development and calculation performance, critical analysis of the calculations

The author has read and approved the final manuscript.

Original article

Peculiarities of Interseasonal Variability of Alongshore Wind Circulation and Coastal Currents off the Southern Coast of Crimea

A. S. Kuznetsov

Marine Hydrophysical Institute of RAS, Sevastopol, Russia
e-mail: kuznetsov_as@mhi-ras.ru

Abstract
The paper analyses decade-average (2013–2022) statistical and spectral characteristics of mesoscale and synoptic variability of the wind field for the atmosphere surface layer and the surface current to reveal regularities and peculiarities of the wind variability and quasi-stationary alongshore current near Cape Kikineiz of the Southern Coast of Crimea. Complex instrumental monitoring was carried out under open sea conditions using clusters of hydrometeorological and oceanological meters at the stationary oceanographic platform of the Black Sea hydrophysical sub-satellite testing area of Marine Hydrophysical Institute of RAS. The author used a dataset of chronological sequences of mean-hourly vector-averaged data for May–October and November–April half-year periods to quantify the values and identify trends in the interseasonal variability of wind and current field characteristics. During the selected time periods, clear seasonal differences in the thermal structure and dynamics of both the surface wind field and coastal waters were observed near the coast. Based on instrumental monitoring materials, peculiarities of coastal water circulation under seasonal variability of local wind conditions were studied. The spectral analysis results estimate the energy contribution of breeze wind circulation to the seasonal intensification of the mesoscale variability of the alongshore current. During the entire annual cycle, multiscale alongshore reciprocating wind fluctuations, parallel to the Main Ridge of the Crimean Mountains, apart from the background large-scale wind field, were detected at the seacoast. Such wind fluctuations influence the variability of the coastal-waters alongshore circulation, which allows studying the conditions and peculiarities of the bimodal distribution formation of the direction recurrence of the quasi-stationary alongshore current near Cape Kikineiz.

Keywords: Black Sea, Southern Coast of Crimea, coastal zone, instrumental monitoring, local wind field, alongshore current, energy spectrum

Acknowledgements: The work was performed under state assignment of Marine Hydrophysical Institute of RAS on topic FNNN-2021-0005 “Complex interdisciplinary research of oceanologic processes, which determine functioning and evolution of the Black and Azov Sea coastal ecosystems”.

For citation: Kuznetsov, A.S., 2024. Peculiarities of Interseasonal Variability of Alongshore Wind Circulation and Coastal Currents off the Southern Coast of Crimea. *Ecological Safety of Coastal and Shelf Zones of Sea*, (1), pp. 31–44.

Особенности межсезонной изменчивости вдольбереговой циркуляции ветра и прибрежного течения у Южного берега Крыма

А. С. Кузнецов

Морской гидрофизический институт РАН, Севастополь, Россия
e-mail: kuznetsov_as@mhi-ras.ru

Аннотация
По результатам анализа средних за десятилетие 2013–2022 гг. статистических и спектральных характеристик мезомасштабной и синоптической изменчивости поля ветра приводного слоя атмосферы и приповерхностного течения выделены закономерности и особенности изменчивости ветра и квазистационарного вдольберегового течения у м. Кикинеиз Южного берега Крыма. Комплексный инструментальный мониторинг выполнен кластерами гидрометеорологических и океанологических измерителей в условиях открытого моря со стационарной океанографической платформы Черноморского гидрофизического подспутникового полигона Морского гидрофизического института РАН. Для количественных оценок значений и выявления тенденций в межсезонной изменчивости характеристик поля ветра и течения использован набор хронологических последовательностей среднечасовых векторно-осредненных данных за полугодия май – октябрь и ноябрь – апрель. В выделенные временные периоды у побережья наблюдались явные сезонные различия в термической структуре и динамике как приповерхностного поля ветра, так и прибрежных вод. На основе материалов инструментального мониторинга исследованы особенности циркуляции прибрежных вод при сезонной изменчивости местных ветровых условий. По результатам спектрального анализа получены оценки энергетического вклада бризовой циркуляции ветра в период сезонной интенсификации мезомасштабной изменчивости вдольберегового течения. В течение всего годового цикла у побережья в море наряду с фоновым крупномасштабным полем ветра выявлены разномасштабные вдольбереговые возвратно-поступательные колебания ветра, ориентированные параллельно хребту Главной гряды Крымских гор. Такие колебания ветра влияют на изменчивость вдольбереговой циркуляции прибрежных вод, что позволяет исследовать условия и особенности формирования бимодального распределения повторяемости направления квазистационарного вдольберегового течения у м. Кикинеиз.

Ключевые слова: Черное море, Южный берег Крыма, прибрежная зона, инструментальный мониторинг, поле местного ветра, вдольбереговое течение, энергетический спектр

Благодарности: работа выполнена в рамках темы государственного задания ФГБУН ФИЦ МГИ FNNN-2021-0005 «Комплексные междисциплинарные исследования океанологических процессов, определяющих функционирование и эволюцию экосистем прибрежных зон Черного и Азовского морей».

Для цитирования: *Кузнецов А. С.* Особенности межсезонной изменчивости вдольбереговой циркуляции ветра и прибрежного течения у Южного берега Крыма // Экологическая безопасность прибрежной и шельфовой зон моря. 2024. № 1. С. 31–44. EDN EBWSKZ.

Introduction

Research into the causes of intense variability of currents off the coast of Crimea is due to the need for reliable navigation support for maritime transport, as well as the extraction and reproduction of resources in the Black Sea coastal zone. The sphere of recreational services and the construction of housing and utility complexes are intensively developing at the Southern Coast of Crimea (SCC), and a network of port, hydraulic engineering and treatment facilities with sewer collectors for the bottom discharge of industrial wastewater from land into the coastal zone of the sea has been formed in the zone of interface between land and sea.

Under such conditions, the preservation of the SCC natural ecosystem depends on the balanced consumption and reproduction of natural resources while limiting the flow of pollution into the sea during waste disposal. The existence and sustainable economic development of such a social eco-economic system is possible only with rational management of environmental activities and effective quality control of the marine environment [1].

Specific structure of the transport of coastal waters and contaminants off the coast of Crimea is a natural factor that invariably minimizes the consequences of technogenic and anthropogenic loads on the marine environment. Long-term instrumental monitoring of the dynamics of coastal waters carried out by Marine Hydrophysical Institute (MHI) at the Black Sea hydrophysical sub-satellite testing area (BSHSTA) near Cape Kikineiz makes it possible to estimate the impact of changes in natural, climatic and anthropogenic factors on the state of the coastal ecosystem reliably.

This work is aimed at obtaining new scientific knowledge about the peculiarities of interseasonal variability of alongshore wind circulation and coastal currents based on the results of statistical and spectral analysis of the 2013–2022 instrumental monitoring data.

Materials and methods of study

Since 1929, a system of hydrometeorological and oceanographic observations has been in operation and is constantly being improved at the BSHSTA of MHI in the settlement of Katsiveli located near Cape Kikineiz [2]. Instrumental monitoring of the characteristics of the coastal waters is carried out by hydrometeorological and oceanological meters from an oceanographic platform located in the open sea at a distance of ~500 m from the coast.

The wind field characteristics are studied using data from a set of automated hydrometeorological complexes with primary measuring transducers of wind indicator M-63 and IPV-M as part of complex MGI-6503 [2] and small-sized wind sensors (DVM) as part of the hydrometeorological data collection complex (KSGD) [3] installed compactly at a height of 18 m above sea level on the oceanographic platform communication mast. The complexes operate in a second-by-second measurement mode with a nominal sensitivity of the wind speed module measuring channel of no more than 0.1 m/s and wind direction channel of no more than 3°. A vector-averaged series of 87,648 pairs of mean-hourly samples of vector components was formed for the 2013–2022 monitoring period.

Data from current meters MGI-1308 [2, 4] are used on hydrological horizons from the surface layer to the bottom one at a depth of ~28 m to study the circulation of coastal waters. The meters record vector-averaged second-by-second readings of the speed and direction of the current vector over a time interval of 5 minutes with a nominal sensitivity of the speed module measuring channel of 0.1 cm/s and a current direction channel of 3°. Basic vector-averaged series of 87,648 pairs of mean-hourly readings of the current vector components were formed for each 5, 10, 15, 20 m measuring horizon over the 10-year period specified above.

Primary measuring transducers of the complexes undergo metrological certification in the MHI metrology and standardization service in the prescribed manner. Further operational technological quality control of measurements ensures compliance with metrological unity during long-term measurements of the characteristics of coastal currents and wind, thus eliminating the impact of faulty values and significant methodological measurement errors. Further averaging of data processing results makes it possible to increase the accuracy of statistically mean values of both current and wind to the level of maximum random errors limited by the resolution (nominal sensitivity) of corresponding primary measuring transducers of the complexes.

Scientific novelty of the set of the 2013–2022 systematized materials used in this work is proved by certificates of state registration [1), 2), 3)]. Materials from vector databases of synchronous monitoring of the coastal current and wind of the atmosphere surface layer were used in statistical and spectral analysis. The intensity and spatiotemporal peculiarities of the dynamics of water and wind near the SCC were studied based on the obtained quantitative estimates. Spectral analysis of the variability of the energy intensity of current and wind fluctuations was carried out under a linear estimate of the spectrum through smoothing of periodograms using a processing program developed by MHI based on work [4)] and applied in [4–6].

[1)] Kuznetsov, A.S. and Zima, V.V., 2019. *Database for Monitoring the Dynamics of the Black Sea Coastal Currents near the Southern Coast of Crimea for 2008–2015 According to Measurements on a Stationary Oceanographic Platform near Cape Kikineiz* [Database]. Moscow. State Registration No. 2019620377 (in Russian).

[2)] Kuznetsov, A.S. and Zima, V.V., 2020. *Database for Monitoring the Current Field of the Coastal Zone of the Black Sea near the Southern Coast of Crimea for 2016–2019* [Database]. Moscow. State Registration No. 2020621445 (in Russian).

[3)] Kuznetsov, A.S., Garmashov, A.V. and Zima, V.V., 2023. *Database for Wind Characteristics Monitoring for the Black Sea Coastal Ecotone at Cape Kikineiz of the Southern Coast of Crimea for 2013–2022* [Database]. Moscow. State Registration No. 2023622482 (in Russian).

[4)] Konyaev, K.V., 1981. [*Spectral Analysis of Random Oceanological Fields*]. Leningrad: Gidrometeoizdat, 207 p. (in Russian).

Results and discussion

As part of monitoring, the problem of estimation of the coastal wind circulation contribution to the formation of the peculiarities of interseasonal variability of the alongshore currents is urgent. According to [4], a quasi-stationary alongshore current is reliably expressed in the coastal zone near Cape Kikineiz and the main modes of its variability have been studied. As noted in [7], the spatial peculiarities of water dynamics near the coast are determined by the configuration of the coastline and the bottom topography. Work [4] presents the results of studies of the main axis orientation of wave-vortex elliptical orbital water movements transformed near the coast. In general, the directions of such reciprocating fluctuations are oriented along the direction of the current which is oriented along the corresponding isobath of the bottom topography at a specific measuring horizon [8]. The 2013–2022 average speed of the alongshore quasi-stationary current is 7.9 cm/s in a west-southwest direction (253°) in the sea surface layer at a horizon of 5 m and 6.7 cm/s in a direction of 215° in the bottom layer at a horizon of 20 m. Figure 1 shows the 2013–

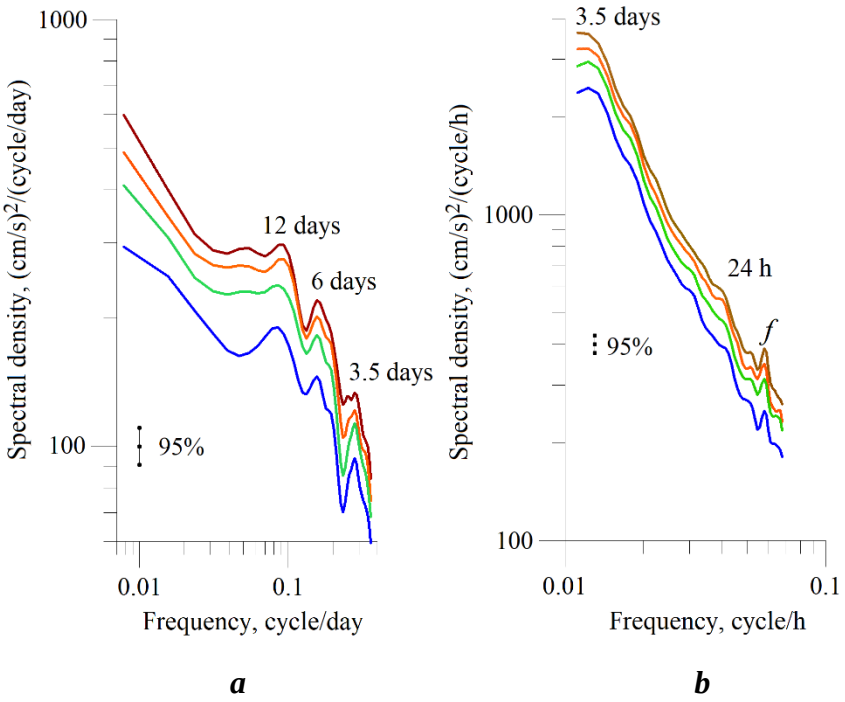

F i g . 1 . Full energy spectra of coastal current fluctuations near the Southern Coast of Crimea at 5, 10, 15, 20 m hydrological horizons (brown, orange, green, blue lines, respectively) at 95% confidence interval in the range of periods: 3–128 days (*a*); 14–96 h (*b*); *f* is local inertial frequency

2022 average energy spectra of coastal current fluctuations at hydrological horizons in the range of periods 3–128 days (Fig. 1, *a*) and 14–96 h (Fig. 1, *b*), similar to the results obtained earlier [4, 5].

It is noted in [7] that the variability of wind conditions near the SCC causes rapid restructuring of coastal currents. Next, we consider the results of wind conditions regime and variability analysis obtained from the 2013–2022 instrumental monitoring materials, which are necessary for further discussion.

Peculiarities of mean long-term wind variability. The total wind field of the Black Sea region is formed by the background wind and the superposition of local winds of thermal and orographic origin which play a significant role in the formation of the atmosphere surface layer wind field [7, 9, 10]. This instrumental monitoring made it possible to identify reliably and specify the spectral composition of wind field fluctuations near the SCC. Fig. 2 shows the 2013–2022 average energy spectra of wind variability in the atmosphere surface layer in the range of periods 3–128 days (Fig. 2, *a*), 6–96 h (Fig. 2, *b*) and 14–96 h (Fig. 2, *c*).

Fig. 2, *a* shows the energy spectrum of wind fluctuations in the range of mesoscale and synoptic variability where spectral peaks are reliably identified at periods of about 4 and 6 days and the intensification of synoptic wind fluctuations is expressed at periods of 8, 13 and 21 days.

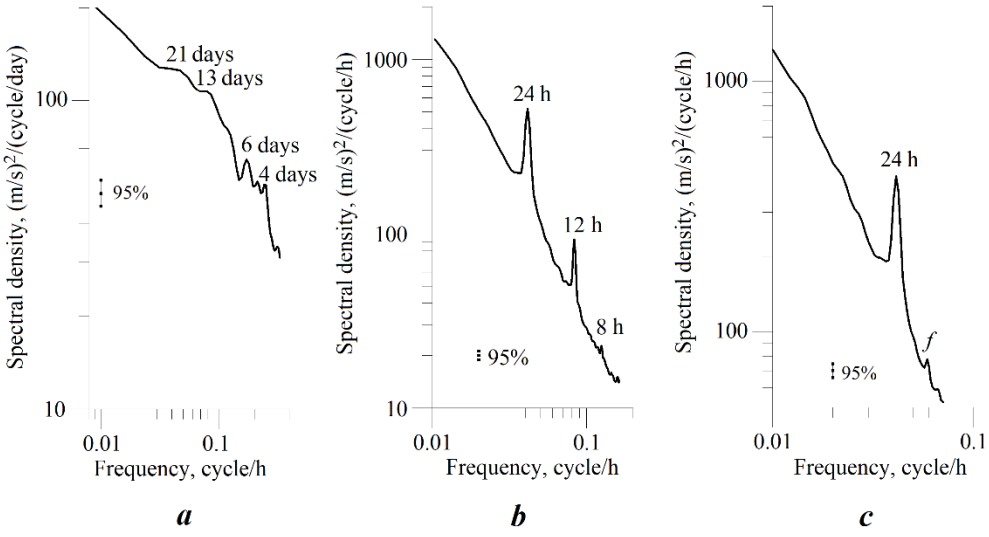

Fig. 2. Full energy spectrum of wind variability in the atmosphere surface layer in the coastal marine ecotone zone near the Southern Coast of Crimea at 95% confidence interval in the range of periods: 3–128 days (*a*); 6–96 h (*b*), 14–96 h (*c*), where *f* is local inertial frequency

It is noted in [9] that the orographic effect should consist in the generation of stationary inertia-gravity waves trapped by the surface when the wind flows around the mountainous relief surrounding the Black Sea. According to the results of numerical modelling [10–12] and analysis of *in situ* data [6], local breezes and mountain slope winds have a pronounced daily periodicity. Figure 2, *b* shows the energy spectrum of wind fluctuations containing spectral maxima of wind fluctuations at periods of about 8, 12 and 24 h.

In order to isolate inertial wind fluctuations in the presence of intense intraday fluctuations, the contribution of gravitational fluctuations with periods of less than 14 h was removed from the initial data by digital filtering. Figure 2, *c* shows the energy spectrum of wind fluctuations calculated in the range of periods of 14–96 h where the spectral peak of wind fluctuations with a period of ~ 17 h (local inertial frequency) was reliably identified.

Peculiarities of the wind field spatial orientation. According to the results obtained, peculiarities of the spatial orientation of the total wind field main components in the region were identified in the atmosphere surface layer. Figure 3, *a* shows empirical probability density function of the distribution of wind field directions calculated in angular segments ±5° for 2013–2022. Three main directions of air masses movement in the atmosphere surface layer near Cape Kikineiz were identified. The winds of the alongshore east-northeast (~ 65°) and west-southwest (~ 245°) points are almost collinear and parallel to the Main Ridge range of the Crimean Mountains in the region, and the wind of the northern (~ 355°) points is directed downslope towards the sea normal to the mountain range.

Alongshore air flows can be periodically formed owing to certain natural conditions near the SCC and disturbances introduced by the Crimean Mountains into the background wind speed fields, and a zone of mesoscale wind speed fluctuations is created in such a way [12].

Figure 3, *b* shows empirical probability density function of wind directions calcu-lated after removing the contribution of inertia-gravitaty and daily wind variability from the initial data by digital filtering. After filtering, the alongshore directions of the reverse movement of air masses parallel to the mountain range are preserved, but at the same time the contribution of the wind from the northern directions is radically transformed. Figure 3, *c* shows empirical probability density function of wind directions, calculated after removing the contribution of inertia-gravity, daily fluctuations and large-scale background wind from the initial data. The background wind of north-northeast (~ 25°) points with a speed module of 1.5–1.6 m/s was calculated for a 10-year monitoring period. Upon completion of the processing, the contribution of wind fluctuations along the coastal points is reliably identified, but the wind of the northern points is not self-identified (Fig. 3, *c*). As a result, it was established that alongshore fluctuations of the coastal wind of various time scales dominate annually in the atmosphere surface layer at a distance of ~ 500 m from the coast with the contribution of local and regional background wind.

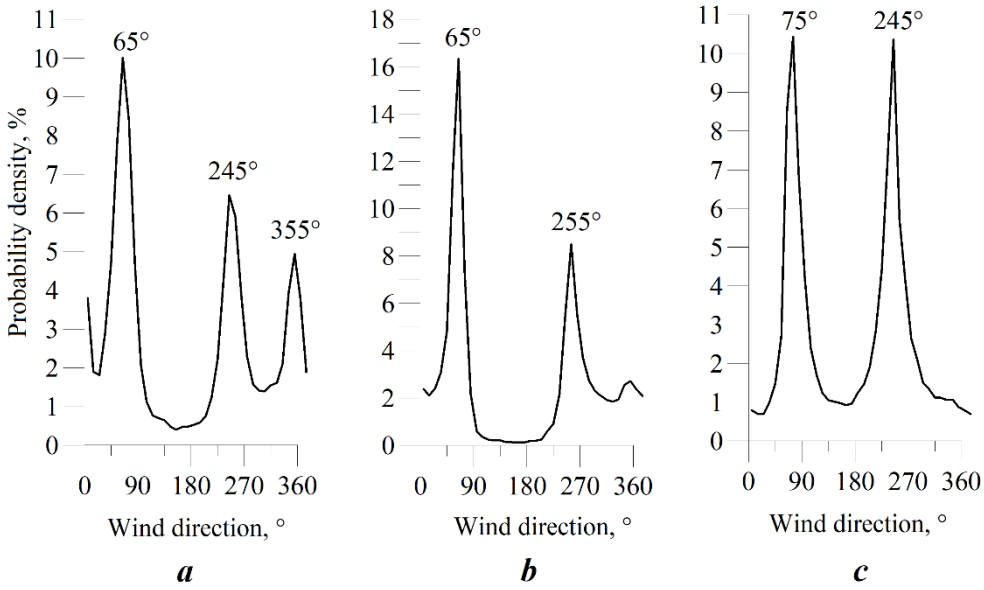

Fig. 3. Empirical probability density distribution function for wind directions in the atmosphere surface layer: *a* – based on the initial data; *b* – after removing the contribution of inertia-gravity and daily wind variability from the initial data; *c* – after removing the contribution of inertia-gravity, daily and large-scale background wind variability from the initial data

Data from the surface horizon of 5 m only were used to compare the statistical and spectral characteristics of wind variability in the atmosphere surface layer and corresponding variability of the coastal current in the upper active layer of the sea. Two separate sets of mean-hourly data were generated for May–October (half-year I) and November–April (half-year II) to calculate the characteristics of both wind and current for 2013–2022. It should be noted that chronological data sets for the indicated half-years are also used when numerically modelling the Crimean region wind regime, its seasonal variability and breeze circulation peculiarities [10, 11].

Interseasonal peculiarities of large-scale wind and current variability. Figure 4 shows full energy spectra of variability of winds in the atmosphere surface layer (Fig. 4, *a*) and currents in the sea surface layer (Fig. 4, *b*) calculated for half-years I and II in the range of periods 3–128 days. In Fig. 4, *a*, spectral peaks of wind fluctuations were reliably identified at periods of 5–6 days, 8, 13 and 21 days in half-years I, and in half-years II, a peak was reliably identified at a period of 4 days and intensification of synoptic wind fluctuations was noted in the range of periods of 8–21 days compared to spectrum calculated for half-years I. In Fig. 4, *b*, spectral peaks

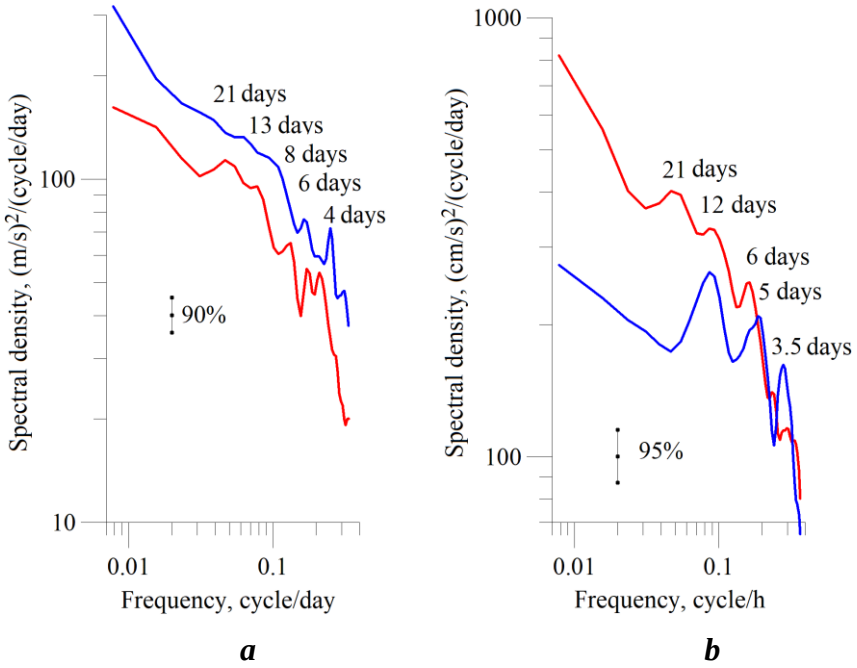

Fig. 4. Full energy spectra of long-wave fluctuations in the range of periods 3–128 days: *a* – winds in the atmosphere surface layer; *b* – currents in the sea surface layer, calculated for the half-year periods May–October and November–April 2013–2022 (red and blue lines, respectively)

of long-wave current fluctuations were reliably identified at periods of ~3.5, 6, 12 and 21 days calculated for half-years I and at periods of ~3.5, 5 and 12 days for half-years II. These long-wave movements propagate along with the alongshore current leaving the coast on the right-hand side.

Research of interseasonal differences in the spectral composition of long-wave fluctuations in the coastal current is possible as part of *in situ* and numerical model studies of long-wave motions including coastal trapped waves [5]. Work [4] presents review of the results obtained earlier in studies of long-wave movements near the SCC which determine trapping and accumulation of wave energy, meandering of currents and formation of mesoscale eddy structures.

Coastal trapped waves are known to be mainly generated by alongshore wind stress fluctuations. According to Fig. 4, *c*, such wind fluctuations are reliably present near the SCC, and the spatiotemporal characteristics of coastal trapped waves

[5] Ivanov, V.A. and Yankovsky, A.E., 1992. [*Long-Wave Motions in the Black Sea*]. Kyiv: Naukova Dumka, 110 p. (in Russian).

are determined by the scale of forcing atmosphere influences in the region [13]. Long-wave current fluctuations with a period of about 6 days in summer are caused by the Black Sea surge circulation with a periodicity of 5–7 days, and fluctuations with a period of about 12 days were previously identified as long coastal trapped waves and generated by remote wind action [13]. Energy spectra in the mesoscale and synoptic range of variability calculated from synchronous cur-rent and wind data have similar spectral ranges of the intensification of fluctuations. Detailed studies of cause-and-effect statistical relationships among the characteristics of these long-wave fluctuations are planned to be carried out in the future.

Interseasonal peculiarities of inertia-gravity and daily variability of wind and current. Figure 5 shows full energy spectra of inertia-gravity and daily fluctuations of winds in the atmosphere surface layer (Fig. 5, *a*) and currents in the sea surface layer (Fig. 5, *b*) calculated for half-years I and II in the range of periods 6–96 h. In Fig. 5, *a*, energy maxima were reliably identified for a pair of spectra of wind

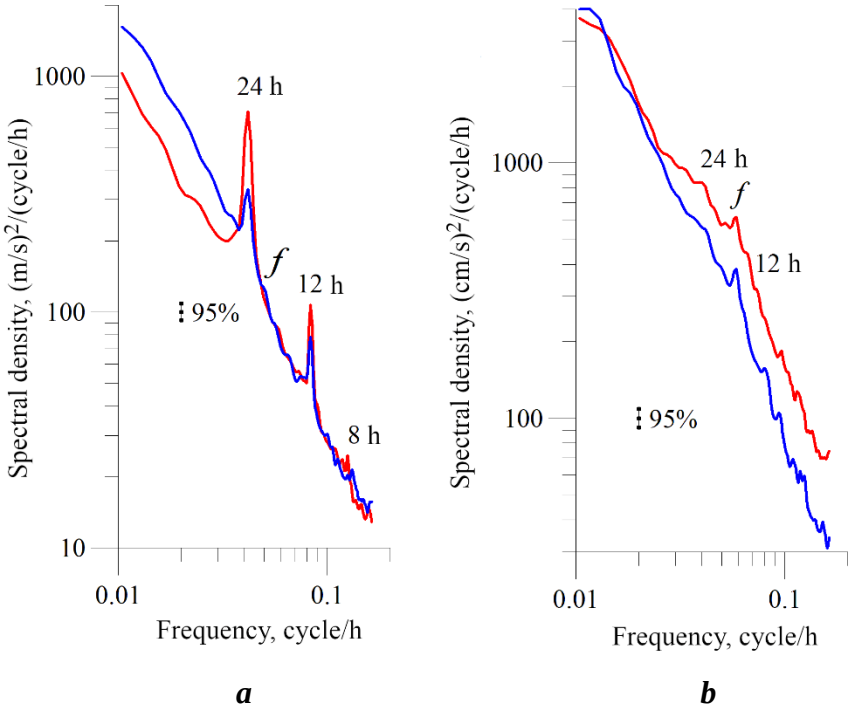

Fig. 5. Full energy spectra of inertia-gravity and daily fluctuations in the range of periods 3–128 days: *a* – winds in the atmosphere surface layer; *b* – currents in the sea surface layer calculated for the half-year periods May–October and November–April 2013–2022 (red and blue lines, respectively)

fluctuations at periods of 12 and 24 h, as well as fluctuations at local inertial frequency *f* and at a period of 8 h. In Fig. 5, *b*, spectral peaks are reliably identified for a pair of spectra of coastal current fluctuations at local inertial frequency *f*.

In order to assess significance and reliability of the identified spectral maxima of fluctuations of both wind and current in the prescribed manner [4], corresponding 95% confidence intervals were calculated for an actual number of degrees of freedom of ~ 1600. This allowed evaluation of differences when comparing the spec-tral levels of the formed pairs of spectra with high accuracy.

In Fig. 5, *a*, the mean long-term amplitudes of wind fluctuations in the range of periods of 36–96 h for half-years II exceed the amplitude of corresponding fluctuations for half-years I by ~ 40%. Further along the spectrum, type and compared levels of wind spectra in the range of fluctuations of 6–26.5 h coincide while differing in the values of the levels of spectral maxima at periods of 12 and 24 h. According to the results obtained previously *in situ* [6, 7] and in model [10, 11] experiments, breeze circulation strengthens from May to October causing significant interseasonal differences in the fluctuation intensity for periods of 12 and 24 h (Fig. 5, *a*).

Figure 5, *b* shows the distribution of the current energy spectral density in the surface layer of the sea for half-years I and II with no energy differences in the spectral levels in the range of fluctuations of 36–96 h. Further along the spectrum in the range of fluctuations of 6–36 h, these differences exceed the limits of 95% confidence interval. The mean long-term amplitudes of current fluctuations in the range of periods of 6–36 h for half-years I exceed the amplitudes of fluctuations for half-years II by ~ 25%. Such differences in the inertia-gravity and daily range of current fluctuations occur from May to October in the upper active layer of the Black Sea under conditions of stable thermal (density) stratification of waters [14]. As is known, a field of intense short-period internal waves is formed in the active layer during this period of the year, thus providing energy sink of the current long-wave fluctuations on the Black Sea shelf. *In situ* studies of the dynamics of inertia-gravity and short-period internal waves on the shelf in the Black Sea upper active layer are constantly being improved and new scientific results of such studies are given in [15–17].

It should be noted that the coastal waters off the SCC including the continental shelf with bays and harbours are the marginal part of the Black Sea shelf zone connected to the land. Currently, some researchers believe that the only statistically reliable characteristic of the water circulation regime near the coast is the bimodal distribution of current direction frequency. However, according to the MHI *in situ* results [4], a monomodal alongshore current directed in the same way as the Rim Current was reliably identified near Cape Kikineiz. At the same time, work [5] reveals that the dominant contribution (~ 80%) is made by fluctuations in the inertia-

gravity and daily range, whereas 20% of the contribution is distributed in the mesoscale range of current fluctuations with periods up to 4–5 days during the formation of the reverse mode of current direction bimodal distribution near the SCC.

As is known, inertial fluctuations take place in the Black Sea with acting force changes and represent a circular or elliptical anticyclonic rotation of the current speed vector which is radically transformed near the coast. Inertial currents near the coast (quasi-reversible water circulation) are observed near the SCC, usually after the cessation of the long-term alongshore wind, when the inertial current vector rotates clockwise for periods of about 17 h at a spatial scale of the anticyclonic eddy of less than ten kilometers [7]. According to the 2013–2022 monitoring studies, inertial fluctuations of currents near Cape Kikineiz arise regularly and exist in the form of periodic packets, and it is noted in [7] that the duration of a series of such inertial anticyclonic eddies is typically 3–4 days.

The presented results of the 2013–2022 comprehensive studies of the wind field variability for the atmosphere surface layer and the coastal current are the basis for further research of the formation of the bimodal distribution of alongshore current directions in the inertia-gravity and mesoscale range of wave-eddy fluctuations for periods of 4–5 days.

Conclusion

The peculiarities of the interseasonal variability of the alongshore circulation of coastal waters and wind off the Southern Coast of Crimea were revealed as a result of processing and analysis of materials from long-term *in situ* studies carried out by MHI of RAS at the BSHSTA. The unique opportunity to conduct a long-term (2013–2022) comprehensive *in situ* experiment in the waters of the coastal ecotone near the SCC was ensured by the reliable operation of clusters of domestic oceanological and hydrometeorological meters from the stationary oceanographic platform of the BSHSTA of MHI under open sea conditions.

Comprehensive studies were carried out using verified information technology for instrumental monitoring which ensures high accuracy in long-term instrumental measurements. The results of statistical and spectral analysis were obtained by processing arrays of synchronous databases of variability in the characteristics of coastal current and wind.

1. Intense wind field variability in the atmosphere surface layer is established throughout the entire annual cycle in the range of periods of 12 and 24 h, 4–6 days and 13–21 days with the dominance of alongshore fluctuations of the local wind direction. Therein, regular mesoscale wind fluctuations can be a source of generation of trains of intense short-period internal waves off the coast.

2. Full energy spectra of current and wind fluctuations have close spectral ranges of intensification of fluctuations in the mesoscale and synoptic ranges of variability.

Further identification of statistical cause-and-effect relationships between the characteristics of current and wind fluctuations is a promising task for the physical understanding of their interaction.

3. Synoptic fluctuations of the coastal current at periods of ~12 days have significant interseasonal differences in the upper layer of the sea to depths of 15 m. Further *in situ* and numerical model studies of long-wave motions will reveal the reasons for such differences. Current regional numerical models of coastal water areas can be validated and improved based on representative empirical results.

4. Inertia-gravity fluctuations of the coastal current in the range of periods of 6–36 h have significant interseasonal differences. Therein, further research should also be carried out in the range of short-period gravity internal waves. This allows detailed studying their contribution to the formation of the bimodal distribution of alongshore water circulation directions. Moreover, it is necessary to continue research into the peculiarities of the energy wave-eddy interaction of inertia-gravity and mesoscale disturbances of the alongshore coastal current.

The presented results form the basis for further studies of the multiscale variability of coastal water circulation near the SCC as a significant natural factor influencing the sustainable social and economic development of the Crimean coastal region, and this remains one of the priority tasks of Marine Hydrophysical Institute of RAS.

References

1. Timchenko, I.E. and Igumnova, E.M., 2011. Control over the Ecological-Economic Processes in the Integral Model of the Coastal Zone of the Sea. *Physical Oceanography*, 21(1), pp. 45–62. https://doi.org/10.1007/s11110-011-9103-9
2. Kuznetsov, A.S. and Zima, V.V., 2019. Development of Observing System of the Black Sea Hydrophysical Polygon in 2001–2015. *Ecological Safety of Coastal and Shelf Zones of Sea*, (4), pp. 62–72. https://doi.org/10.22449/2413-5577-2019-4-62-72
3. Toloknov, Yu.N., Garmashov, A.V., Korovushkin, A.I. and Polonsky, A.B., 2014. [Equipment for Monitoring Hydrometeorological Parameters on the Oceanographic Platform at Katsiveli]. In: V. A. Ivanov and V. A. Dulov, 2014. *Monitoring of the Coastal Zone in the Black Sea Experimental Sub-Satellite Testing Area*. Sevastopol: ECOSI-Gidrofizika, pp. 150–153 (in Russian).
4. Kuznetsov, A.S., 2022. Mean Long-Term Seasonal Variability of the Coastal Current at the Crimea Southern Coast in 2002–2020. *Physical Oceanography*, 29(2), pp. 139–151. https://doi.org/10.22449/1573-160X-2022-2-139-151
5. Kuznetsov, A.S. and Ivashchenko, I.K., 2023. Features of Forming the Alongcoastal Circulation of the Coastal Ecotone Waters nearby the Southern Coast of Crimea. *Physical Oceanography*, 30(2), pp. 171–185. https://doi.org/10.29039/1573-160X-2023-2-171-185
6. Kuznetsov, A.S., 2023. Spectral Characteristics of Wind Variability in the Coastal Zone of the South Coast of Crimea 1997–2006. *Ecological Safety of Coastal and Shelf Zones of Sea*, (2), pp. 6–20. https://doi.org/10.22449/2413-5577-2022-2-6-20

7. Koveshnikov, L.A., Ivanov, V.A., Boguslavsky, L.G., Kazakov, S.I. and Kaminsky, S.T., 2001. Problems of Heat and Dynamics Interaction in a Sea–Atmosphere–Land System of the Black Sea Region. In: MHI, 2001. *Ekologicheskaya Bezopasnost' Pribrezhnoy i Shel'fovoy Zon i Kompleksnoe Ispol'zovanie Resursov Shel'fa* [Ecological Safety of Coastal and Shelf Zones and Comprehensive Use of Shelf Resources]. Sevastopol: ECOSI-Gidrofizika. Iss. 3, pp. 9–52 (in Russian).
8. Ivanov, V.A., Kuznetsov, A.S. and Morozov, A.N., 2019. Monitoring Coastal Water Circulation along the South Coast of Crimea. *Doklady Earth Sciences*, 485(2), pp. 405–408. https://doi.org/10.1134/S1028334X19040044
9. Efimov, V.V., Shokurov, M.V. and Barabanov, V.S., 2002. Physical Mechanisms of Wind Circulation Forcing over the Inland Seas. *Izvestiya, Atmospheric and Oceanic Physics*, 38(2), pp. 217–227.
10. Efimov, V.V., Barabanov, V.S. and Iarovaya, D.A., 2014. [Mesoscale Processes in the Atmosphere of the Black Sea Region]. In: Ivanov, V.A. and Dulov, V.A., 2014. *Monitoring of the Coastal Zone in the Black Sea Experimental Sub-Satellite Testing Area*. Sevastopol: ECOSI-Gidrofizika, pp. 250–271 (in Russian).
11. Efimov, V.V., 2017. Numerical Simulation of Breeze Circulation over the Crimean Peninsula. *Izvestiya, Atmospheric and Oceanic Physics*, 53(1), pp. 84–94. https://doi.org/10.1134/S0001433817010042
12. Efimov, V.V. and Komarovskaya, O.I., 2019. Disturbances in the Wind Speed Fields due to the Crimean Mountains. *Physical Oceanography*, 26(2), pp. 123–134. https://doi.org/10.22449/1573-160X-2019-2-123-134
13. Ivanov, V.A. and Yankovsky, A.E., 1994. Dynamics of the Crimea shelf waters in summer. *Physical Oceanography*, 6(3), pp. 201–217. https://doi.org/10.1007/BF02197518
14. Ivanov, V.A. and Belokopytov, V.N., 2013. *Oceanography of Black Sea*. Sevastopol: ECOSI-Gidrofizika, 210 p.
15. Bondur, V.G., Sabinin, K.D. and Grebenyuk, Yu.V., 2017. Characteristics of Inertial Oscillations According to the Experimental Measurements of Currents on the Russian Shelf of the Black Sea. *Izvestiya, Atmospheric and Oceanic Physics*, 53(1), pp. 120–126. https://doi.org/10.1134/S0001433816050030
16. Khimchenko, E.E. and Serebryany, A.N., 2018. Internal Waves on the Caucasian and Crimean Shelves of the Black Sea (According to Summer-Autumn Observations 2011–2016). *Journal of Oceanological Research*, 46(2), pp. 69–87. https://doi.org/10.29006/1564-2291.JOR-2018.46(2).7 (in Russian).
17. Serebryany, A., Khimchenko, E., Popov, O., Denisov, D. and Kenigsberg, G., 2020. Internal Waves Study on a Narrow Steep Shelf of the Black Sea Using the Spatial Antenna of Line Temperature Sensors. *Journal of Marine Science and Engineering*, 8(11), 833. https://doi.org/10.3390/jmse8110833

Submitted 01.11.2023; accepted after review 10.12.2023;
revised 27.12.2023 ; published 25.03.2024

About the author:

Alexander S. Kuznetsov, Leading Research Associate, Head of the Shelf Hydrophysics Department, Marine Hydrophysical Institute of RAS (2 Kapitanskaya St., Sevastopol, 299011, Russian Federation), Ph.D. (Tech.), **ORCID ID: 0000-0002-5690-5349; Scopus Author ID: 57198997777**, *kuznetsov_as@mhi-ras.ru*

The author has read and approved the final manuscript.

Original article

Lithodynamics of the Coastal Zone in the Inkit-Pitsunda Area (Abkhazia)

G. V. Tlyavlina *, V. A. Petrov, R. M. Tlyavlin

Research center "Sea coasts" (Branch of JSC TsNIITS), Sochi, Russia
** e-mail: TlyavlinaGV @Tsniis.com*

Abstract
The paper studies lithodynamic processes in the Black Sea coastal zone from Cape Inkit to Cape Pitsunda in the Republic of Abkhazia. A review of past studies of the coastal lithodynamics in this area was carried out. The principles of allocation of lithodynamic areas were shown and the characteristics of the transverse and longitudinal structures of coastal systems were described. A scheme of lithodynamic zoning of the studied area has been developed. The paper describes sources of sediments intake and their movement in the studied coastal zone of the Inkit-Pitsunda area of Abkhazia and provides characteristics of the longshore sediment flow in the area. The coastline dynamics on a fragment of the Bzyb-Pitsunda coast was investigated. The paper estimates the volume of sediments carried out by the Bzyb River and compares it with the value of the total longshore flow of pebble sediments in the area. The coastline dynamics based on research materials of previous years was analysed, the aerial photographs taken into account. The paper also estimates sediment runoff into the tops of underwater erosion hollows (canyons) located on the underwater coastal slope from the Bzyb River to Cape Pitsunda. The paper shows that although the width of pebble beaches may reach fifty meters, in the upper part of the coastal zone, the ancient barrier beach and low terrace, which are composed of highly erodible sediments, are exposed to washouts. These washouts are caused by large waves during passing storms, and their run-up is not completely damped on the surface of even such wide beaches. The authors conclude that the existing beach is not wide enough to completely damp storm waves, as evidenced by the washouts of ancient barrier beaches. In addition, the erosion of the ancient barrier beach bases is due to the general retreat of the coastline within the sea terrace located between the mouth of the Bzyb River and Cape Pitsunda.

Keywords: abrasion, alluvial deposits, lithodynamics, lithodynamic zoning, beach, underwater canyons, sediment flow, coastal zone, accumulative terraces

For citation: Tlyavlina, G.V., Petrov, V.A. and Tlyavlin, R.M., 2024. Lithodynamics of the Coastal Zone in the Inkit-Pitsunda Area (Abkhazia). *Ecological Safety of Coastal and Shelf Zones of Sea*, (1), pp. 45–56.

Литодинамика береговой зоны Инкит-Пицундского района Абхазии

Г. В. Тлявлина *, В. А. Петров, Р. М. Тлявлин

Научно-исследовательский центр «Морские берега» (ОП АО ЦНИИТС), Сочи, Россия

* *e-mail: TlyavlinaGV@Tsniis.com*

Аннотация

Исследованы литодинамические процессы в береговой зоне Черного моря на участке от м. Инкит до м. Пицунда в Республике Абхазия. Выполнен обзор исследований литодинамики данного участка берега прошлых лет. Показаны принципы выделения литодинамических районов. Описаны характеристики поперечной и продольной структур береговых систем. Разработана схема литодинамического районирования исследуемого участка. Описаны источники поступления наносов и их движение в береговой зоне исследуемого участка Инкит-Пицундского района Абхазии. Даны характеристики вдольберегового потока наносов на участке. Исследована динамика береговой линии на фрагменте берега Бзыбь – Пицунда. Выполнена оценка объема наносов, выносимых р. Бзыбью, и его сравнение с величиной общего вдольберегового потока галечных наносов на участке. Проанализирована динамика береговой линии по материалам исследований прошлых лет с учетом аэрофотосъемок. Оценен сток наносов в вершины подводных эрозионных ложбин (каньонов), расположенных на подводном береговом склоне от р. Бзыби до м. Пицунда. Показано, что, хотя ширина галечных пляжей может достигать 50 м, в верхней части береговой зоны наблюдаются подмывы древнего берегового вала и низкой террасы, сложенных легко размываемыми отложениями. Эти подмывы обусловлены воздействием больших волн во время шторма, накат которых не гасится полностью на надводной части даже таких широких пляжей. Сделан вывод о том, что ширина существующего пляжа недостаточна для полного гашения штормовых волн, о чем свидетельствуют подмывы древних береговых валов. Кроме того, такие подмывы обусловлены общим отступанием береговой линии в пределах морской террасы, расположенной между устьем р. Бзыби и м. Пицунда.

Ключевые слова: абразия, аллювиальные отложения, литодинамика, литодинамическое районирование, пляж, подводные каньоны, поток наносов, прибрежная зона, аккумулятивные террасы

Для цитирования: *Тлявлина Г. В., Петров В. А., Тлявлин Р. М.* Литодинамика береговой зоны Инкит-Пицундского района Абхазии // Экологическая безопасность прибрежной и шельфовой зон моря. 2024. № 1. С. 45–56. EDN GGICDK.

Introduction

The investigated section of the shore is located on the southwestern flank of the Pitsunda Peninsula between Capes Inkit and Pitsunda. The adjacent section of the bottom between the mouth of the Bzyb River and Cape Pitsunda is complicated by an extensive system of underwater canyons, the tops of which come close to the shore. The largest of them is the Akula Canyon [1], which opens to Cape Inkit (Fig. 1). Erosion hollows on the underwater slope complicate coastal processes.

A reliable estimate of the natural processes occurring in the coastal zone of the sea and their direction is of very important scientific and practical importance. Thus, the reliability and effectiveness of coast protecting structures against wave

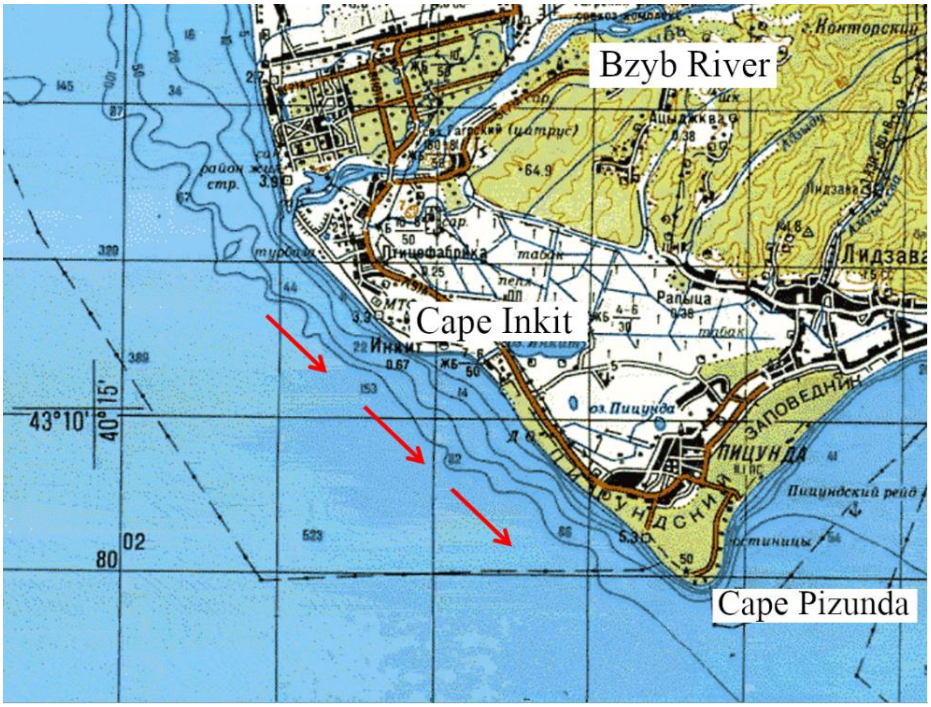

F i g . 1 . The investigated shore. The arrows show the direction of the longshore sediment flow (adapted from https://satmaps.info/map.php?s=100k&map=k-37-033)

action depend largely on the knowledge and correct estimate of the lithodynamics and morphology of the section [2, 3]. Moreover, only long-term observations of the shore state can reveal the influence of various factors.

No comprehensive studies of coastal processes in order to estimate their direction have been carried out on the shore section between the mouth of the Bzyb River and Cape Pitsunda from the end of the last century to the present. The dynamics of the pebble beach was also not observed. After the Abkhazia conflict (1992–1993), only some researchers of the Academy of Sciences of Abkhazia with limited participation of the Russian scientists have carried out special coastal studies [4]. All this makes it difficult to estimate objectively the coastal processes currently occurring in the section under consideration and the direction of their development.

Based on the analysis of available data on the state of the coastal zone between the mouth of the Bzyb River and Cape Pitsunda and the processes occurring in this zone, as well as the influence of the anthropogenic factor on them, the degree of knowledge of these processes at the present stage can be characterized as insufficient.

The study aims at the estimate of the geomorphological conditions of the coastal zone between Capes Inkit and Pitsunda and identification of the direction of lithodynamic processes.

Materials and methods of study

The study used materials from field work carried out by the authors in the summer of 2023 (bathymetric and topographic surveys, investigation of the coastal zone), as well as data obtained from an analysis of ongoing coastal processes, taking into account the supply of beach-forming material from rivers and the coastline configuration [5].

Results and discussion

A lithodynamic system is a set of characteristic natural and anthropogenic factors that determine the interconnected coastal processes occurring on the coastal section under consideration independently of neighbouring sections and state the stability of the system itself.

The coastal lithodynamic system is characterized by transverse and longitudinal structures. The transverse structure includes data on the formation of the transverse profile of a pebble beach under the influence of waves and its longshore changes. As for the pebble beaches, the coastal lithodynamic system on the sea side is limited by the place where pebble material is pulled back during a storm, which corresponds to the depth of the last wave breaking [5]. The top of the wave run-up is the upper limit on the shore. Consequently, the width of the coastal lithodynamic system is equal to the run-up length of the maximum possible (calculated) storm in terms of the cross section. Transverse drifting of pebble material with its differentiation and formation of a beach profile occur within this designated zone. Surface waves (wind and swell ones) and various currents excited by them, which play a crucial role in the sediment drifting and transformation of the coastal zone topography, are the main factor determining the pebble beach profile formation and the underwater slope topography. Sea depth is one of the main characteristics that determines wave propagation direction and velocity and, as a consequence, shore and bottom deformation. The influence of the bottom topography on wave heights and angles of their approach to the shore begins to manifest itself from the depths equal to half the wavelength.

The longitudinal longshore structure of the lithodynamic system is primarily characterized by the volumes of drifted material and their changes in different sections of the shore, as well as changes in the transverse structure caused by the configuration of the coastline, supply of beach-forming material from watercourses and abrasion processes, changes in depths, etc.

The main lithodynamic characteristics, information about which is obtained during the study, are the direction of movement and volumes of sediment drifting under the influence of hydrogenic factors, as well as subsequent transformations of the topography of the beach and adjacent underwater slope. Therefore, the most complete estimate of the processes occurring in the coastal zone can be obtained by studying the longshore and transverse structures of the sediment flow as an integral factor determining its state. The boundaries of the lithodynamic system along the shore

determine the beginning and end of the sediment flow, and the transverse structure of the sediment flow determines the depth of the sea to which it is necessary to analyze the lithodynamic processes occurring in the coastal zone. Thus, the lithodynamic system is primarily identified by the longshore sediment flow determined by the influence of waves on the beach-forming material entering the coastal zone. The longshore sediment flow is resulting material drifting influenced by the entire spectrum of waves over a long period (usually a year) or, more precisely, of the longshore projection of the wave energy resultant, which is distributed very unevenly along the shore and the magnitude of which depends on the exposure of a particular section of the shore. Beach material can move along the coast in opposite directions under the influence of waves of different directions.

A fragment of the shore between the mouth of the Bzyb River and Cape Pitsunda adjoin the younger near shore part (the age of which does not exceed 2.0–2.5 thousand years) of the accumulative plain of the Pitsunda Peninsula, which is part of the all1uvial-marine terrace formed over the last 11–12 thousand years. The coastal plain is composed of highly erodible sediments 90–100 m thick. The sediments are represented by separate layers of silty clays and sands, reaching a thickness of 6–18 m, which are covered by peat bogs up to 4–5 m thick. In the north, the Pitsunda Lowland adjoins the southern slopes of the Myusser Upland. The western border of the lowland runs along the left bank of the Bzyb River lower course [6], and the southern border is limited by the sea coastline. Low elevations of the lowland surface contributed to the formation of relict lakes, the largest of which is Lake Inkit.

The investigated shore section located between Capes Inkit and Pitsunda includes three morphologically different shore fragments. Inkit Bay is located on the northern flank, smoothly turning into a relatively straight central shore fragment, giving way to a bay-shaped shore stretching to Cape Pitsunda on the eastern flank. The straightness of the middle section of the shore composed of highly erodible sediments with their azimuth of 140° is explained by its turn parallel to the front of the resultant of the waves.

As studies [1), 2)] [1] showed, due to the peculiarities of the hydrodynamic regime of the sea within the shore section from Cape Kodosh, a natural barrier to sediment drifting located north-west of the city of Tuapse, and to Cape Pitsunda for 160 km earlier (before the construction of various hydraulic structures, such as enclosing breakwaters of the ports of Tuapse, Sochi, Imereti) a single longshore sediment flow was expressed. This fact makes it possible to distinguish this shore fragment into a single Kodosh-Pitsunda lithodynamic system.

[1)] Zenkovich, V.P., 1958. [*Coasts of the Black and Azov Seas*]. Moscow: Gosudarstvennoe izdatelstvo geograficheskoy literatury, 374 p. (in Russian).

[2)] Zenkovich, V.P., 1958. [*Morphology and Dynamics of the Soviet Coasts of the Black Sea*]. Moscow: Izdatelstvo AN SSSR. Vol. 1, 187 p. (in Russian).

The beach strip on the coast of the Krasnodar Krai and Abkhazia from Cape Kodosh to Cape Pitsunda is composed of sand and pebbles. The main source of nutrition for the pebble beaches of the region under consideration is predominantly coarse material supplied by rivers [3] [7]. A small part of the fragmentary material, which is not of decisive importance, comes from abrasion of the beach scarp and physical weathering of its constituent rocks and also as a result of bedrock abrasion.

In the structure of the longshore sediment flow, three components are distinguished, each of which is characterized by the dominance of certain development processes [4]. The first part is the zone of sediment flow origin, within which abrasion and erosion predominate. The second part is the transit area of the longshore sediment flow, where abrasion and erosion alternate with the deposition of beach material. The third part is the discharge area, where the accumulation of material drifted under the influence of waves occurs.

Under natural conditions, in the longshore sediment flow from Cape Kodosh to Cape Pitsunda, no classical division into zones of its origin, transit and discharge (accumulation) took place. The processes of sediment accumulation and drifting in the coastal zone of the considered shore fragment were associated with solid river runoff, its redistribution under the influence of wave and surf flows and currents generated by these flows. Surge phenomena and wind (drift) currents play a subordinate role in the distribution of beach pebble material.

No single source of beach material entering the coastal zone was observed in the identified natural Kodosh-Pitsunda lithodynamic system. Throughout the entire system, there was a constant replenishment of beach material from a single longshore sediment flow due to the solid runoff of large and small rivers, as well as streams and temporary watercourses. Under complex orographic conditions in the presence of numerous temporary watercourses, small streams and relatively large rivers (Ashe, Psezuapse, Shakhe, Sochi, Mzymta, Bzyb), the zones of origin, replenishment and transit of the longshore sediment flow merged into a single zone, i.e. the zone of sediment flow saturation [5].

Without taking into account anthropogenic intervention, the discharge zones of longshore sediment flow (accumulation of beach material) are adjacent to the northwestern flanks of the cuspate forelands of the Ashe, Psezuapse, Sochi, Mzymta and Bzyb Rivers. Areas of accumulation of beach material can also be observed near such capes as, e.g., Uch-Dere, Vidny, Pitsunda.

The magnitude of the longshore flow of pebble sediments can vary within the identified lithodynamic system depending on the supply of beach material to the coastal zone and changes in the drifting ability of waves determined by the relationship between their direction and coastline contour. No classical division of the lithodynamic system into zones of origin of longshore sediment flow and its transit is observed on the coastal section (Cape Kodosh – Cape Pitsunda).

---

[3] Makarov, K.N., Tlyavlina, G.V. and Tlyavlin, R.M., 2019. [*Scientific and Methodological Rationale for the Master Layout of Coastal Protection of the Sochi Agglomeration Morskoy Fasad*]. Sochi: Sochinsky Gosudarstvenny Universitet, 213 p. (in Russian).

[4] Safyanov, G.A., 1996. *Coastal Geomorphology*. Moscow: MGU, 400 p. (in Russian).

As the flow moved in the southeast direction, its magnitude changed constantly as a result of the replenishment of the flow with beach-forming pebble material due to solid river runoff.

The entry of beach-forming pebble material into the coastal zone caused by solid river runoff and determining the change in the magnitude of the longshore flow of pebble sediments can be taken as the basis for the division of a single lithodynamic system into subsystems. Based on this, the boundaries of lithodynamic subsystems can be the mouths of rivers that are most significant in terms of solid runoff. The factors listed above provide the basis for identifying lithodynamic subsystems in a single lithodynamic system [5]. From Cape Kodosh to Cape Pitsunda, taking into account the main sources of material supply (large rivers of the region under consideration, such as the Ashe, the Psezuapse, the Shakhe, the Sochi, the Mzymta, the Bzyb), several lithodynamic subsystems can be distinguished, which are integral parts of the single Kodosh-Pitsunda lithodynamic system. They are Ashe-Tuapse, Ashe-Psezuapse, Shakhe-Psezuapse, Shakhe-Sochi, Sochi-Mzymta, Psou-Mzymta, Psou-Bzyb and Bzyb-Pitsunda ones. The common feature of these lithodynamic subsystems was a longshore sediment flow directed from northwest to southeast (from Tuapse towards Cape Pitsunda). The sediment flow does not bypass Cape Kodosh, but passes through the mouths of the above rivers and bypasses such capes as Uch-Dere, Vidny and some others. Final discharge of the longshore flow of pebble sediments, which, being deposited on the beach and underwater slope, contributed to the general extension of the cape towards the sea, took place at Cape Pitsunda [8]. Therefore, the lithodynamic subsystems under consideration were previously open (before the construction of the enclosing breakwaters of the ports of Sochi and Imereti). The erected breakwaters of the ports of Sochi (1936) and Imereti (2008) interrupted the single longshore flow of pebble sediments, as a result of which the Sochi-Mzymta and Psou-Mzymta lithodynamic subsystems became separate.

Based on the proposed principle of identifying lithodynamic subsystems which is based on the longshore sediment flow replenished from a significant source of beach-forming material (large rivers of the region under study), the shore section under consideration is included in the Bzyb-Pitsunda lithodynamic subsystem. Similar to this is the idea of identifying six independent shore dynamic systems, including the Bzyb one, in the coastal zone in the area between the mouths of the Psou and Inguri rivers according to the criterion of the presence of separate longshore sediment flows formed by river sediments [9].

Such identified large structural cells as the lithodynamic system and its subsystems include extended shore sections determining general direction of the coastal processes occurring there. When choosing engineering solutions for coast protecting structures, it is necessary to identify smaller lithodynamic structures within which detailed lithodynamic studies should be carried out for a detailed accounting of coastal processes occurring on the shore section under consideration.

Based on the influence of the coastline configuration (Cape Inkit extending into the sea) on the longshore sediment flow, the Bzyb-Inkit and Inkit-Pitsunda lithodynamic areas can be distinguished in the identified Bzyb-Pitsunda lithodynamic subsystem. Taking into account the configuration of the coastline, three lithodynamic sections can be distinguished within the Inkit-Pitsunda lithodynamic area (Fig. 2):

1) western section, located within Inkit Bay,

2) central section, representing a flat fragment of the shore,

3) eastern section, bay-shaped, ending with Cape Pitsunda.

The division of a single lithodynamic system into parts is stipulated by the need for more detailed lithodynamic studies, e. g., to justify coast protecting measures.

In this regard, it is necessary to consider, on the one hand, the possible influence of anthropogenic intervention on them and, on the other hand, their influence on the constructed coast protecting structures for a reliable estimate of modern processes occurring in the coastal zone. In addition, it is necessary to forecast possible state of the beaches and longshore sediment flow of the Bzyb-Inkit lithodynamic area located upstream of the flow, i.e., starting from the mouth of the Bzyb River.

The shore section under consideration is located within the Inkit-Pitsunda lithodynamic area, which is part of the Bzyb-Pitsunda lithodynamic subsystem. The dynamics of the beaches of this lithodynamic subsystem is primarily determined by the longshore sediment flow directed towards Cape Pitsunda. The main volume of sediment entering the coastal zone and, under the influence of waves, forming the longshore flow, which determines the condition of the beaches on the shore section under consideration, comes from the Bzyb River. Of this volume, the share of

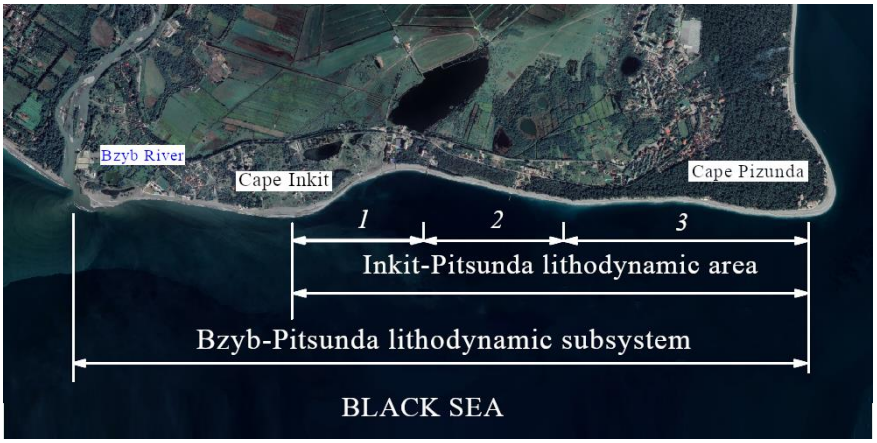

F i g . 2 . Scheme of lithodynamic zoning of the studied area. Google Earth image (available at https://www.google.com/intl/ru/earth/)

suspended sediments accounts for [5] 715 thousand tons, and the runoff of bed load amounts to 205 thousand tons. According to expeditions of Tbilisi University carried out from 1972 to 1978, in the runoff of bed load of the Bzyb River, the proportion of particles with a diameter of more than 50 mm is 26% of the total weight, with a diameter from 50 to 100 mm – 31%. During spring floods, almost half of bed load carried by the river accounted for particles with a diameter of 20 to 100 mm. The alluvial deposits contained small amounts of sediment with a diameter of more than 200 mm. In a long-term context, the volume of sediment carried out by the Bzyb River exceeds the volume of the longshore flow of pebble sediments, and therefore its mouth is mainly formed under the predominant influence of the river factor [9]. The state of beaches on the shore from the mouth of the Bzyb River to Cape Pitsunda is significantly influenced by the considerable depth of the underwater slope complicated by a system of underwater erosion hollows – canyons. They cause high waves to approach the shore, which change little compared to the open sea waves. Under the influence of disturbances in the western directions, sediments carried out by the Bzyb River are lost in the tops of underwater canyons during their drifting. The most active and closest to the shore is the Akula Canyon located in the area of the Inkit cuspate foreland [1]. The sediment runoff into the top of this canyon can reach 50 thousand m^3 per year, which is more than a half of the longshore sediment flow in the considered shore section [6], according to estimates equal to 80 thousand m^3 per year [1]. Losses of beach sediments in the Akula Canyon are the main reason for the incision of Inkit Bay [1], where coastal retreat is estimated on average at 0.3–0.5 m/year [6]. The area under study near the shore reveals no erosion hollows at the bottom that affect the longshore drifting of beach-forming material and wave conditions.

Dynamics of the coastline in the section from the mouth of the Bzyb River to Cape Pitsunda is subject to cyclic fluctuations causing alternating stages of erosion and accumulation of beaches. The condition of the beaches on the western coast of the Pitsunda Peninsula is influenced by both long-term changes in the wave activity of the sea and changes in the amount of solid runoff of the Bzyb River. Periods of high wave activity usually coincide with a general decrease in solid runoff from rivers. As a result, the western coast of the peninsula begins to erode. Comparison of data on the amount of solid runoff from the Bzyb River shows that an acute sediment deficit or excess is periodically created in its pre-estuary area. When periods of decreased solid flow of the river coincide with a phase of increased wave activity, erosion of the beaches of the Pitsunda western coast is observed, as, e.g., in the early 1960s [10]. The variability of the Bzyb River solid runoff and the wave regime of the sea also affects the flow of sediment into underwater canyons.

Dynamic changes in the contour of the coastline stipulated by different cycles of wave activity and changes over time in the runoff of beach-forming sediments from the Bzyb River are developing against the background of a general retreat of the coastline of the Pitsunda Peninsula southwestern coast. In the long-term plan,

---

[5] Khmaladze, G.N., 1978. [*Sediment Load Discharged by Rivers on the Black Sea Caucasian Coast*]. Leningrad: Gidrometeoizdat, 167 p. (in Russian).

this section of the Cape Pitsunda coast belongs to the area in which abrasion processes in the coastal zone are intensively developing [11]. A comparison of aerial photographs and satellite images indicates that over the past 80 years the shore in the area of Cape Inkit has retreated by 65–70 m [4]. The predicted rate of coastline retreat over the past hundred years was 60–110 m south of Inkit Bay [12].

Although the width of pebble beaches may reach 50 m, in its upper part, the ancient barrier beach and low terrace, which are composed of highly erodible sediments, are exposed to washouts. These washouts are caused by large waves during passing storms, and their run-up is not completely damped on the surface of even such wide beaches.

The washout scarp of the ancient barrier beach composed of sand mixed with gravel and small pebbles is shifting towards the shore. Waves wash the barrier beach and low terrace out which leads to the fall of pine trees (Fig. 3).

The rate of coastline retreat is significantly influenced by the frequency of strong storms, as well as the shore configuration which determines the heterogeneous distribution of wave energy. According to estimates, the rate of retreat of the coastline as a whole between Capes Inkit and Pitsunda has been 0.3–0.4 m/year over the past 20 years.

The topography of the underwater slope is not uniform. To a depth of 10–11 m, on the bottom composed of loose sediments, several erosion hollows can be traced, the tops of which reach depths of 5–5.5 m. The incision depth of these hollows relative to the surrounding surface of the bottom does not exceed 0.6 m. In the area of 5–5.5 m, the relatively flat bottom topography turns into a steeper one, the formation of which is caused by the displacement of large beach-forming material to the zone of final breaking of storm waves.

The underwater part of the beach (up to a depth of 5 m) is complicated by a number of shallow transverse hollows. Apparently, these hollows are formed during storms as channels for sediment flow to depth. Coarse sediments are not drifted seaward of the wave breaking zone, and small sediments are carried to lower horizons along the above-mentioned erosion hollows.

Fig. 3. The washout and fall of pine trees from the north side of the investigated shore section

Conclusion

Based on the performed lithodynamic studies and data analysis, the following results were obtained:

– the main source of beach material entering the shore section under consideration is the Bzyb River runoff;

– under the influence of waves, the beach pebble material drifting in the longshore sediment flow is directed to the southeast towards Cape Pitsunda;

– the shore and bottom of the underwater slope in the shore section under consideration are composed of easily eroded alluvial deposits;

– currently, the coastal zone is represented by a beach 50–55 m wide;

– in its upper part, the beach is composed of sand which changes to pebble and gravel sediment as it moves towards the sea;

– the width of the beach is maintained by the longshore flow drifting from the mouth of the Bzyb River;

– the depth of the existing beach is not sufficient to damp completely storm waves, as evidenced by the erosion of ancient barrier beaches;

– erosion of the bases of ancient barrier beaches is caused by the general retreat of the coastline within the marine terrace located between the mouth of the Bzyb River and Cape Pitsunda.

References

1. Peshkov, V.M., 2005. [*Pebble Beaches of Tideless Seas. Main Issues of Theory and Practice*]. Krasnodar, 444 p. (in Russian).
2. Tlyavlina, G.V., 2022. Laboratory and Field Studies to Ensure the Regulatory Framework Development and the Transport Facilities' Safety in the Wave Effect Conditions. *Russian Journal of Transport Engineering*, 9(4). doi:10.15862/10SATS422 (in Russian).
3. Tlyavlina, G.V., 2023. Methods of Scientific Substantiation of Regulatory Requirements in the Field of Engineering Protection of Transport Structures from Wave Impact. *News KSUAE*, (2), pp. 80–91. doi:10.52409/20731523_2023_2_80 (in Russian).
4. Van, V.G., Eremenko, E.A., Kazhukalo, G.A., Kotenkov, A.V., Kuznetsov, M.A., Smirnova, A.P., Smirnova, V.V., Smirnova, S.V., Avdonina, A.M. [et al.], 2022. [Morphogenetic Types of Abkhazian Coasts and Current Trends in the Development of the Coastal Zone]. In: M. S. Savoskul and N. L. Frolova, eds., 2022. [*Collected Papers of Participants of Winter Student Expeditions*]. Moscow: Izdatel Erkhova I. M., pp. 33–45 (in Russian).
5. Petrov, V.A., 2021. *Wave Dampening Pebble Beaches*. Moscow: Ekon-Inform, 295 p. (in Russian).
6. Dbar, R.S., Zhiba, R.Yu. and Ivlieva, O.V., 2019. Artificial Regulation of the Seaside Hydroecological System of Peninsula Pitsunda. *Geopolitics and Ecogeodynamics of Regions*, 5(1), pp. 206–216 (in Russian).
7. Tlyavlina, G.V. and Tlyavlin, R.M., 2019. Problems of Monitoring of Hazardous Processes of the Imereti Lowlands. In: SSC RAS, 2019. *Regularities of Formation and Impact of Marine and Atmospheric Hazardous Phenomena and Disasters on the Coastal Zone of the Russian Federation under the Conditions of Global Climatic and Industrial Challenges ("Dangerous Phenomena"): Proceedings of the International Scientific Conference (Rostov-on-Don, 13–23 June 2019)*. Rostov-on-Don: SSC RAS Publishers, pp. 300–302 (in Russian).

8. Menshikov, V.L. and Peshkov, V.M., 1981. [On Influence of Pre-Mouth Canyons of the Bzyb River on the Coastal Sediment Budget]. In: V. P. Zenkovich, E. I. Ignatova, and S. A. Lukianova, eds., 1981. [*Coastal Zone of Sea*]. Moscow: Nauka, pp. 101–108 (in Russian).
9. Ekba, Ya.A. and Dbar, R.S., 2009. Features of Dynamics of Coastal Deposits of the Black Sea Coast of Abkhazia. *Izvestiya SFedU. Engineering Sciences*, (6), pp. 71–80 (in Russian).
10. Peshkov, V.M., 2005. [Cyclic Dynamics of Sea Coasts]. *Geologiya i Poleznye Iskopaemye Mirovogo Okeana*, (1), pp. 111–122 (in Russian).
11. Balabanov, I.P., 2009. *Paleogeographical Prerequisites of Formation of the Modern Environments and the Long-term Forecast of the Holocene Terraces Development on the Black Sea Coast of the Caucasus*. Moscow, Vladivostok: Dalnauka, 350 p. (in Russian).
12. Balabanov, I.P. and Nikiforov, S.P., 2016. *Bay of Gagra. Recreational Potential of Natural and Geological Conditions of the Coastal and Marine Area*. Moscow: Izd-vo Avtorskaya Kniga, 288 p. (in Russian).

Submitted 29.07.2023; accepted after review 30.09.2023;
revised 27.12.2023; published 25.03.2024

About the authors:

Galina V. Tlyavlina, Head of the Laboratory of Modeling, Calculations and Rationing in Hydraulic Engineering, Subdivision of JSC TsNIITS "Research Center "Sea Coasts" (1, Iana Fabritsiusa St., Sochi, 354002, Russian Federation), Ph.D. (Tech.), **ORCID ID: 0000-0003-4083-9014**, *TlyavlinaGV@Tsniis.com*

Viktor A. Petrov, Senior Researcher, Subdivision of JSC TsNIITS "Research Center "Sea Coasts" (1, Iana Fabritsiusa St., Sochi, 354002, Russian Federation), Ph.D. (Geogr.), **Scopus Author ID: 7402842652**, *demmi8@mail.ru*

Roman M. Tlyavlin, Head of the Subdivision of JSC TsNIITS "Research Center "Sea Coasts" (1, Iana Fabritsiusa St., Sochi, 354002, Russian Federation), Ph.D. (Tech.), **ORCID ID: 0000-0002-8648-0492**, *TlyavlinRM@Tsniis.com*

Contribution of the authors:

Galina V. Tlyavlina – scientific management of work, formulation and setting of tasks, development of research methods, analysis of the research results

Viktor A. Petrov – review of the literature on the research problem, field survey of the site, processing and description of the research results, formulation of conclusions

Roman M. Tlyavlin – development of the research concept, processing and description of the research results

All the authors have read and approved the final manuscript.

Original article

Sea-Air CO_2 Flux in the Northeastern Part of the Black Sea

N. A. Orekhova *, E. V. Medvedev, I. N. Mukoseev, A. V. Garmashov

Marine Hydrophysical Institute of RAS, Sevastopol, Russia
** e-mail: natalia.orekhova@mhi-ras.ru*

Abstract
Carbon dioxide is one of the green gases and its entry into the atmosphere and further redistribution in the waters of the World Ocean not only plays a significant role in the climate on the Earth, but also affects the characteristics of waters. The research of inland seas, e.g. the Black Sea, makes it possible to study the influence of atmospheric CO_2 on the characteristics of waters and to assess the contribution of regional ecosystems to the total budget of the CO_2 flux of the World Ocean. The paper presents numerical estimates of the sea–air CO_2 flux, analyzes its direction and identifies factors that determine the values of the CO_2 flux in the northeastern part of the Black Sea during a cold period. For the analysis, the data obtained during the cruise of R/V *Professor Vodyanitsky* in December 2022 were used. The values of the sea–air flux of carbon dioxide were calculated taking into account the wind speed and pCO_2 gradient between the sea surface and the near sea surface atmosphere. According to the direct measurements of pCO_2, the value of the CO_2 flux in December 2022 varied widely from –0.05 to –8.74 mmol·m^{-2}·day^{-1}, the average value being –2.11 ± 1.79 mmol·m^{-2}·day^{-1}. It was established that during the cold season, the CO_2 flux was directed from the atmosphere to the sea surface. Thus, the waters of the Crimean coast serve as a stock of atmospheric CO_2. Local minima of flux values were observed in the southeastern regions of the Crimean coast. When analyzing the correlation of the CO2 flux with temperature, wind speed and ΔpCO_2, the strongest relationship was found with wind speed (–0.93), while the weakest one was with ΔpCO_2 (0.22). Therefore, the intensity of the sea–air CO_2 flux was determined by wind speed, while the direction of the flux was determined by ΔpCO_2. The temperature contribution manifested as change in the concentration of CO_2 in the water column.

Keywords: CO_2 flux, Black Sea, carbon dioxide, partial pressure of carbon dioxide, carbon cycle

Acknowledgements: The work was carried out within the framework of grant no. 169-15-2023-002 dated 01.03.2023 of the Federal Service for Hydrometeorology and Environmental Monitoring.

For citation: Orekhova, N.A., Medvedev, E.V., Mukoseev, I.N. and Garmashov, A.V., 2024. Sea-Air CO_2 Flux in the Northeastern Part of the Black Sea. *Ecological Safety of Coastal and Shelf Zones of Sea*, (1), pp. 57–67.

Поток CO_2 на границе с атмосферой в северо-восточной части Черного моря

Н. А. Орехова *, Е. В. Медведев, И. Н. Мукосеев, А. В. Гармашов

Морской гидрофизический институт РАН, Севастополь, Россия
* *e-mail: natalia.orekhova@mhi-ras.ru*

Аннотация
Углекислый газ является одним из климатообразующих веществ, его поступление в атмосферу и дальнейшее перераспределение в водах Мирового океана играют значительную роль в формировании климата на Земле и влияют на характеристики вод. Изучение внутренних морей, таких как Черное море, позволяет исследовать влияние атмосферного CO_2 на характеристики вод и оценить вклад региональных экосистем в общий бюджет CO_2 вод Мирового океана. В работе приведены количественные оценки потока CO_2 на границе с атмосферой, проанализирована его направленность, выделены факторы, определяющие величину потока CO_2 в северо-восточной части Черного моря в холодный период. Для анализа использованы данные, полученные в ходе экспедиционных исследований на НИС «Профессор Водяницкий» в декабре 2022 г. Величина потока углекислого газа на границе вода – атмосфера рассчитывалась с учетом скорости ветра и градиента pCO_2 между поверхностью моря и приводным слоем атмосферы. По данным прямого определения pCO_2, значения потока CO_2 в декабре 2022 г. изменялись в широких пределах от –0.05 до –8.74 ммоль·м$^{-2}$·сут$^{-1}$, среднее значение соответствовало –2.11 ± 1.79 ммоль·м$^{-2}$·сут$^{-1}$. Установлено, что в холодный период года поток CO_2 был направлен из атмосферы в поверхностный слой вод. Таким образом, воды Крымского побережья служат стоком атмосферного CO_2. Локальные минимумы потока наблюдались в юго-восточной части Крымского побережья. При анализе корреляционной связи потока CO_2 с температурой, скоростью ветра и ΔpCO_2 наиболее сильная связь выявлена со скоростью ветра (–0.93), слабая – с ΔpCO_2 (0.22). Следовательно, интенсивность потока CO_2 на границе с атмосферой определялась скоростью ветра. Однако направление потока зависело от ΔpCO_2. Вклад температуры проявлялся в изменении концентрации CO_2 в водной толще.

Ключевые слова: поток CO_2, Черное море, углекислый газ, парциальное давление углекислого газа, цикл углерода

Благодарности: работа выполнена с использованием средств гранта № 169-15-2023-002 от 01.03.2023 Федеральной службы по гидрометеорологии и мониторингу окружающей среды.

Для цитирования: Поток CO_2 на границе с атмосферой в северо-восточной части Черного моря / Н. А. Орехова [и др.] // Экологическая безопасность прибрежной и шельфовой зон моря. 2024. № 1. С. 57–67. EDN GNFAZA.

Introduction

The global cycle of natural substances includes their transport among various biogeochemical reservoirs and regulating balance and budget of substances in the atmo-, litho- and hydrosphere. One of such natural cycles is the carbon cycle, the most important component of which is carbon dioxide (CO_2) [1)] [1–5].

[1)] Raven, J., Caldeira, K., Elderfield, H., Hoegh-Guldberg, O., Liss, P., Riebesell, U., Shepherd, J., Turley, C. and Watson, A., 2005. *Ocean Acidification due to Increasing Atmospheric Carbon Dioxide*. London: The Royal Society, 57 p.

CO_2 is one of the green gases [1–6] and its entry into the atmosphere and further redistribution in the waters of the World Ocean not only plays a significant role in the formation of the climate on the Earth [1], but also affects the characteristics of waters [1, 6, 7].

The waters of the World Ocean are still its natural stock despite the continuous increase in the level of atmospheric CO_2 (about 0.4% per year) and to date its content achieves more than 420 μatm (https://gml.noaa.gov/ccgg/trends/mlo.html). They absorb up to 25% atmospheric CO_2 from anthropogenic emission, thereby support to reduce CO_2 concentrations in the atmosphere [7]. However, its accumulation in the water column leads to negative consequences for the ecosystems of the World Ocean which is revealed in the disruption of natural balances, in particular carbonate ones, decrease in pH and oxygen concentration and emergence of oxygen deficiency zones. The Ocean's ability to absorb carbon dioxide from the atmosphere decreases over time [8–10] and waters can even become a source of CO_2 for the atmosphere in some extreme cases [7].

The primary factor determining the influence of CO_2 on the state of marine systems is its flux from the atmosphere which depends, other things being equal, on the ratio of the partial pressure of CO_2 in the near sea surface atmosphere and the equilibrium partial pressure of CO_2 in the sea surface. This ratio determines the direction and values of the CO_2 flux.

An important aspect of the research of the sea–air CO_2 flux and the pCO_2 value in the sea surface is the study of the nature of changes on time scales from seasonal to interannual which is associated with significant spatial and temporal variability of biological and physical processes affecting these characteristics.

Inland seas are characterized by more intense physical and biogeochemical processes compared to open areas of the World Ocean. As a result, their ecosystem is more dynamic on a temporal and spatial scale and any external influence manifests itself more quickly. First of all, such manifestations include changes in the characteristics of the system: oxygen and CO_2 concentrations, pH values, as well as speed and direction of production and destruction processes [10]. Moreover, these ecosystems are characterized by a more pronounced response to changes in CO_2 concentration in the atmosphere which manifests itself primarily in a shift in the carbonate system equilibrium, as well as changes in redox conditions [1)] [5–7, 10].

The research of inland seas makes it possible to study the influence of atmospheric CO_2 on the characteristics of waters and to assess the contribution of regional ecosystems to the total budget of the CO_2 flux of the World Ocean.

The Black Sea is one of such inland seas. The shelf water characteristics of the northern part of the sea are largely determined by freshwater river runoff and atmospheric contribution, of the northeastern part – by the Azov Sea waters, of the deep-water part – by the Rim Current [11]. This sea is characterized by a wide range

of changes in salinity and temperature [11], high intensity and seasonal changes in primary production processes [12], high values of alkalinity and total inorganic carbon content [13–15]. All this largely determines the state of the carbonate system of sea waters, the CO_2 content in the sea surface and the formation of the sea–air CO_2 flux.

The factors listed above are influenced by seasonal variability. Accordingly, both CO_2 concentration and CO_2 flux also show intra-annual variability.

It can be assumed that during a cold period, the CO_2 concentration should be primarily determined by an abiotic factor – temperature and vertical transport of CO_2 by deep waters, as well as sea–air metabolic processes. In summer, the predominant factor should be biotic due to the occurrence of biogeochemical processes involving organic matter.

The purpose of this work was to obtain numerical estimates of the sea–air CO_2 flux and to identify its direction and the factors that determine the values of the CO_2 flux in the area of the Crimean coast of the Black Sea during the cold period when the contribution of the abiotic factor predominates.

Previously, the CO_2 flux estimates for this Black Sea ecosystem were carried out based on calculated data [13] or for a local area [14].

Materials and methods

The data obtained during the cruise of R/V *Professor Vodyanitsky* in December 2022 (the 125th cruise, 02–27.12.2022) were used in this work. According to [11], this period refers to late autumn.

Fig. 1 shows the area under study and sampling map. The studied area includes a 12-mile zone of the Crimean coast in the northern part of the Black Sea.

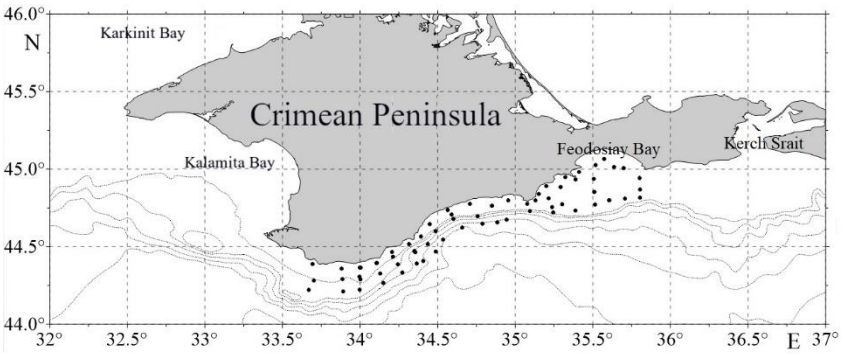

F i g . 1 . Sampling map

Samples from the near sea surface atmosphere were taken at a height of 10 m above sea level. The air intake tube was located in such a way as to avoid the CO_2 influx from the working mechanisms of the vessel, if possible. An LI-7000 by LI-COR infrared analyzer with a working range of CO_2 concentration of 0–3000 ppm and water vapor of 0–60 mmol/mol was used to determine the volumetric concentration and partial pressure of CO_2 directly. In this case, the measurement error is less than 1% of the measured values [15].

Water samples were taken from the sea surface (1–3 m) using a continuous seawater supply system. Next, the water was transported at a constant speed to an equilibrator with the help of which equilibrium was established with a certain volume of atmospheric air at the temperature of sea water according to the method described in [15]. Air from the equilibrator was pumped at a constant speed through the cell of the LI-7000 by LI-COR infrared analyzer in which the concentration of CO_2 and water vapor was determined at the cell temperature. The temperature of the cell is determined by a temperature sensor installed inside it and is in equilibrium with the temperature of the atmosphere surrounding the equilibrator. Next, the carbon dioxide concentration was converted to the partial pressure of carbon dioxide:

$$pCO_2 = x(CO_2) \cdot p_{ATM},$$

where $p(CO_2)$ is partial pressure of carbon dioxide, μatm; $x(CO_2)$ is carbon dioxide concentration, μmol/mol; p_{ATM} is atmospheric pressure, atm.

The temperature and salinity of the sea surface were measured with an IDRONAUT OCEAN SEVEN 320PlusM WOCE-CTD multiparameter probe, and at shallow water stations (less than 50 m) – with the GAP AK-16 hydrological CTD probe.

Meteorological parameters were measured with recording equipment of the hydrometeorological data collection complex [16]. A sensor for measuring wind speed and direction was installed on a side boom 1.5 m long in the direction of the port side on the foremast, with the north direction chosen according to the vessel's heading. The sensor is installed at a height of about 8 m from sea level. The data passed quality control with the rejection of unreliable fragments and were reduced to a standard observation height (10 m) [17]. According to the recommendations of the World Meteorological Organization, the measured parameters were averaged over 10 minutes, and further analysis was carried out for the averaged values. Wind gusts are given as instantaneous wind speed values over 5 s [17].

The values of the sea–air flux of carbon dioxide were calculated using the equations and assumptions described in [18] taking into account the wind speed and pCO_2 gradient between the sea surface and the near sea surface atmosphere:

$$F_{CO_2} = k \cdot K_0 \cdot \Delta pCO_2, \quad (1)$$

where F_{CO_2} is sea–air flux of carbon dioxide, $mmol \cdot m^{-2} \cdot day^{-1}$; K_0 is CO_2 solubility, $mol \cdot m^{-3} \cdot atm^{-1}$; ΔpCO_2 is gradient between partial pressure of carbon dioxide

in the sea surface and the near sea surface atmosphere, atm; k is gas transport rate, $m \cdot day^{-1}$, parameterized as a wind speed function:

$$k = 0.251 \cdot U^2 \cdot (Sc/660)^{-0.5},$$

where U is wind speed, $m \cdot s^{-1}$; Sc is Schmidt number; ratio 0.251 is empirically de-rived parameter, $cm \cdot h^{-1} \cdot (m \cdot s^{-1})^{-2}$ [19].

In [18], it has been established that the intensity of the carbon dioxide flux is determined by the state of the sea surface (bubbles, roughness) at wind speeds of more than 15 $m \cdot s^{-1}$. Wind speeds of more than 15 $m \cdot s^{-1}$ were not recorded during the 125th cruise. Thus, only wind speed and pCO_2 gradient were taken into account when assessing fluxes.

Results

In December 2022, the average wind speed was 4.2 ± 3.8 $m \cdot s^{-1}$ with its minimum of 0.7 $m \cdot s^{-1}$ and maximum of 8.2 $m \cdot s^{-1}$. The sea surface temperature varied within 9.6–14.1 °C with its average value of 13.04 ± 1.06 °C.

The average pCO_2 value of the sea surface was 388 ± 9 μatm while pCO_2 of the near sea surface atmosphere varied within a narrower range and the average value was 434 ± 4 μatm. Thus, the pCO_2 gradient between the sea surface and near sea surface atmosphere (ΔpCO_2) was predominantly determined by the pCO_2 variability in the sea surface. The values of ΔpCO_2 varied from –32.7 to –70.90 μatm with its average of $–45.64 \pm 8.56$ μatm. It can be noted that the sea surface was undersaturated with carbon dioxide relative to the atmosphere during the period under study.

Based on the data obtained from equation (1), the CO_2 flux values were calculated.

The CO_2 flux intensity varied over a wide range from –0.04 to –8.74 $mmol \cdot m^{-2} \cdot day^{-1}$, the average value being $–2.11 \pm 1.79$ $mmol \cdot m^{-2} \cdot day^{-1}$. Negative flux values indicate that the Black Sea waters absorb CO_2 from the atmosphere serving as its stock during the period under study. The calculated flux values are consistent with previously obtained data concerning the waters of the Crimean coast [14] and of the European shelf northwestern part [5].

Spatial variability of CO_2 flux values was characterized by heterogeneity (Fig. 2, *a*). Local minimum values and maximum flux intensity were observed in the area of the eastern coast of Crimea, as well as in its southern part (Fig. 2, *a*).

In terms of quality, the CO_2 flux spatial variability coincides with the distribution of temperature, wind speed and ΔpCO_2 in the sea surface (Fig. 2). Minima of temperature and ΔpCO_2 of the sea surface, as well as maximum wind speed were observed in zones of maximum intensity and minimum flux (Fig. 2).

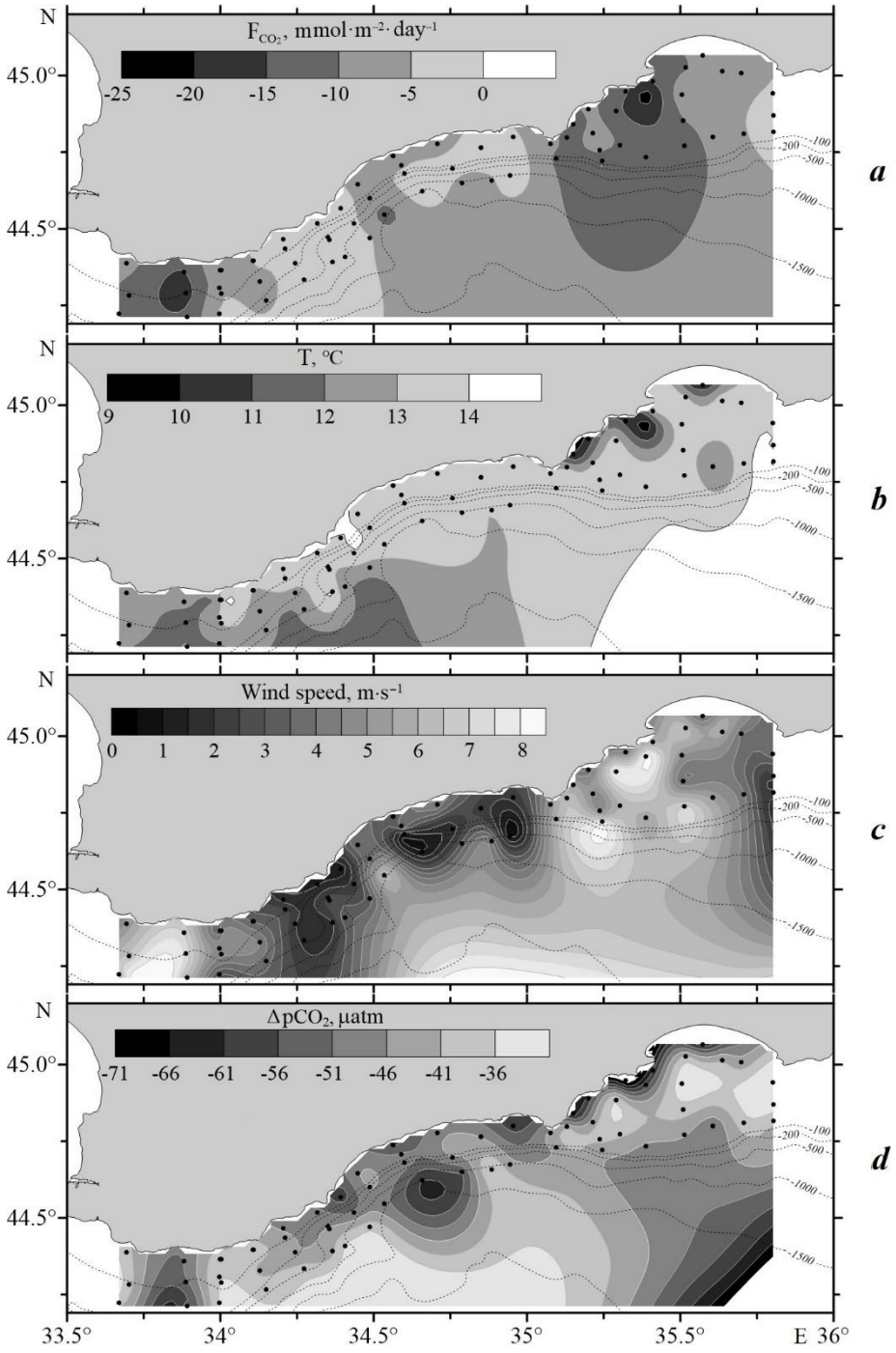

Fig. 2. Spatial variability of the sea-air CO_2 flux (*a*), temperature (*b*), wind speed (*c*) and gradient of pCO_2 (*d*) by data of the 125th cruise of R/V *Professor Vodyanitsky*

Discussion of results

It is known that the CO_2 flux value depends on wind speed and ΔpCO_2 to the greatest extent [18, 19].

Analysis of our data showed that the CO_2 flux was determined primarily by wind speed in December 2022 (Fig. 3). The correlation ratio (–0.93, it is statistically significant with probability belief p = 0.99) indicates a strong linear relationship. The relationship is inverse in itself. Flux direction determines ΔpCO_2 between the sea surface and the near sea surface atmosphere. In turn, ΔpCO_2 is determined by the ratio of the partial pressure of CO_2 in the atmosphere and the equilibrium partial pressure of CO_2 in the sea surface.

The pCO_2 value of the sea surface is proportional to the concentration of CO_2 in water. The concentration of CO_2 depends on the biogeochemical factor when the production or removal of CO_2 occur due to the transformation of organic matter and the formation of carbonates, proceeding according to the following equations:

$$6CO_2 + 6H_2O \leftrightarrow 6H^+ + 6HCO_3^- \leftrightarrow C_6H_{12}O_6 + 6O_2,$$
$$Ca^{2+} + 2HCO_3^- \leftrightarrow CaCO_3 + CO_2 + H_2O\,.$$

In addition, the CO_2 content in the sea surface depends on temperature which affects not only the CO_2 solubility, but also the intensity of biological processes, as well as the shift in chemical equilibria in the carbonate system [19]:

$$CO_{2(g)} \leftrightarrow CO_{2(aq)} \leftrightarrow CO_{2(aq)} + H_2O \leftrightarrow H^+ + HCO_3^- \leftrightarrow 2H^+ + CO_3^{2-}.$$

Changes in CO_2 concentration can also be caused by water dynamics, in particular by the CO_2 influx with waters from underlying layers [20].

Therein, the weak correlation of the CO_2 flux with ΔpCO_2 was unexpected (correlation ratio 0.22, it is statistically significant with probability belief p = 0.95).

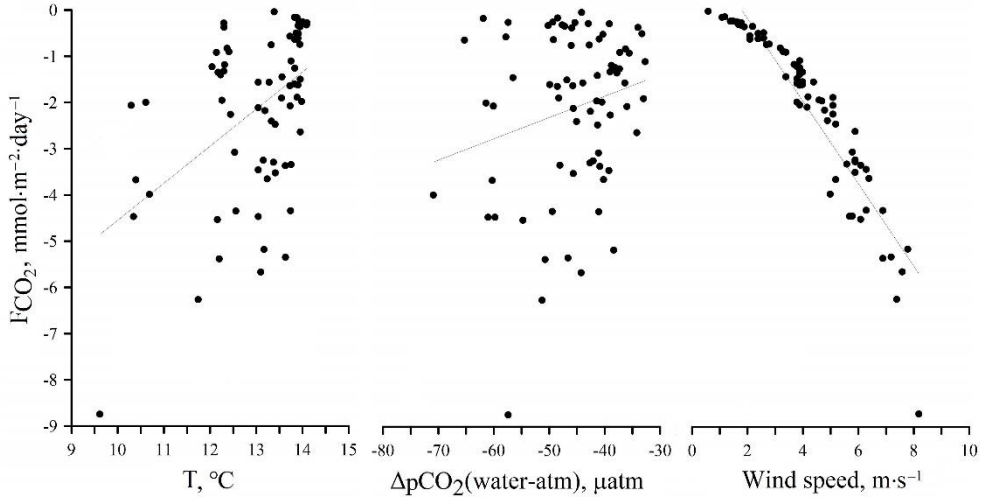

F i g . 3 . Dependence of CO_2 flux (F_{CO_2}) on temperature, ΔpCO_2 and wind speed

A decrease in ΔpCO_2 is characterized by a decrease in the flux (Fig. 3). In turn, a decrease in ΔpCO_2 indicates a decrease in the difference between pCO_2 of the sea surface and the near sea surface atmosphere. As pCO_2 of the near sea surface atmosphere showed almost no changes during the period under study (fluctuation range ±1 %, average pCO_2 = 434 μatm), the decrease in the difference is due to an increase in pCO_2 and, accordingly, in the CO_2 concentration in the sea surface.

An increase in the CO_2 concentration in the sea surface at its low temperatures (about 13 °C) can be caused either by an increase in the CO_2 solubility with a decrease in temperature, or by the dynamics of water ensuring the CO_2 influx from underlying water layers, as well as by the decomposition of organic matter formed during the autumn blooming [12, 21].

The correlation of the CO_2 flux with the sea surface temperature was moderate enough (correlation ratio 0.47, it is statistically significant with probability belief $p = 0.99$). The sea–air intensity of the CO_2 flux decreased with increasing temperature (Fig. 3). However, since the intensity of the flux is also affected by ΔpCO_2 in addition to the wind speed, in this case it is advisable to consider the absolute values (to modulo) of the flux which determine its intensity. Thus, it should be noted that an increase in temperature leads to a decrease in ΔpCO_2 and, accordingly, a decrease in CO_2 flux during the cold season.

Therefore, we can conclude that in December 2022, the predominant contribution to the intensity of the flux is made by the wind speed while the direction of the CO_2 flux is determined by the difference in pCO_2 between the sea surface and the near sea surface atmosphere.

Conclusions

The waters of the northeastern part of the Black Sea serve as a stock of atmospheric CO_2 during the cold season.

According to the direct measurements of pCO_2 in the sea surface and in the near sea surface atmosphere, the values of the CO_2 flux in December 2022 varied widely from –0.048 to –8.74 $mmol \cdot m^{-2} \cdot day^{-1}$, the average value being -2.11 ± 1.79 $mmol \cdot m^{-2} \cdot day^{-1}$. At the same time, no pronounced features of spatial variability were identified. Local minima of flux values were observed in the eastern and southern regions of the Crimean peninsula.

In terms of quality, the CO_2 flux spatial variability coincided with the distribution of temperature, wind speed and ΔpCO_2.

When analyzing the correlation of the CO_2 flux with temperature, wind speed and ΔpCO_2, the strongest relationship was found with wind speed (–0.93), while the weakest one was with ΔpCO_2 (0.22). When the wind speed increases, an increase in the intensity of the CO_2 flux is observed, while the direction of the CO_2 flux is determined by ΔpCO_2 and, accordingly, by the value of pCO_2 and the CO_2 concentration in the sea surface.

The measurements were carried out at the Center for Collective Use R/V *Professor Vodyanitsky* of A.O. Kovalevsky Institute of Biology of the Southern Seas of RAS.

REFERENCES

1. Feely, R.A., Sabine, C.L., Takahashi, T. and Wanninkhof, R., 2001. Uptake and Storage of Carbon Dioxide in the Ocean: The Global CO_2 Survey. *Oceanography*, 14(4), pp. 18–32. https://doi.org/10.5670/oceanog.2001.03
2. Friedlingstein, P., O'Sullivan, M., Jones, M.W., Andrew, R.M., Gregor, L., Hauck, J., Le Quéré, C., Luijkx, I.T., Olsen, A. [et al.], 2022. Global Carbon Budget 2022. *Earth System Science Data*, 14(11), pp. 4811–4900. https://doi.org/10.5194/essd-14-4811-2022
3. Mignot, A., von Schuckmann, K., Landschützer, P., Gasparin, F., van Gennip, S., Perruche, C., Lamouroux, J. and Amm, T., 2022. Decrease in Air-Sea CO_2 Fluxes Caused by Persistent Marine Heatwaves. *Nature Communications*, 13, 4300. https://doi.org/10.1038/s41467-022-31983-0
4. Watson, A.J., Schuster, U., Shutler, J.D., Holding, T., Ashton, Ian, G.C., Landschützer, P., Woolf, D.K. and Goddijn-Murphy, L., 2020. Revised Estimates of Ocean-Atmosphere CO_2 Flux are Consistent with Ocean Carbon Inventory. *Nature Communications*, 11, 4422. https://doi.org/10.1038/s41467-020-18203-3
5. Marrec, P., Cariou, T., Macé, E., Morin, P., Salt, L.A., Vernet, M., Taylor, B., Paxman, K. and Bozec, Y., 2015. Dynamics of Air–Sea CO_2 Fluxes in the Northwestern European Shelf Based on Voluntary Observing Ship and Satellite Observations. *Biogeosciences*, 12(18), pp. 5371–5391, https://doi.org/10.5194/bg-12-5371-2015
6. Gehlen, M., Gruber, N., Gangstø, R., Bopp, L. and Oschlies, A., 2011. Biogeochemical Consequences of Ocean Acidification and Feedbacks to the Earth System. In: J.-P. Gattuso and L. Hansson, eds., 2011. *Ocean Acidification*. Oxford: Oxford University Press, pp. 230–248. https://doi.org/10.1093/oso/9780199591091.003.0017
7. Addey, C., Jiang, Z., Chen, J., Afelumo, A., Adesina, B. and Osanyintuyi, A., 2021. The Variability of Partial Pressure of Carbon Dioxide (pCO_2) in a River-Influenced Coastal Upwelling System: A Case of the Northeast Pacific Coast. *Journal of Geoscience and Environment Protection*, 9(7), pp. 133–148. https://doi.org/10.4236/gep.2021.97009
8. Park, J., 2009. A Re-Evaluation of the Coherence Between Global-Average Atmospheric CO_2 and Temperatures at Interannual Time Scales. *Geophysical Research Letters*, 36(22), L22704. https://doi.org/10.1029/2009GL040975
9. Fung, I.Y., Doney, S.C., Lindsay, K. and John, J., 2005. Evolution of Carbon Sinks in a Changing Climate. *Proceedings of the National Academy of Sciences*, 102(32), pp. 11201–11206. https://doi.org/10.1073/pnas.0504949102
10. Borges, A.V. and Gypens, N., 2010. Carbonate Chemistry in the Coastal Zone Responds More Strongly to Eutrophication Than to Ocean Acidification. *Limnology and Oceanography*, 55(1), pp. 346–353. https://doi.org/10.4319/lo.2010.55.1.0346
11. Ivanov, V.A. and Belokopytov, V.N., 2013. *Oceanography of Black Sea*. Sevastopol: ECOSI-Gidrofizika, 210 p. EDN XPERZR.
12. Kovalyova, I.V. and Suslin, V.V., 2022. Integrated Primary Production in the Deep-Sea Regions of the Black Sea in 1998–2015. *Physical Oceanography*, 29(4), pp. 404–416. https://doi.org/10.22449/1573-160X-2022-4-404-416
13. Medvedev, E.V., Moiseenko, O.G. and Khoruzhy, D.S., 2013. [Long-Term Changes in the Carbonate System of the Black Sea in 1932–2010]. In: MHI, 2013. *Ekologicheskaya Bezopasnost' Pribrezhnoy i Shel'fovoy Zon i Kompleksnoe Ispol'zovanie Resursov Shel'fa* [Ecological Safety of Coastal and Shelf Zones and Comprehensive Use of Shelf Resources]. Sevastopol: MHI. Iss. 27, pp. 318–321 (in Russian).
14. Khoruzhy, D.S., 2018. Variability of the CO_2 Flux on the Water-Atmosphere Interface in the Black Sea Coastal Waters on Various Time Scales in 2010–2014. *Physical Oceanography*, 25(5), pp. 401–411. https://doi.org/10.22449/1573-160X-2018-5-401-411

15. Khoruzhiy, D.S., 2010. Usage of Device Complex AS-C3 for Detection of Carbon Dioxide Partial Pressure and Inorganic Carbon Concentration in Sea Environment. In: MHI, 2010. *Ekologicheskaya Bezopasnost' Pribrezhnoy i Shel'fovoy Zon i Kompleksnoe Ispol'zovanie Resursov Shel'fa* [Ecological Safety of Coastal and Shelf Zones and Comprehensive Use of Shelf Resources]. Sevastopol: MHI. Iss. 23, pp. 260–272 (in Russian).
16. Toloknov, Yu.N. and Korovushkin, A.I., 2010. Hydrometeorological Information Collection System. *Monitoring Systems of Environment*, 13, pp. 50–53 (in Russian).
17. Garmashov, A., 2020. Hydrometeorological Monitoring on the Stationary Oceanographic Platform in the Black Sea. In: SGEM, 2020. *20th International Multidisciplinary Scientific GeoConference SGEM 2020: proceedings*. Sofia. Book 3.1, pp. 171–176. https://doi.org/10.5593/sgem2020/3.1/s12.023
18. Wanninkhof, R., 2014. Relationship between Wind Speed and Gas Exchange over the Ocean Revisited. *Limnology and Oceanography: Methods*, 12(6), pp. 351–362. doi:10.4319/lom.2014.12.351
19. Millero, F.J., 2007. The Marine Inorganic Carbon Cycle. *Chemical Reviews*, 107(2), pp. 308–341. https://doi.org/10.1021/cr0503557
20. Cai, W.-J., Xu, Y.-Y., Feely, R.A., Wanninkhof, R., Jönsson, B., Alin, S.R., Barbero, L., Cross, J.N., Azetsu-Scott, K. [et al.], 2020. Controls on Surface Water Carbonate Chemistry Along North American Ocean Margins. *Nature Communications*, 11, 2691. https://doi.org/10.1038/s41467-020-16530-z
21. Demidov, A.B., 2008. Seasonal Dynamics and Estimation of the Annual Primary Production of Phytoplankton in the Black Sea. *Oceanology*, 48(5), pp. 664–678. https://doi.org/10.1134/S0001437008050068

Submitted 07.08.2023; accepted after review 14.12.2023;
revised 27.12.2023 ; published 25.03.2024

About the authors:

Natalia A. Orekhova, Leading Research Associate, Head of Marine Biogeochemistry Department, Marine Hydrophysical Institute of RAS (2 Kapitanskaya St., Sevastopol, 299011, Russian Federation), Ph.D. (Geogr.), **ORCID ID: 0000-0002-1387-970X, ResearcherID: I-1755-2017, Scopus Author ID: 35784884700**, *natalia.orekhova@mhi-ras.ru*

Eugene V. Medvedev, Junior Research Associate, Marine Hydrophysical Institute of RAS (2 Kapitanskaya St., Sevastopol, 299011, Russian Federation), **ORCID ID: 0000-0002-6093-5102**, *eugenemedvedev@mhi-ras.ru*

Igor N. Mukoseev, Senior Engineer, Marine Hydrophysical Institute of RAS (2 Kapitanskaya St., Sevastopol, 299011, Russian Federation)

Anton V. Garmashov, Senior Research Associate, Marine Hydrophysical Institute of RAS (2 Kapitanskaya St., Sevastopol, 299011, Russian Federation), Ph.D. (Geogr.), **Scopus Author ID: 54924806400**, **ResearcherID: P-4155-2017**, *ant.gar@mail.ru*

Contribution of the authors:

Natalia A. Orekhova – problem statement, processing, analysis and description of the study results, article text editing

Eugene V. Medvedev – *in situ* data obtaining, measurement data processing, discussion of the results

Igor N. Mukoseev – *in situ* data obtaining, graphic material preparation

Anton V. Garmashov – meteodata obtaning and processing, discussion of the results

All the authors have read and approved the final manuscript.

Original article

Field of Total Suspended Matter Concentration of Anthropogenic Nature at the Southern Coast of the Heraclean Peninsula (Crimea)

P. D. Lomakin *, A. I. Chepyzhenko

Marine Hydrophysical Institute of RAS, Sevastopol, Russia
* *e-mail: p_lomakin@mail.ru*

Abstract

Based on the data of a series of expeditions conducted in 2008–2019, the paper analyzes features of the structure of the total suspended matter concentration field in the areas of underwater discharge outlets of urban wastewaters. The linear scale of their influence was estimated. The regularities of domestic wastewaters distribution were considered for three types of background stratification of the water column. It was revealed that the field of the analyzed value was extremely heterogeneous in the studied coastal areas. At the sea surface, against the background of low natural concentration, individual spots were observed with a concentration ten times higher than the surrounding background. The main mass of suspended matter in the outlet area was accumulating in the 0–7 m layer. In the subsurface waters, the structure of the field under consideration shows local maxima, as well as isolated lenses with low salinity. The anthropogenic suspension spread to a distance of 0.4–1.5 miles from the discharge sites. The paper confirms the known regularities of the distribution of wastewaters from deep-sea outlets. These regularities are determined by the water column stratification and are as follows: free penetration to the surface in a homogeneous environment, predominantly horizontal transport in the presence of a seasonal thermocline, and rise to the sea surface in a situation of wind upwelling against a developed seasonal thermocline.

Key words: total suspended matter, temperature, salinity, anthropogenic impact, Heraclean Peninsula, Black Sea

Acknowledgements: The work was performed under state assignment of Marine Hydrophysical Institute of RAS on topic FNNN-2021-0005 “Complex interdisciplinary research of oceanologic processes, which determine functioning and evolution of the Black and Azov Sea coastal ecosystems”.

For citation: Lomakin, P.D. and Chepyzhenko, A.I., 2024. Field of Total Suspended Matter Concentration of Anthropogenic Nature at the Southern Coast of the Heraclea Peninsula (Crimea). *Ecological Safety of Coastal and Shelf Zones of Sea*, (1), pp. 68–81.

Поле концентрации общего взвешенного вещества антропогенной природы у южного берега Гераклейского полуострова (Крым)

П. Д. Ломакин, А. И. Чепыженко

Морской гидрофизический институт РАН, Севастополь, Россия
* *e-mail: p_lomakin@mail.ru*

Аннотация
На базе данных серии экспедиций, проведенных в 2008–2019 гг., проанализированы особенности структуры поля концентрации общего взвешенного вещества на участках подводных выпусков городских стоков. Оценен линейный масштаб их влияния. Рассмотрены закономерности распространения сточных хозяйственно-бытовых вод при трех типах фоновой стратификации водной толщи. Выявлено, что на исследуемых прибрежных участках поле анализируемой величины крайне неоднородно. На поверхности моря на фоне низкой природной концентрации наблюдались отдельные пятна с концентрацией в десятки раз выше окружающего фона. Основная масса взвеси в районе выпусков накапливалась в слое 0–7 м. В подповерхностных водах в структуре рассматриваемого поля отмечены локальные максимумы, а также обособленные линзы с пониженной соленостью. Антропогенная взвесь распространялась на расстояние 0.4–1.5 мили от мест выпуска. Подтверждены известные закономерности распространения сточных вод из глубоководных выпусков, определяемые стратификацией водной толщи: свободное проникновение к поверхности в условиях однородной среды, преимущественно горизонтальный перенос при наличии сезонного термоклина и выход на поверхность моря в ситуации ветрового апвеллинга на фоне развитого сезонного термоклина.

Ключевые слова: общее взвешенное вещество, температура, соленость, антропогенное воздействие, Гераклейский полуостров, Черное море

Благодарности: работа выполнена в рамках государственного задания по теме № FNNN-2021-0005 «Комплексные междисциплинарные исследования океанологических процессов, определяющих функционирование и эволюцию экосистем прибрежных зон Черного и Азовского морей».

Для цитирования: *Ломакин П. Д., Чепыженко А. И.* Поле концентрации общего взвешенного вещества антропогенной природы у южного берега Гераклейского полуострова (Крым) // Экологическая безопасность прибрежной и шельфовой зон моря. 2024. № 1. С. 68–81. EDN NVHRIB.

Introduction

Since 2016, hydrological and hydrochemical monitoring of the state of sea waters has been carried out in the Sevastopol region, near sources of pollution in bays and open coastal area, including the studies of hydrodynamic factors that determine the transfer and accumulation of suspended matter and pollutants.

In [1], the first results of these studies with a comprehensive estimate of the flow of sources and the level of pollution of the marine environment, analysis of hydrophysical processes and hydrochemical parameters have been published. In particular, they concern two main most polluted open sites of the Sevastopol coastal

area: 1 – at the entrance to Balaklava Bay, 2 – near the southwestern section of the coast of the Heraclean Peninsula (area of Cape Fiolent), where the Balaklava and Sevastopol domestic wastewater sewers are located (Fig. 1).

The article examines the structure of the total suspended matter (TSM) content field in these areas.

The selected parameter is considered one of the most informative indicators of water pollution in coastal waters, and the structure of the concentration field of this matter contains information about the sources of anthropogenic load, degree of their influence on the aquatic environment, trajectories of the spread of pollutants, places of their accumulation and dispersion [2].

Active oceanological studies of the field of TSM content in the oceans, seas and freshwater bodies began about 30 years ago. Then, sounding complexes based on the optical principle were invented in a number of foreign countries (Midas CTD+Valeport Ltd, the UK; EXO2 Multiparameter Sonde, YSI Incorporated, the USA; CTD90M – Probe Sea & Sun Technology GmbH, Germany; Metrec•XL AML Oceanographic, Canada). They determine quickly the TSM concentration *in situ* with good spatial resolution. The accuracy of measuring the content of this matter has increased by an order of magnitude compared to the previously used method of evaporation and subsequent dry residue weighing in selected water samples.

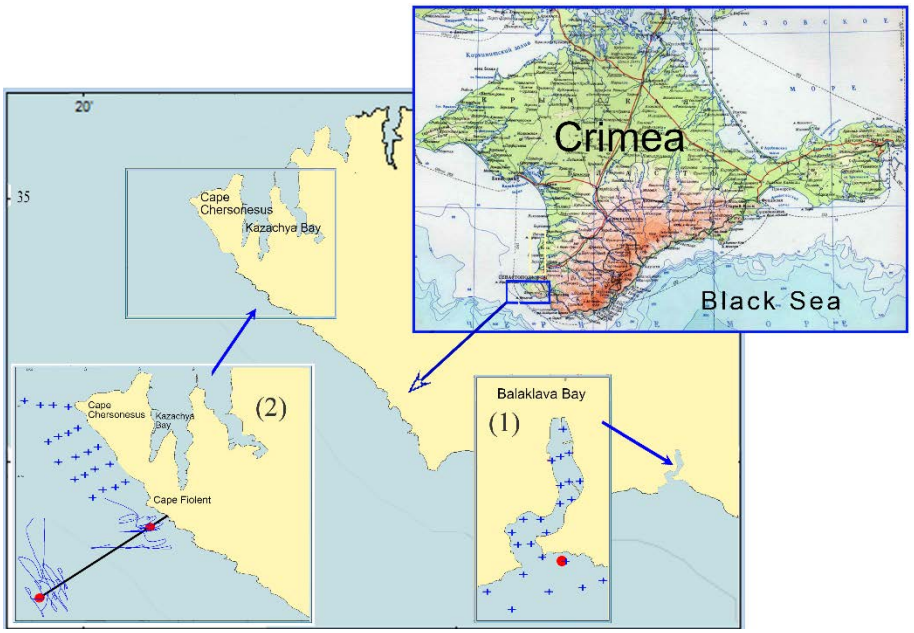

F i g . 1 . The studied areas on the map of the southern coast of the Heraclean Peninsula. The red dots are for municipal wastewater sewers

Since the beginning of this century, a similar probe has been used in the practical coastal expeditionary research of Marine Hydrophysical Institute, in particular in the study of the distribution of wastewaters from underwater discharge outlets in the Sevastopol region.

The article aims at:

– identification of signs of anthropogenic impact on the aquatic environment in the structure of the TSM concentration field and the thermohaline field in two sites of the Sevastopol coastal area, where underwater discharges of Balaklava and Sevastopol domestic wastewaters are located;

– estimate of the horizontal and vertical scales of the anthropogenic impact of each source on the environment;

– consideration of the influence of background stratification on the nature of the spread of wastewaters from the bottom layer to the sea surface;

– comparison of the result with known patterns of distribution of sewage runoffs from deep-sea outlets, previously obtained by other methods, depending on the stratification of the water column.

Initial data and methods of study

Materials from seven complex expeditions conducted by Marine Hydrophysical Institute (MHI) and Institute of Biology of the Southern Seas (IBSS) in 2008–2019 were analyzed.

The Table shows the distribution of initial information by region and over time. The text of the article shows details and features of specific surveys.

Data from expeditions with recording the total suspended matter content in the analyzed Sevastopol coastal areas

Area	Organization	Date of survey, site of water area
1	IBSS	9 May 2008, Balakalava Bay + coastal area 14 April 2010, Balakalava Bay + coastal area
	MHI	29 May 2012, Balakalava Bay + coastal area 6 June 2012, Balakalava Bay + coastal area
2	MHI	27–28 May 2016, coastal area * 12–13 September 2016, coastal area * 23 August 2019, coastal area

* The ship was underway.

All analyzed information was obtained by two instruments. Submersible autonomous hydrobiophysical multiparametric optical probe "Kondor" [1)] Scientific Production Enterprise "Akvastandart," TU 431230-006-00241904-2015; EAEU code 9027 50 000 0; EAEU Declaration of Conformity N RU D-RU.EM03.A.00096/19) was used during standard field oceanographic surveys. During the surveys while the ship was underway, a turbidity meter was used as part of the flow-through complex of MHI associated studies (Table).

During each sounding, the TSM concentration, temperature, and salinity were recorded synchronously (in situ) with a depth discreteness of 0.1 m. The accuracy of determining the indicated values is ±0.2 mg/L, ±0.01 °C, ±0.05 PSU, respectively.

In 1970–1980s, researchers of Institute of Biology of the Southern Seas of the National Academy of Sciences of Ukraine headed by the famous oceanologist Professor V.I. Zats conducted comprehensive experimental and theoretical studies of the processes of self-purification and distribution of wastewaters from sewer discharge outlets in the Black Sea. Monographs [3, 4] show the summarized results of these studies. According to these sources, deep-sea outlet sewers should be placed below the pycnocline (thermocline). This layer prevents the diluted sewage from rising to the sea surface and ensures its predominantly horizontal distribution.

In [4], it is shown that a similar scheme works well off the coast of Crimea in the warm months of the year when water column is sharply stratified. In the cold half of the year, when there is no vertical stratification, wastewater plumes rise freely to the sea surface. The situations of upwelling in the warm season of the year, which weaken the vertical stratification of the water column and in which wastewater plumes penetrate to the surface from a depth of 50–75 m through the seasonal thermocline, are considered separately.

This result was obtained by tracking the movement and transformation of rhodamine (used to color wastewaters) spots on the sea surface. The distribution of pollutants in the water column from a point sewer is considered based on numerical modeling methods.

To solve this problem, we used another method based on an analysis of the structure of the TSM concentration field and information about the background stratification of the thermohaline field.

High accuracy and vertical discreteness of the empirical data at our disposal made it possible to trace the distribution of sewage runoff from the considered deep-sea outlets in each of the situations noted above: in the absence of a thermocline, in the presence of a developed thermocline and under conditions of wind upwelling against the background of a developed thermocline.

To date, the TSM content maximum permissible concentration has not been stated as a numerical indicator of pollution of the aquatic environment. Therefore, to estimate the significance of the anthropogenic component in the concentration field of this matter, its actual content was compared with the concentration

---

[1)] HYDROoptics Ltd. *Complex Hydrobiophysical Multiparametric Submersible Autonomous "CONDOR"*. 2023. [online] Available at: http://ecodevice.com.ru/ecodevice-catalogue/multiturbidimeter-kondor [Accessed: 04 March 2024].

characteristic of the natural environment – waters with the TSM insignificant anthropogenic component.

Based on the results of the analysis of materials from numerous expeditions, we established that the content of TSM varies in a wide range of 0.2–19 mg/L in the waters of the Sevastopol region in the 0–30 m layer, and the structure of the actual field of this matter in bays and open coastal areas is characterized by spottiness due to the presence of local maxima of anthropogenic nature. After the filtration of corresponding concentration extremes from the actual fields, we came to the conclusion that a concentration of 0.8 mg/L corresponds to the environment with the TSM minimal anthropogenic component [5–7].

This value, accepted conditionally as the natural norm for the content of this matter in the waters of the Sevastopol region, was used as a criterion to determine the sites with no anthropogenic impact.

The presence of anthropogenic (from sewage runoff) suspended matter is confirmed by the heterogeneity in the field of TSM concentration in the form of spots (on a plane) or lenses (in space) with a TSM concentration of more than 0.8 mg/L. Sometimes these waters appeared in the salinity field in the form of local minima.

Based on the location of heterogeneities with TSM concentrations of more than 0.8 mg/L and their special haline characteristics, the sites of the water area subject to anthropogenic load were identified, and the linear scale of the influence of the wastewater discharges under consideration was estimated.

To analyze the atmospheric synoptic situation and weather conditions that accompanied the expeditionary research, synoptic maps of the *Wetterzentrale* Hydrometeorological Center website were used (http://old.wetterzentrale.de/topkarten/fsreaeur.html). Weather data are available at: http://rp5.am/Погода_на_Херсонесском_маяке.

Results and discussion

Let us consider the structure of the TSM concentration field under conditions of different background stratification in the coastal areas of the Balaklava and Sevastopol wastewater sewers (Fig. 1).

Area 1 – Balaklava Bay and the adjacent coastal area

The main source of pollution in this area is the Balaklava wastewater sewer located on the approaches to the bay near the southeastern coast at a distance of 55 m from the edge of water at a depth of 9 m [1] (Fig. 1).

The upper boundary of the seasonal pycnocline (thermocline) in this area of the sea is on average located at a depth of about 15 m [8], which creates favorable conditions for the free rise of polluted waters from the bottom horizons and their release to the surface throughout the year.

This effect is confirmed by the results of five oceanographic surveys of Balaklava Bay and the adjacent sea area carried out by the IBSS researchers in 2000–2006 during monitoring studies of this bay and the adjacent Megalo-Yalo Bay [8].

Analysis of expedition materials showed no qualitative changes in the structure of the TSM concentration field characteristic properties from survey to survey.

In the area of discharge outlet, a local maximum in the content of this matter was observed, which varied in the range of 7.1–18.6 mg/L. At the same time, the bottom maximum was less significant and approximately 1.5–3 times higher than the natural norm. The entire water column contained anthropogenic suspended matter mainly concentrated in the upper layer 3–7 m thick. The horizontal scale of the lens of polluted water on the sea surface was 0.4–0.6 miles. According to hydrochemical studies, transformed wastewaters from the discharge area penetrated into the apex of the bay with the wind from the southern quarter.

Fig. 2 shows the situation of maximum contamination of the site under consideration, observed in August 2006. In the surface layer of the sea, the TSM concentration reached 18.6 mg/L, near the bottom it was 2.8 mg/L, and the horizontal scale of the polluted water lens was approximately 0.6 miles. The main amount of the matter under study was concentrated in the 0–5 m layer.

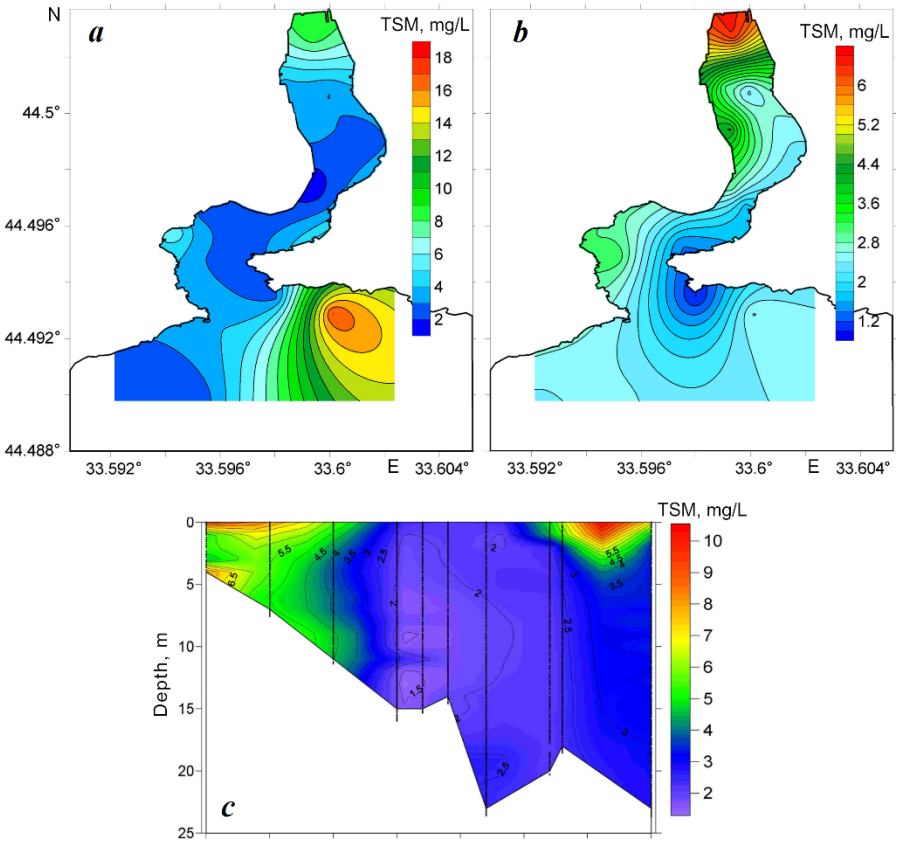

Fig. 2. TSM concentration in the area of Balaklava Bay in August 2006: *a* – in the surface layer; *b* – near the bottom; *c* – at the longitudinal transect of the bay [8]

Analysis of data from subsequent expeditions conducted in 2008–2012 (Table) showed the same basic properties of the field structure of the content of the matter under study identified earlier, as well as its significant concentration an order of magnitude higher than the natural norm (Fig. 3). This indicates significant consumption and stability of the parameters of the source of pollution under consideration and the degree of its impact on the aquatic environment.

The Balaklava wastewater discharge area is distinguished by the maximum concentration of TSM of anthropogenic nature compared to other open areas of the coast and bays of the Sevastopol region.

The response of the aquatic environment to local anthropogenic impact on the approaches to Balaklava Bay is also noted in the salinity field. In the area of discharge outlet, a noticeable desalination of the surface layer of water was observed in the form of a local minimum of salinity in the center of the lens with the maximum TSM concentration. Salinity at the point of this extreme was 0.2–0.5 PSU below the surrounding background.

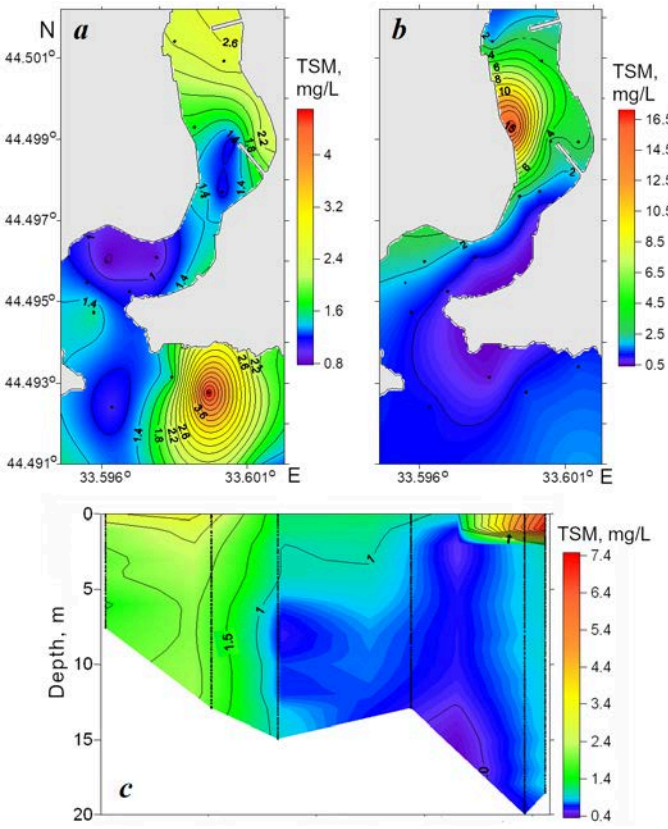

Fig. 3. TSM concentration in the area of Balaklava Bay in April 2010: *a* – in the surface layer; *b* – near the bottom; *c* – at the longitudinal transect of the bay

For comparison, the desalination effect in the area of the natural Georgievsky source of submarine discharge located off the southwestern coast of Balaklava Bay is tens of times less (a similar extremum is not more than 0.02 PSU) [8], which indicates the importance of the wastewater discharge from Balaklava as a water pollution factor.

Area 2 – water area off the southwestern coast of the Heraclean Peninsula where sewage facilities Yuzhnye are located

Let us note the peculiarity of the structure of this water area – here, a constant (main) pycnocline corresponding to the main Black Sea halocline is observed at depths from 50 to 100 m. A known source of pollution in this coastal area is wastewater from sewage facilities *Yuzhnye*, City of Sevastopol [1]. The pipeline head of these structures is located at a distance of ~3 km from the coast at a depth of 88 m. In 2014, a leak developed in the underwater pipeline at a distance of ~ 700 m from the coast at a depth of 34–37 m, which turned into a significant source of anthropogenic suspended matter [1].

The spread of wastewater of high turbidity from the leak is clearly observed on satellite images in the visible range (Fig. 4).

In May and September 2016, two expeditions were conducted in the area of sewage facilities *Yuzhnye* in order to record the content of TSM while the ship was underway (Table). TSM concentration measurements were carried out in a flow-through complex installed onboard the vessel, where a turbidity meter was placed. In the area of the pipe, the ship moved on irregular tacks. The distance between adjacent tacks was reduced in the most polluted areas which were visible on the sea surface as spots of increased turbidity.

In May 2016, areas in the vicinity of both discharge outlets were studied (Fig. 1; Fig. 5, *a*). In September of that year, only the site of the discharge outlet closest to the coast was studied, namely from the beach area to half the length of the wastewater pipeline (Fig. 5, *b*).

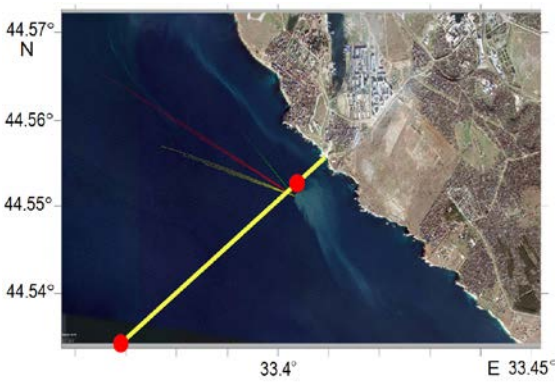

Fig. 4. Satellite image (http://dvs.net.ru/SWCrimea/stoki_ru.shtml) of the studied water area with a scheme of a pipeline of sewage facilities *Yuzhnye*. The red dots are for discharge outlets

In May 2016, the work was performed in hot low-wind weather determined by an anticyclonic low-gradient field of surface atmospheric pressure. The survey was carried out at the beginning of the warm season, when the Black Sea thermocline (pycnocline) had not formed yet and the vertical exchange was not limited to this stratification element.

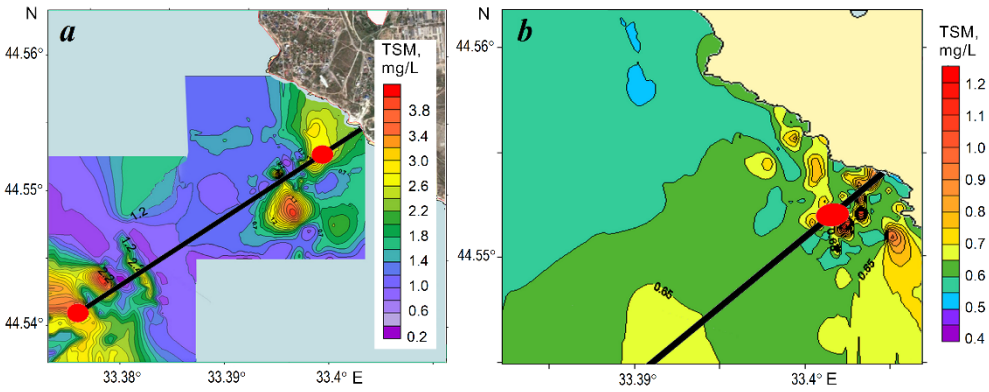

F i g . 5 . TSM Concentration in the 0–1 m layer in Area *2* in May (*a*) and September (*b*) 2016. The black line is for the pipeline with discharge outlets (red dots)

Analysis of experimental data showed the presence of a significant amount of anthropogenic suspended matter in the upper layer of water. Against the background of low (0.2–0.4 mg/L) TSM concentration typical for the open part of the Black Sea, anthropogenic suspended matter from two discharge outlets, the concentration of which was several times and an order of magnitude higher than the background values, was observed in the predominant part of the water area. Local maximum concentration of the studied matter of 4.0–4.2 mg/L was found above both discharge outlets. The anthropogenic suspended matter in the form of spots with a diameter of about 100 m spread into shallow water from the discharge outlet closest to the coast. In the area of the seaward discharge outlet, extensive spots with a diameter of up to ~ 200 m were observed with a TSM concentration 3–5 times higher than the natural norm.

The survey on 12–13 September 2016 was carried out in clear low-wind (variable wind speeds of 2–3 m/s) weather determined by a low-gradient field of surface atmospheric pressure. The September survey was carried out under conditions of developed vertical stratification of the density field typical for the Black Sea at the end of the summer season. This survey confirmed the significant screening role of the seasonal thermocline preventing the spread of the wastewater plume from the bottom horizons to the upper layer of the sea.

In the predominant part of the studied water area, the TSM content (0.4–0.8 mg/L) corresponded to the natural norm. Only in the coastal zone, in the area of the closest wastewater discharge outlet, separate small spots with a diameter of 10–50 m were detected with a TSM concentration of 1.0–1.2 mg/L, which is approximately four times lower than the concentration confirmed by the May survey (Fig. 5, *b*).

In August 2019, the MHI researchers conducted a comprehensive oceanological survey at a test site located half a mile northwest of the pipeline of sewage facilities *Yuzhnye* under conditions of strong northeasterly offshore winds (Table, Fig. 1). This successful experiment made it possible to understand the features of water structure

and the TSM distribution from real sources of pollution in a situation of upwelling and maximally stratified water column.

A developed seasonal thermocline was observed in the coastal area under study. Its upper boundary was located at a depth of 7–11 m and was raised near the coast. The vertical gradient in the thermocline (in absolute value) exceeded 1 °C/m.

The source of upwelling on the sea surface was clearly visible in the field of temperature and TSM concentration in the form of a minimum of these values extended along the coast: 21.6–22.1 °C and 0.4–0.8 mg/L (Fig. 6, *a, b*).

Despite a well-defined seasonal thermocline that prevented vertical exchange, anthropogenic suspended matter that penetrated through this screening layer in the system of ascending upwelling circulation was found in the upper layer of water almost throughout the entire test site water area. Everywhere in the area under study, with the exception of the northwestern sites most remote from the pipeline of sewage facilities *Yuzhnye*, the TSM concentration exceeded the natural norm and varied in the range of 0.8–2.6 mg/L.

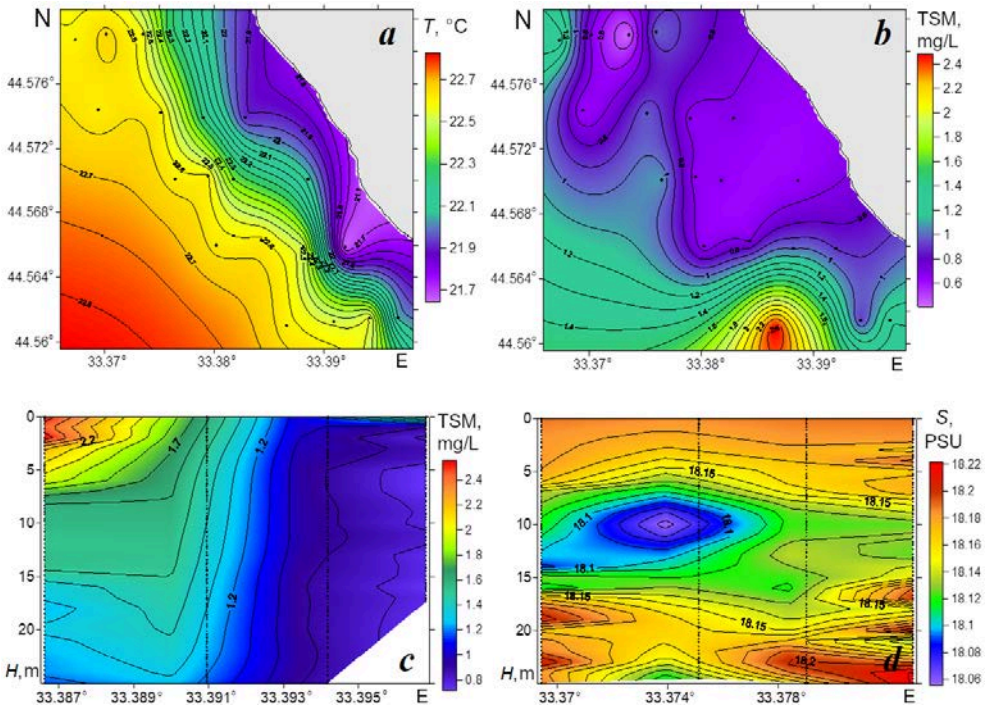

Fig. 6. Distribution of hydrophysical parameters in August 2019: temperature, °C (*a*) and TSM concentration, mg/L (*b*); TSM concentration, mg/L (*c*) and salinity, PSU (*d*) at transects normal to the coast

A fragment of a lens with a vertical scale of 3–5 m and a maximum TSM concentration of 2.4–2.6 mg/L was recorded in the southern part of the test site, in close proximity to the pipe. Anthropogenic suspended matter was observed in the upper layer of water in an area with a linear size of about 1.0–1.5 miles (Fig. 6, *b*, *c*).

The structure of the haline field reflects clearly the response to anthropogenic interference in the state of the aquatic environment in the coastal area under study. The vertical structure of the transformed wastewaters discharged to the sea surface showed signs of anthropogenic impact. They were especially clearly manifested in the stratification of the salinity field in the subsurface layer of 5–20 m in the form of heterogeneities that should not exist in an unpolluted aquatic environment.

Against the surrounding background, these formations were represented by isolated lenses with a vertical size of 3–10 m and salinity reduced by 0.05–0.2 PSU (Fig. 6, *d*).

Note that traces of wastewater discharge on the sea surface were also discovered in the Sevastopol region due to the analysis of high spatial resolution data from satellites Landsat8 and Sentinel1 [10, 11].

The results of this study concerning the features of the distribution of suspended matter from underwater discharge of Balaklava and Sevastopol domestic wastewaters with different stratification of the water column correspond to the main patterns of distribution of sewage discharge outlets from underwater runoff off the Crimean coast identified by the authors of monographs [3 , 4].

It should be noted that the above mentioned authors studied the distribution of artificial dye, while in our case we consider the TSM, a parameter of the aquatic environment actual state. These are two different substances, and each of them could be distributed differently under the same type of background stratification. The discovered similarity of the results determines the possibility of using the method discussed in this article to study the distribution of sewage runoff from deep-sea discharge outlets. It is quick and less expensive.

Thus, a comprehensive survey using probe “Kondor” with recording the TSM concentration in the areas where wastewater discharge outlets are located in Balaklava and Sevastopol takes several hours at a ship speed of 6–8 knots and a sounding depth of 100 m.

In addition, the method based on determining the TSM concentration is more informative, since it gives an idea of the three-dimensional structure of the actual suspended matter field which makes it possible to trace the distribution of this substance in the water column. Observations of the dye [3, 4] were carried out only on the sea surface through aerial photography. The distribution of suspended matter in the water column was modeled.

Conclusion

Based on the data provided by seven expeditions conducted in 2008–2019, the structure of the TSM concentration field and the thermohaline field was analyzed at the sites off the southern coast of the Heraclean Peninsula, where the Balaklava (area 1) and Sevastopol (area 2) underwater discharge outlets of domestic

wastewaters are located. Signs of domestic wastewaters were identified. The scale of the anthropogenic impact of each of the considered sources on the environment was estimated. The influence of background stratification on the distribution of wastewaters from the bottom layer to the sea surface was considered.

It is shown that domestic wastewaters appear in the field of TSM concentration in the form of local maxima with a concentration several times and tens of times higher than the natural norm in each of the studied areas. Sometimes these waters were detected in the salinity field in the form of local minima.

In area 1, the location of the Balaklava wastewater sewer above the seasonal thermocline facilitates the free rise of anthropogenic suspended matter from the bottom horizon to the sea surface throughout the year.

In this area, the structure of the TSM concentration field was stable and was characterized by the following properties during 2000–2018. A local maximum of 7.1–18.6 mg/L was observed in the surface layer 3–7 m thick. The entire water column contained anthropogenic suspended matter. The impact of the sewer extended over a distance of 0.4–0.6 miles from the discharge outlet. Area 1 is distinguished by the maximum anthropogenic TSM concentration compared to other open areas and bays of the Sevastopol region.

In area 2, a qualitative dependence of the anthropogenic TSM distribution on water stratification was traced. In a situation where the seasonal thermocline was not formed (May 2016), anthropogenic suspended matter was found in the surface layer with its concentration several times and an order of magnitude higher than the background values. The TSM content corresponded to the natural norm with a developed seasonal thermocline (September 2016) in the predominant part of the water area. In August 2019, anthropogenic suspended matter was observed in the surface layer of water throughout the entire water area of the test site in a situation of upwelling and a developed seasonal thermocline.

In area 2, the impact of wastewaters extends over a distance of 1–1.5 miles from the discharge outlet.

The results of this study based on an analysis of the structure of the TSM concentration field confirm the dependence of the distribution of sewage runoff on the background stratification of water for deep-sea discharge outlets in the Crimean region, previously identified using other methods. This makes it possible to apply the method we used to study the distribution of sewage runoff from deep-sea discharge outlets.

References

1. Gruzinov, V.M., Dyakov, N.N., Mezenceva, I.V., Malcheko, Y.A., Zhohova, N.V. and Korshenko, A.N., 2019. Sources of Coastal Water Pollution near Sevastopol. *Oceanology*, 59(4), pp. 523–532. https://doi.org/10.1134/S0001437019040076
2. Eisma, D., 2011. *Suspended Matter in the Aquatic Environment*. Berlin: Springer, 315 p. https://doi.org/10.1007/978-3-642-77722-6
3. Zats, V.I., Nemirovsky, M.S., Andryushchenko, B.F., Kandybko, V.V., Stepanov, V.N., Agarkov, A.K., Shulgina, E.F., Kiseleva, M.I., Senichkina, L.G. and Fedorenko, L.V., 1973. [*Experience of Theoretical Experimental Study of the Problem of Deep-Water Sewage Discharge: the Case of the Yalta Area*]. Kiev: Naukova Dumka, 274 p. (in Russian).

4. Zats, V.I. and Goldberg, G.A., eds., 1991. *Modelling of Water Selfpurification Processes of the Shelf Zone of Sea Water*. Leningrad: Gidrometeoizdat, 230 p. (in Russian).
5. Lomakin, P.D. and Chepyzhenko, A.A., 2019. Hydrophysical Conditions and Characteristics of Water Pollution of the Kazachya Bay (Crimea Region) in September of the Year 2018. *Monitoring Systems of Environment*, (1), pp. 48–54. https://doi.org/10.33075/2220-5861-2019-1-48-54 (in Russian).
6. Lomakin, P.D., Chepyzhenko, A.I. and Grebneva, E.A., 2019. Fields of Hydrophysical and Hydrochemical Elements in South and Ship Bays (Crimea) in December 2018. *Monitoring Systems of Environment*, (3), pp. 44–50. https://doi.org/10.33075/2220-5861-2019-3-44-50 (in Russian).
7. Lomakin, P.D. and Chepyzhenko, A.I., 2022. The Structure of Fields of Oceanological Quantities in the Upwelling Zone at the Herakleian Peninsula (Crimea) in August 2019. *Ecological Safety of Coastal and Shelf Zones of Sea*, (1), pp. 31–41. https://doi.org/10.22449/2413-5577-2022-1-31-41
8. Lomakin, P.D. and Popov, M.A., 2013. *Oceanological Characteristic and Estimation of the Water Pollution in the Balaklava Bay*. Sevastopol: ECOSI-Gifrofizika, 220 p. (in Russian).
9. Bondur, V.G., Ivanov, V.A., Dulov, V.A., Goryachkin, Yu.N., Zamshin, V.V., Kondratiev, S.I., Lee, M.E., Mukhanov, V.S., Sovga, E.E. and Chukharev, A.M., 2018. Structure and Origin of the Underwater Plume near Sevastopol. *Fundamentalnaya i Prikladnaya Gidrofizika*, 11(4), pp. 42–54. https://doi.org/10.7868/S2073667318040068 (in Russian).
10. Bondur, V.G. and Grebenyuk, Yu.V., 2001. Remote Indication of Anthropogenic Influence on Marine Environment Caused by Depth Wastewater Plum: Modelling, Experiments. *Issledovanie Zemli iz Kosmosa*, (6), pp. 49–67 (in Russian).
11. Dulov, B.A., Yurovskaya, M.V. and Kozlov, I.E., 2015. Coastal Zone of Sevastopol on High Resolution Satellite Images. *Physical Oceanography*, (6), pp. 39–54. https://doi.org/10.22449/1573-160X-2015-6-39-54

Submitted 09.08.2023; accepted after review 19.10.2023;
revised 27.12.2023; published 25.03.2024

About the authors:

Pavel D. Lomakin, Leading Research Associate, Marine Hydrophysical Institute of RAS (2 Kapitanskaya St., Sevastopol, 299011, Russian Federation), Dr.Sci. (Geogr.), **ResearcherID: V-7761-2017,** *p_lomakin@mail.ru*

Alexey I. Chepyzhenko, Senior Research Associate, Marine Hydrophysical Institute of RAS (2 Kapitanskaya St., Sevastopol, 299011, Russian Federation), Ph.D. (Tech.), *ecodevice@yandex.ru*

Contribution of the authors:

Pavel D. Lomakin – general scientific supervision of the study, statement of the aim and objectives, interpretation of the results, article writing

Alexey I. Chepyzhenko – performance of the expeditionary studies, data processing and analysis, preparation of graphic materials, interpretation of the results

All the authors have read and approved the final manuscript.

Original article

Variability of Nutrient Concentration in Waters of the Chernaya River Estuarine Zone (Sevastopol Region)

S. V. Narivonchik

Marine Hydrophysical Institute of RAS, Sevastopol, Russia
e-mail: Narivonchik_s@mail.ru

Abstract

Nutrient concentration in the water of sea mouths of rivers is a limiting factor in the life activity of hydrobionts. Therefore, studying this parameter is important for assessing the current state of mouth ecosystems and its forecasting. Until now, the variability of nutrients has been analysed by their average concentrations over heterogeneous or short-term periods, extremes or individual surveys, which do not reflect the regime of these elements in the modern climatic period. The paper aims to give a modern description of the nutrient concentration variability in the Chernaya River estuarine zone and to assess water quality based on these components of the ecosystem. For the analysis, we used data from hydrochemical surveys for 1991–2020. Water quality was assessed by the nutrient water pollution index, whereas self-purifying capacity of the estuarine zone was assessed using a transformation index of selected nutrients. The distributions of nutrient concentrations were found to be extremely asymmetrical. In this regard, we obtained for the first time the distributions of medians of nitrates, nitrites, ammonium nitrogen and phosphates in the water of the Chernaya River estuarine zone. In the study area, these median concentrations of nutrients did not exceed the maximum permissible values. Analysis of the temporal variability of average annual nutrient concentrations showed the absence of significant trends. The obtained results can be used for balance estimates and calculations of the assimilation capacity of the Chernaya River estuarine zone.

Keywords: Chernaya River, estuary, Sevastopol region, nutrient concentration variability, nutrients, water pollution index, water quality

Acknowledgments: The work was carried out under state assignment on topic 0555-2021-0005 “Complex interdisciplinary studies of oceanological processes that determine the functioning and evolution of ecosystems in the coastal zones of the Black and Azov Seas” (code “Coastal Research”). The author is grateful to senior researcher R. Ya. Minkovskaya, DSc (Geogr.), for her help in working on the article and to the director of the SB SOI N. N. Dyakov, PhD (Geogr.), for providing the observational data.

For citation: Narivonchik, S.V., 2024. Variability of Nutrient Concentration in Waters of the Chernaya River Estuarine Zone (Sevastopol Region). *Ecological Safety of Coastal and Shelf Zones of Sea*, (1), pp. 82–97.

Изменчивость концентрации биогенных веществ в воде устьевого взморья реки Черной (Севастопольский регион)

С. В. Наривончик

Морской гидрофизический институт РАН, Севастополь, Россия
e-mail: Narivonchik_s@mail.ru

Аннотация
Концентрация биогенных веществ в воде морских устьев рек является лимитирующим фактором жизнедеятельности гидробионтов. Поэтому исследование этого параметра важно для оценки и прогнозирования современного состояния устьевых экосистем. До настоящего времени изменчивость концентрации биогенных веществ анализировали по средним значениям за неоднородные или короткие периоды, экстремумам или данным отдельных съемок, что не отражало режима этих элементов в современный климатический период. Цель работы – дать современную характеристику изменчивости содержания биогенных веществ в воде устьевого взморья р. Черной и оценить качество воды по этим компонентам экосистемы. Для анализа использовались материалы гидрохимических съемок за 1991–2020 гг. Качество воды оценивали по индексу загрязненности воды биогенными веществами, а самоочищающую способность устьевого взморья – по индексу трансформации отдельных биогенных веществ. Установлено, что распределения концентраций биогенных веществ крайне асимметричные. В связи с этим впервые использованы распределения медианных концентраций нитратов, нитритов, аммонийного азота и фосфатов в воде устьевого взморья р. Черной, которые в рассматриваемом районе не превышали предельно допустимых значений. Анализ временной изменчивости средней годовой концентрации биогенных веществ показал отсутствие значимых тенденций. Полученные результаты могут использоваться в балансовых оценках и расчетах ассимиляционной емкости устьевого взморья р. Черной.

Ключевые слова: Севастопольский регион, устье реки, река Черная, концентрация биогенных веществ, биогенные вещества, индекс загрязненности воды, качество воды

Благодарности: работа выполнена в рамках темы *FNNN*-2021-0005 «Комплексные междисциплинарные исследования океанологических процессов, определяющих функционирование и эволюцию экосистем прибрежных зон Черного и Азовского морей» (шифр «Прибрежные исследования»). Автор благодарит с. н. с. д. г. н. Р. Я. Миньковскую за помощь в работе над статьей, а также директора СО ГОИН к. г. н. Н. Н. Дьякова за предоставленные данные наблюдений.

Для цитирования: *Наривончик С. В.* Изменчивость концентрации биогенных веществ в воде устьевого взморья реки Черной (Севастопольский регион) // Экологическая безопасность прибрежной и шельфовой зон моря. 2024. № 1. С. 82–97. EDN RDAHUK.

Introduction

The development of the natural and economic complex of the Sevastopol region depends on the condition of the sea mouth of the Chernaya River. In the modern climatic period of 1991–2020 adopted by the World Meteorological Organization (WMO) [1)], a change in climate and abiotic components of the ecosystem is observed [1]. In addition, economic activity is actively carried out affecting negatively the ecological state of the estuary, which will reduce the quality of life of the local population.

The most important abiotic factor for hydrobionts is the content in water of nutrients that limit their life activity and affect water quality. Therefore, the study of variability in the concentration of nutrients that affect the trophicity of a water body and the identification of areas of environmental risks are relevant.

Content of nutrients both in certain parts of the estuary (in Sevastopol Bay, the lower reaches of the Chernaya River) [2–14] and in the estuary of the Chernaya River as a whole (see work [2)] and [15, 16]) has been actively studied by the Marine Hydrophysical Institute scientists.

The main sources of nutrients entering the receiving reservoir are the runoff of the Chernaya River, which integrates nutrients carried out from the entire river catchment area during precipitation, as well as wastewater discharges, washout from the shore and precipitation [15, 17]. In [15], it is shown that with river runoff the river estuarine zone receives on average: 3 t/year of phosphates, 10 t/year of ammonium nitrogen, 1 t/year of nitrites, 40 t/year of nitrates. Nitrates account for 80–90% of the structure of river nutrient removal [4].

Since previously (e.g., in [3, 4, 15]) mainly the variability of the concentration of nutrients at the top of the sea mouth of the Chernaya River and in its mouth area was studied, as well as the removal of nutrients with river runoff, the main attention in this article is on the analysis of the variability of nutrient concentration in the surface and bottom layers of the Chernaya River estuarine zone.

The relationship between the concentration of inorganic nitrogen and the amount of precipitation established in [17] indicates the significant role of atmospheric entry in the nutrient balance of coastal waters. An increase in precipitation leads to a decrease in the concentration of nitrogen in the atmosphere and an increase in its content in the catchment area, in the water of the Chernaya River and its estuary. Since the water surface area of the Chernaya River estuary is approximately 16 times smaller than the drainage (washoff) area, the main entry component of the nutrient balance of the river estuarine zone is its runoff.

An analysis of the spatial and temporal variability of nutrient concentration in the considered estuary for 1980–2004, 1978–2016, 2007–2016 and 1976–2012 was carried out previously in [3–6, 15, 16]. Moreover, the distribution schemes for these ingredients were constructed using the arithmetic average values of their concentrations. What is more, it is indicated that the nutrient concentrations did

---

[1)] WMO, 2014. *Guide to Climatological Practices*. WMO no. 100. Geneva: WMO, 156 p.

[2)] Ivanov, V.A. and Minkovskaya, R.Ya., 2008. [*Sea Mouths of Ukrainian Rivers and Mouth Processes*]. Sevastopol: ECOSI-Gidrofizika. Part 1, 448 p. (in Russian).

not have any significant trends during the periods under consideration [5], were multidirectional [15] – positive [6] or negative [16]. The averaging periods in these works were different and did not cover the entire modern climatic period of 1991–2020 (WMO). Different levels of economic activity were not taken into account or analysis of individual hydrochemical surveys was carried out [7, 8]. This approach did not provide a reliable assessment of the current nutrient regime at the mouth of the Chernaya River, therefore, a number of studies substantiated the need to replace the average concentration value with the median and take into account natural and anthropogenic changes in the state of the water body (see work [3)] and [15]).

Biogeochemical zoning of the Sevastopol Bay water surface according to the maps of the distribution of nutrients and suspended matter for 1998–2004 is given in [7, 9, 11]. These works show that the waters of Yuzhnaya Bay and the central region of Sevastopol Bay are the areas most contaminated with nutrients.

The intra-annual variability of the E-TRIX trophicity index, which characterizes water quality based on the content of nutrients and other ecosystem components, is presented in [9]. However, this work does not give an idea of the average long-term content of nutrients in the water of the bay and confirms the conclusions stated in [7] about the most significant pollution of Yuzhnaya Bay with nutrients. At the same time, in contrast to the results presented in [7], it was established in [9] that the central part of Sevastopol Bay was least polluted with mineral forms of nitrogen in 1998–2012. The authors of [13] come to the same conclusion.

Fundamental work [2] analyzes the variability of nutrient concentrations in the Black Sea without detailing their content in the water of the estuarine zone where their concentration is usually higher than in the marine environment.

The ability of various parts of Sevastopol Bay to self-purify from nutrients and the factors influencing it are considered in [10–14]. The authors cited difficult water exchange and wastewater discharges as the reasons of the low self-purification of Yuzhnaya Bay concerning inorganic forms of nitrogen.

To assess water quality, the authors used the water pollution index (WPI) calculated based on the content of chemical ingredients of different groups (oxygen, nutrients, phenols, petroleum hydrocarbons) in work [2)] and [15]. Previously, no integral assessment of water pollution based on the content of nutrients has been carried out.

The sporadic nature of observations of the nutrient concentration with significant temporal variability of these ingredients makes estimates of the average annual concentration insufficiently substantiated, therefore, it was proposed to use the median as the center for grouping data instead of the arithmetic mean value in work [2)]. In the same work, based on an analysis of the distribution law of nutrient concentrations, the rationale for this method is given. In work [3)], it is also recommended to use the median, since the arithmetic mean is a biased estimate of the sample center.

Thus, the analysis of previous works revealed a number of shortcomings of research methods: the use of arithmetic mean concentrations to analyze spatial variability;

[3)] Gagarina, O.V., 2012. [*Assessment and Standardization of Natural Water Quality: Criteria, Methods, Current Issues. Study Guide*]. Izhevsk: Udmurtsky Universitet, 199 p. (in Russian).

the choice of short series of observations or unreasonably long ones that do not take into account climatic factors and the level of economic activity, in order to generalize the results of a study of temporal variability; incorrect use of statistical methods (lack of statistical assessments of the homogeneity and stationarity of series, the significance of trends and the reliability of the obtained dependencies). This makes reliable modern assessment of water quality difficult.

The purpose of this work is to give a modern description of the variability of the nutrient content in the water of the Chernaya River estuarine zone and to assess the quality of water in accordance with these ecosystem components. For this purpose, the database was systematized, statistical characteristics of nutrient concentrations were obtained, their variability in space and time was analyzed, and the quality and self-purifying ability of water was assessed.

The object of the study is the estuarine zone which is influenced by the river runoff and wastewaters and makes up most of the Chernaya River sea mouth (Fig. 1).

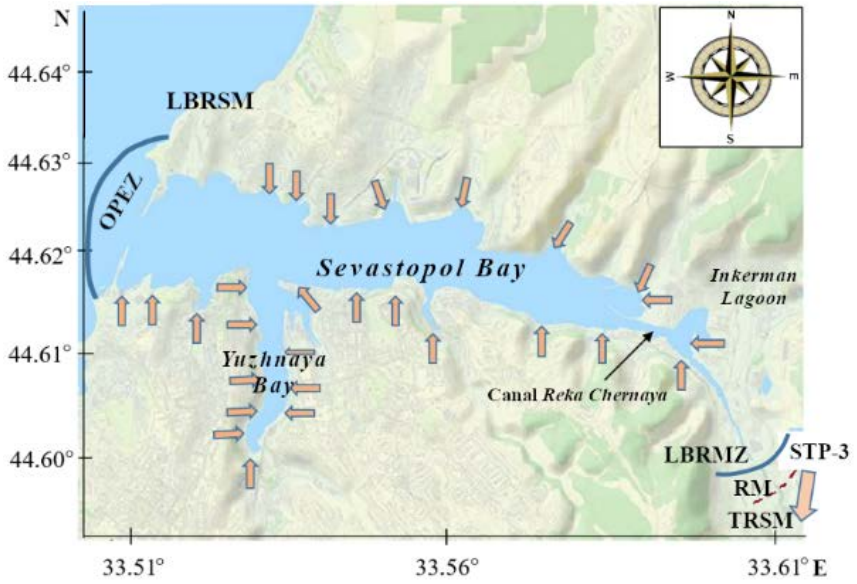

Fig. 1. Sea mouth of the Chernaya River (arrows show constant sources of water pollution taken from paper [4]). LBRSM – lower boundary of the river's sea mouth; OPEZ – open part of the estuarine zone of the Chernaya River; LBRMZ – lower boundary of the river mouth zone; RM – river mouth; TRSM – the top of the river's sea mouth; STP-3 – sewage treatment plant in the village of Sakharnaya Golovka. The blue line shows the boundaries of the Chernaya River estuarine zone

The Chernaya River sea mouth (Fig. 1) includes:

– river mouth (RM);

– complex estuarine zone consisting of Sevastopol Bay with a complex of smaller bays, the Inkerman Lagoon created artificially in the mid-1950s and open part of the estuarine zone (OPEZ) [15].

Due to the lack of data on the Chernaya River OPEZ, the object of our study is limited to the Inkerman Lagoon, Sevastopol and Yuzhnaya bays. The subject of the study is the variability of the content of inorganic forms of nitrogen (nitrates, nitrites, ammonium nitrogen) and phosphorus (phosphates) in the water of the Chernaya River estuarine zone in 1991–2020.

The results obtained can be used in further work for balance calculations, modeling the evolution of the ecosystem and assessing the future state of the abiotic and biotic components of the Chernaya River estuary.

Materials and methods

Monitoring of the Sevastopol Bay and the adjacent part of the sea has been carried out by scientific and regulatory authorities since 1951, while since the 1960s – on a regular basis [15]. The observation network has been optimized several times. Fig. 2 shows its present state on the Chernaya River estuarine zone.

The results of 1991–2020 *in situ* observations provided by N.N. Zubov State Oceanographic Institute (SB SOI) and Marine Hydrophysical Institute of RAS (MHI RAS) were used as initial information. Observations were carried out within the boundaries of the Chernaya River sea mouth (Fig. 1), including its estuarine zone (Fig. 2).

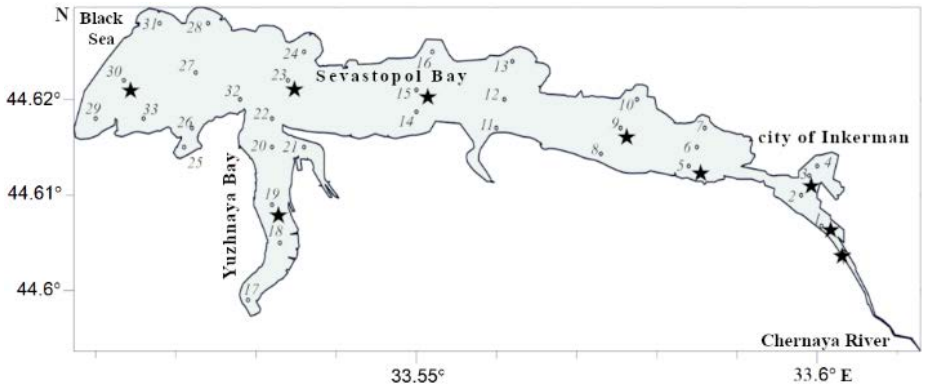

Fig. 2. Map of hydrochemical observational stations of MHI RAS and SB SOI in the Chernaya River estuarine zone in 1991–2020. The dots are for hydrological and hydrochemical surveys carried out by MHI RAS from 1998; the stars are for those carried out by the SB SOI from 1961

The availability of primary hydrochemical data is sufficient to assess the variability of the nutrient concentration in space and time. The generalization period was selected in accordance with the recommendations [1)] taking into account changes in the regional economy occurred in the 1990s. The correctness of this choice is confirmed by the previously performed analysis of climatic and anthropogenic changes in the region under consideration [1].

Water sampling for the nutrient content was carried out at 33 stations of the estuarine zone (Fig. 2) and 1 station at the RM lower boundary (Fig. 1). The concentration of nitrates (NO_3), nitrites (NO_2), ammonium nitrogen (NH_4) and phosphates (PO_4) in the surface and bottom layers of water was studied.

The choice of the studied elements is due to the lack of information on the content of pollutants in the water of the estuarine coastal zone. A reliable statistical assessment of *in situ* data can so far be made only within the largest part (90%) of the Chernaya River estuarine zone, including Sevastopol Bay and the Inkerman Lagoon. Therefore, the characteristics of nutrient variability are given for this part of the estuarine zone (Fig. 2).

Analysis of samples for the content of nutrients was carried out in accordance with standardized methods [4)] in certified hydrochemical laboratories of SB SOI and MHI RAS.

On average, 360 water samples were taken and analyzed for nutrient content at each station in 1991–2020 (Fig. 3). 90 analyzes of each ingredient were performed, i.e., 45 samples from the surface and bottom layers of water. This is sufficient for an objective statistical assessment [18].

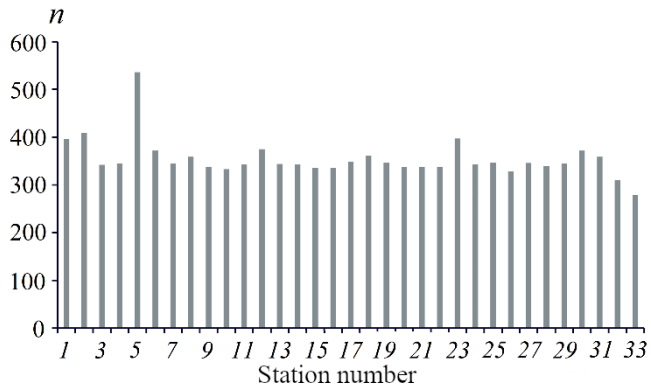

Fig. 3. Number of samples for nutrient content (n) in the water of the Chernaya River estuarine zone in 1991–2020 (data from SB SOI and MHI RAS)

[4)] Oradovsky, S.G., ed., 1993. *Guide on the Chemical Analysis of Sea Waters.* RD 52.10.243-92. Saint Petersburg: Gidrometeoizdat, 264 p. (in Russian).

Nutrient concentrations in water samples were determined by SB SOI and MHI RAS on a unified methodological basis. Therefore, after checking the hydrochemical survey data for homogeneity using the Student's t test [19] for a significance level of 0.95, the series of nutrient concentration values were combined.

Unlike previous works, the distribution diagrams of nutrient concentrations in the surface and bottom layers of water were constructed using medians, since it was established that the distribution of these water quality characteristics was extremely asymmetrical at all stations. Fig. 4 shows the example of a histogram of phosphate distribution at station *30*. Therefore, the arithmetic mean is not a sufficiently representative parameter of the sample center in this case and it is advisable to use the median according to works [2), 3)] and [15, 18]. During the period under review, median concentrations at all stations of the Chernaya River estuarine zone were 15–95% less than their arithmetic average values due to right-sided asymmetry (Fig. 4).

To calculate statistical characteristics, standard statistical generalization methods were used [19], and distribution diagrams of nutrient concentrations were constructed with the standard Surfer 13 software package.

The use of integral and complex indices for assessing water quality (pollution coefficient, water quality index, water pollution index, combinatorial water pollution index, specific combinatorial water pollution index, etc.) discussed in work [3)] is difficult due to the lack of data on many indicators. Therefore, a simplified version of assessing water quality using the nutrient water pollution index (WPI_N) was used as follows:

$$WPI_N = \left(\sum_{i=1}^{4} \frac{C_i}{MPC_i} \right) \Big/ 4, \qquad (1)$$

where C_i is average long-term nutrient concentration; MPC_i is its maximum permissible concentration.

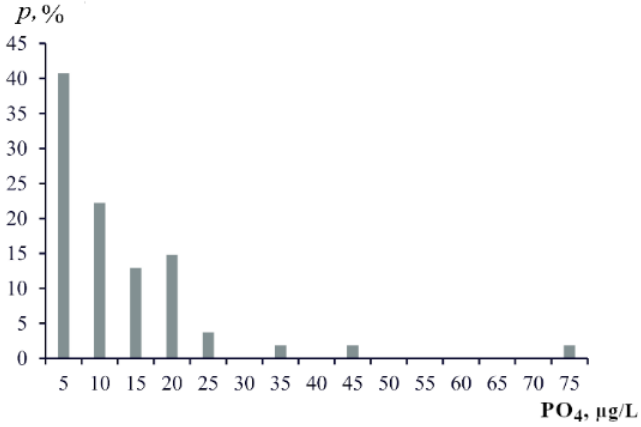

F i g . 4 . Repeatability of phosphate concentration at the western Sevastopol Bay

WPI_N characterizes the total impact of nutrients on the aquatic environment without taking into account the influence of other water quality indicators.

For an approximate assessment of the average long-term transformation of nutrients in the water of the Chernaya River estuarine zone under the influence of hydrophysical, hydrochemical and hydrobiological factors, the transformation index of nutrients (TI_N, %/km) was used showing by what percentage on average the concentration of an individual nutrient changed for each kilometer of the longitudinal axial section of the estuarine zone. Work [4, p. 291] proposes the following formula to calculate TI_N

$$TI_N = \left(\frac{\Delta C}{C_{\text{нач}} \cdot L} \right) \cdot 100\%, \quad (2)$$

where ΔC is difference between the average long-term nutrient concentration at the final and initial sections of the area under study; L is distance between sections.

The significance of trends in the concentration of the studied ingredients was assessed using the F-criterion (Fisher test) for the probability of inequality of the slope to zero at the level of 95% [20].

Discussion of results

Temporal variability. For 1991–2020, the average annual nutrient concentration calculated from 3–4 hydrochemical surveys per year did not exceed the MPC at all stations. Although some surveys showed the extreme concentrations of elements 2–500 times higher than the MPC: 595 μg/L of phosphates (MPC 150 μg/L) (27.04.2016), 10,471 μg/L of nitrites (MPC 20 μg/L) (05.09.2016), 17,755 μg/L of nitrates (MPC 9000 μg/L) (04.02.2014). Such anomalies can be caused by emergency wastewater discharges and rainfall.

Analysis of the variability of the nutrient concentration in the bottom and surface layers of water in the Chernaya River estuarine zone revealed no significant trends. Fig. 5 shows typical distribution of nutrient concentrations in the surface layer of water in the central part of the river estuarine zone (Sevastopol Bay), where the most intense interaction of heterogeneous waters (river, sea, bay and wastewaters) occurs.

Earlier works (e.g., in [16]) in 1989–2008 revealed a decrease in the concentration of ammonium nitrogen (by 10 μg/L/year) and nitrites (by 2 μg/L/year) entering the water of the estuarine zone with the Chernaya River runoff, and work [6] identified trends towards an increase in the content of phosphates and nitrates in the water of Sevastopol Bay in 2007–2016 since 2012.

The absence of significant trends in nutrient concentration changes in 1991–2020 confirms the conclusions made in [5, 15]. During the same period, no significant trends in other abiotic components of the ecosystem, such as river runoff, precipitation and water level, were observed [1]. During this period, multidirectional trends in the nutrient concentrations were identified in wastewaters [4]. Obviously, the integral influence of all these factors (economic activity and warming) and sources of nutrient entry (river runoff and wastewaters) during the period under review did not significantly affect the nutrient temporal variability.

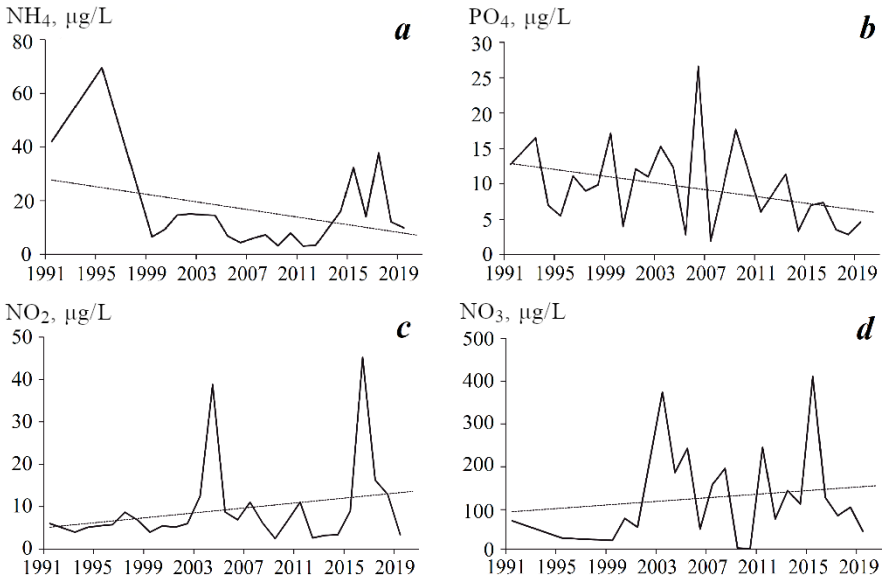

Fig. 5. Nutrient concentrations, µg/L, in the water of the Chernaya River estuarine zone: *a* – ammonium nitrogen, *b* – phosphates, *c* – nitrites, *d* – nitrates

Spatial variability. General character of the distribution of nutrient median concentrations (Fig. 6) indicates that the eastern part of the estuarine zone is influenced by the river runoff, which carries nutrients out of the river basin when washed off during precipitation, and wastewaters.

The content of all nutrients in the bottom layer of water is lower than in the surface one, excluding the concentration of ammonium nitrogen, especially in the area of station *8* (see Fig. 2). Ammonification increases under anaerobic conditions in the deep-sea part of the bay. Therefore, an increased concentration of ammonium nitrogen is observed in the bottom layer of water.

Compared to previous works [5, 15], the distribution of nutrient concentration over depth is less homogeneous (Fig. 6). Obviously, this is due to the use of medians for analysis, and not because of less accurate arithmetic average values of the nutrient concentrations which are significantly influenced by the extreme values of the ingredients.

The highest concentration of all nutrients was observed in the water of Yuzhnaya Bay exposed to the impact of storm water runoff, emergency sewage discharges, under-channel runoff, etc. Pollution of this part of the estuarine zone by nutrients is facilitated by difficult water exchange with Sevastopol Bay due to its geomorphological features (see Fig. 2). The decontaminating effect of sea water with a lower nutrient concentration extends to the western part of the estuarine zone, but at the same time denser sea water and prevailing wind direction (along the axis of the estuarine zone) complicate water exchange between Yuzhnaya and Sevastopol Bays. This promotes the accumulation of pollutants at the top of the stagnant Yuzhnaya Bay.

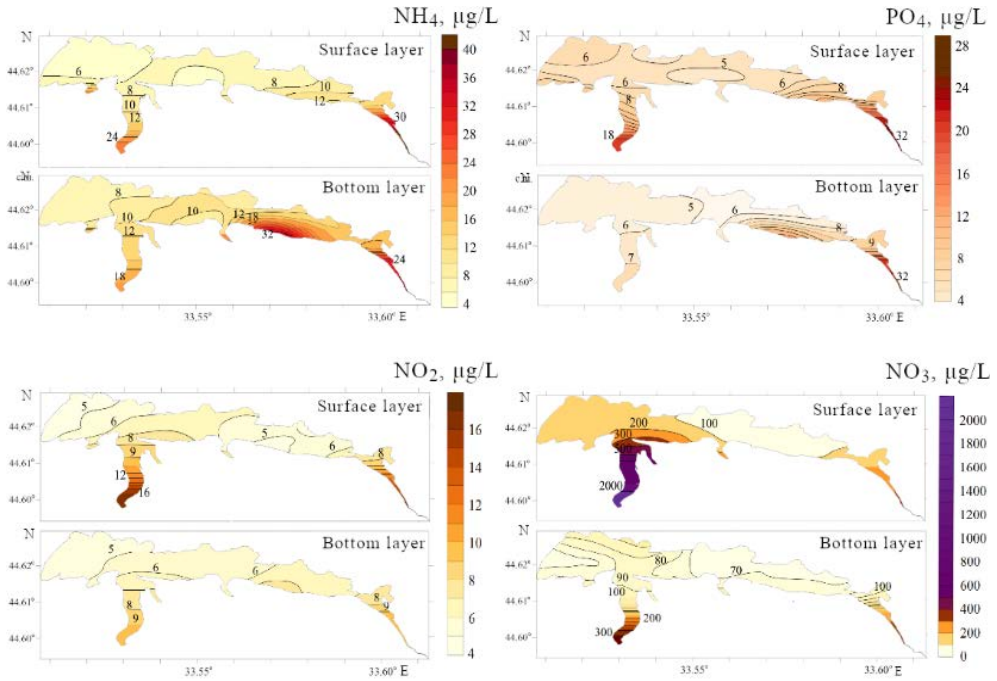

Fig. 6. Distribution of median concentrations of ammonium nitrogen (NH_4), phosphates (PO_4), nitrites (NO_2) and nitrates (NO_3) in the surface and bottom layers of water in the Chernaya River estuarine zone

The median values of nutrient concentrations at all stations did not exceed the MPC (Fig. 6). Their highest values were revealed at station *17* (see Fig. 2) in Yuzhnaya Bay: 18 µg/L – for phosphates and nitrites, 2346 µg/L – for nitrates, 25 µg/L – for ammonium nitrogen.

Nitrates make the greatest contribution to the supply of nutrients to water. They come with river runoff in an amount that is an order of magnitude greater than the amount of other incoming nutrients [4, 15], as well as with precipitation [17], wastewaters [4] and during intra-reservoir hydrochemical and hydrobiological processes [2].

Analysis of the distribution of median nutrient concentrations in the water of the Chernaya River estuarine zone (Fig. 7) showed that under the influence of various self-purification factors (mixing with cleaner sea water, sedimentation, biogeochemical transformation of nutrients and other hydrophysical, hydrochemical and hydrobiological processes), the nutrient concentrations decreased mainly along the axis of the estuarine coastal zone, with the exception of nitrates. The content of nitrates decreased from the top to the middle of the river estuarine zone and then increased (Fig. 7) which is due to their entry into the southern and western parts of the estuarine zone with wastewaters.

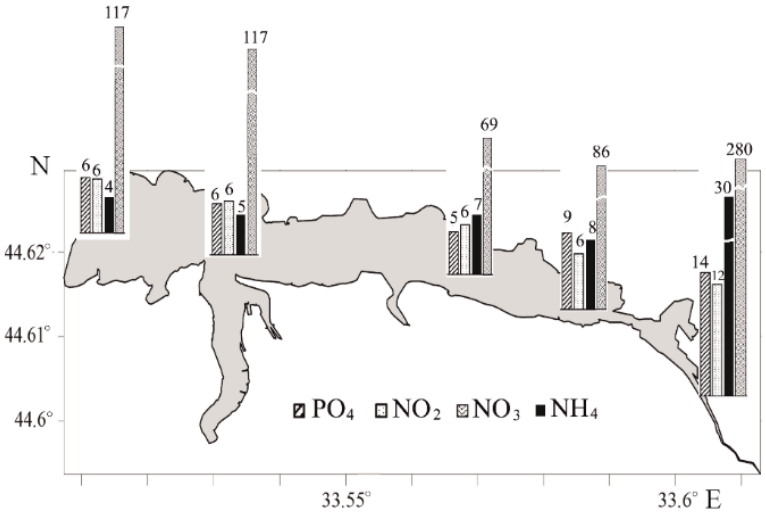

Fig. 7. Variability of the median concentration of the nutrients in the surface water layer in the Chernaya River estuarine zone, μg/L

Fig. 7 shows that the concentration of all nutrients decreased most intensively in the Inkerman Lagoon and the adjacent part of the bay, in the zone of the frontal section of heterogeneous waters, where self-purification processes are most active. The concentration of nitrates decreased by 2.4, ammonium nitrogen by 7.5, nitrites by 2.0, and phosphates by 2.3 times along the axis of the Chernaya River estuarine zone. At the same time, the concentration of phosphates and nitrites changed insignificantly along the axis of Sevastopol Bay (the main part of the estuarine zone).

The resulting schemes can be used for zoning the Chernaya River estuarine zone according to hydrochemical indicators, identifying the most vulnerable ecological areas, assessing water quality comprehensively, as well as calculating the nutrient balance and the accumulative capacity of this receiving reservoir.

Assessment of water quality and self-purification. The assessment of the water quality of the Chernaya River estuarine zone in terms of nutrient content was carried out according to formula (1) using average (Fig. 8, *a*) and median (Fig. 8, *b*) concentration values. Fig. 8 shows that WPI_N calculated from arithmetic mean concentrations is 2–6 times greater than WPI_N calculated from median concentrations. The highest value of WPI_N calculated from median concentrations (Fig. 8, *b*) is observed in the surface layer of water of the Inkerman Lagoon, since the main source of nutrients is the Chernaya River runoff.

The average long-term WPI_N in the bottom layer was 2.5 times less than in the surface layer of water in the Chernaya River estuarine zone in 1991–2020. This is due to the fact that nitrates make the greatest contribution to the structure of water pollution: denitrification processes reducing the concentration of nitrates occur more actively in the bottom layer of water under anaerobic conditions, and nitrates enter the surface layer from various sources with the increase of their concentration

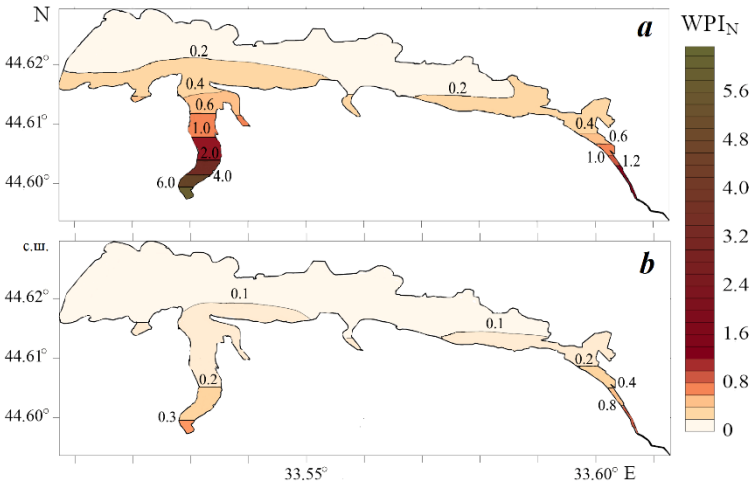

Fig. 8. Distribution of the index of water pollution with nutrients (IWP_N) in the Chernaya River estuarine zone calculated using average (*a*) and median (*b*) concentration values for 1991–2020

due to nitrification processes. The nutrient content in the water of the western and central parts of the estuarine zone was the lowest one (Fig. 8), since the western part of the estuarine zone received sea water depleted of nutrients, and in its central part fewer sewage and storm water collectors are located. (see Fig. 1).

The resulting assessment of water quality based on WPI_N coincides with the conclusions in [7, 15] where WPI was calculated using the generally accepted method [18] taking into account not only nutrients, but also pollutants. The WPI_N distribution (Fig. 8) corresponds to the presence of sources of pollutants at the Chernaya River mouth indicated in Fig. 1 and discussed in [15]. Consequently, the surface layer of water of the Inkerman Lagoon and Yuzhnaya Bay, which are parts of the Chernaya River estuarine zone with the lowest self-purifying ability of the aquatic environment, can be under greatest risk of eutrophication.

To quantify the nutrient transformation along the longitudinal axis of the river estuarine zone, a simplified method was used to calculate the average long-term TI_N using formula (2). This indicator characterizes the ability of water to self-purify from nutrients taking into account the complex influence of abiotic and biotic factors on the concentration of separate nutrients.

The water of the Chernaya River estuarine zone most purified itself from ammonium nitrogen: its concentration decreased by an average of 11.4%/km. The concentration of nitrates decreased by 7.7%/km, phosphates – by 7.3%/km and nitrites – by 6.8%/km.

The self-purification of water from phosphates improved (by 3.5%/km), and from nitrates it worsened (by 2.6%/km) in the modern period in comparison with previously obtained results [15].

TI_N can be applied for approximate estimates of changes in concentration at any point of the estuarine zone depending on the concentration at the source of nutrient entry.

Conclusion

In numerous previous studies, the analysis of the variability of the nutrient content in the water of the Chernaya River estuarine zone for the entire modern period (1991–2020) was carried out on the basis of an arithmetic mean value, which represents an insufficiently correct statistical assessment of primary information.

For the first time, hydrochemical observational data accumulated in the databases of MHI RAS and SB SOI for 1991–2020 were systematized, checked for homogeneity and stationarity and combined into one series, which made it possible to obtain a modern characteristic of the nutrient variability.

It was established that water quality in terms of the content of phosphates, nitrates, nitrites and ammonium nitrogen in 1991–2020 generally corresponded to the standard. No significant trends in the average long-term values nutrient concentrations were detected.

Since the distributions of urgent values of nutrient concentrations are extremely asymmetrical at all stations, the obtained patterns of distribution of their median concentrations in the surface and bottom layers of water in the Chernaya River estuarine zone are more reliable compared to previous works in which less accurate arithmetic average values were used.

It is proposed to use the water pollution index (WPI_N) to assess the integral pollution of the aquatic environment by the complex of nutrients. Differences between WPI_N calculated from medians and arithmetic mean concentrations are shown for the first time. It was established that when median concentrations are used to calculate WPI_N, the highest nutrient content is determined for the water of the eastern part of the estuarine zone. In the future, it will be possible to establish water quality classes based on WPI_N and zone the estuarine zone according to them.

The TI_N (nutrient transformation index) calculation revealed that the concentration decreases naturally from the river to the sea along the axis of the Chernaya River estuarine zone. The nutrient content in the most enriched surface layer of water decreases by an average of 8%/km. The TI_N can be applied for an approximate assessment of changes in the content of various nutrients with a lack of *in situ* data.

The results obtained are applicable for improving the monitoring system, balance and forecast estimates, modeling the evolution of the estuary ecosystem, developing a scientific justification for economic activities in the region, as well as measures to preserve and protect the natural environment of the Chernaya River sea mouth.

REFERENCES

1. Narivonchik, S.V., Minkovskaya, R.Ya., Dyakov, N.N., Malchenko, Yu.A. and Shcherbachenko, S.V., 2022. Variability of the Water Salinity at the Estuary of the Chernaya River (Sevastopol Region) in the Modern Climatic Period. *Hydrosphere. Hazard Processes and Phenomena*, 4(4), pp. 359–380. https://doi.org/10.34753/HS.2022.4.4.359 (in Russian).
2. Simonov, A.I., Ryabinin, A.I. and Gershanovich, D.E., eds., 1992. [*Hydrometeorology and Hydrochemistry of Seas of the USSR. Vol. 4. The Black Sea. Iss. 2. Hydrochemical Conditions and Oceanological Basics of Biological Productivity Formation*]. Saint Petersburg: Gidrometeoizdat, 220 p. (in Russian).
3. Minkovskaya, R.Ya. and Ingerov, A.V., 2010. Hydrochemical Description of the Rivers in the Sevastopol Area. In: MHI, 2010. *Ekologicheskaya Bezopasnost' Pribrezhnoy i Shel'fovoy Zon i Kompleksnoe Ispol'zovanie Resursov Shel'fa* [Ecological Safety of Coastal and Shelf Zones and Comprehensive Use of Shelf Resources]. Sevastopol: ECOSI-Gidrofizika. Iss. 22, pp. 281–295 (in Russian).
4. Verzhevskaya, L.V. and Minkovskaya, R.Ya., 2020. Structure and Dynamics of Anthropogenic Load on the Coastal Zone of the Sevastopol Region. *Ecological Safety of Coastal and Shelf Zones of Sea*, (2), pp. 92–106. https://doi.org/10.22449/2413-5577-2020-2-92-106 (in Russian).
5. Min'kovskaya, R.Ya., Ryabinin, A.I. and Demidov, A.N., 2007. Results of State Monitoring of the Main Parameters in Biogenic Cycle in the Seastopol Bay Water. In: MHI, 2007. *Ekologicheskaya Bezopasnost' Pribrezhnoy i Shel'fovoy Zon i Kompleksnoe Ispol'zovanie Resursov Shel'fa* [Ecological Safety of Coastal and Shelf Zones and Comprehensive Use of Shelf Resources]. Sevastopol: ECOSI-Gidrofizika. Iss. 15, pp. 66–73 (in Russian).
6. Orekhova, N.A. and Varenik, A.V., 2018. Current Hydrochemical Regime of the Sevastopol Bay. *Physical Oceanography*, 25(2), pp. 124–135. https://doi.org/10.22449/1573-160X-2018-2-124-135
7. Ivanov, V.A., Ovsyany, E.I., Repetin, L.N., Romanov, A.S. and Ignatyeva, O.G., 2006. *Hydrological and Hydrochemical Regime of the Sebastopol Bay and Its Changing under Influence of Climatic and Anthropogenic Factors*. Sevastopol: MHI, 90 p. (in Russian).
8. Sovga, E.E. and Khmara, T.V., 2020. Influence of the Chernaya River Runoff during High and Low Water on the Ecological State of the Apex of the Sevastopol Bay Water Area. *Physical Oceanography*, 27(1), pp. 28–36. https://doi.org/10.22449/1573-160X-2020-1-28-36
9. Sovga, E.E., Mezentseva, I.V. and Slepchuk, K.A., 2020. Comparison of Assimilative Capacity and Trophic Index for Various Parts of the Sevastopol Bay Water Area. *Ecological Safety of Coastal and Shelf Zones of Sea*, (3), pp. 63–76. https://doi.org/10.22449/2413-5577-2020-3-63-76 (in Russian).
10. Sovga, E.E., Mezentseva, I.V. and Khmara, T.V., 2022. Simulation of Seasonal Hydrodynamic Regime in the Sevastopol Bay and of Assessment of the Self-Purification Capacity of its Ecosystem. *Fundamental and Applied Hydrophysics*, 15(2), pp. 110–123. https://doi.org/10.59887/fpg/92ge-ahz6-n2pt (in Russian).
11. Mezentseva, I.V. and Sovga, E.E., 2019. Self-Purification Ability of the Ecosystem of the East Part of the Sevastopol Bay with Respect to Inorganic Nitrogen. *Ecological Safety of Coastal and Shelf Zones of Sea*, (1), pp. 71–77. https://doi.org/10.22449/2413-5577-2019-1-71-77 (in Russian).
12. Sovga, E.E. and Mezentseva, I.V., 2019. Ecological Condition of the Central Part of Sevastopol Bay Depending on the Anthropogenic Load Level. *Ecological Safety of Coastal and Shelf Zones of Sea*, (3), pp. 52–60. https://doi.org/10.22449/2413-5577-2019-3-52-60 (in Russian).

13. Ivanov, V.A., Mezentseva, I.V., Sovga, E.E., Slepchuk, K.A. and Khmara, T.V., 2015. Assessment Self-Purification Ability of the Sevastopol Bay Ecosystem in Relation to Inorganic Forms of Nitrogen. *Processes in GeoMedia*, (2), pp. 55–65 (in Russian).
14. Sovga, E.E., Mezentseva, I.V. and Khmara, T.V., 2021. Natural-Climatic and Anthropogenic Factors Determining the Self-Purification Capacity of Shallow-Water Marine Ecosystems in Relation to Reduced Nitrogen Forms. *Ecological Safety of Coastal and Shelf Zones of Sea*, (3), pp. 23–36. https://doi.org/10.22449/2413-5577-2021-3-23-36 (in Russian).
15. Minkovskaya, R.Ya., 2020. *Comprehensive Studies of Different Types of River Mouths (on the Example of the River Mouths in the North-Western Part of the Black Sea)*. Sevastopol: FGBUN FITS MGI, 364 p. https://doi.org/10.22449/978-5-6043409-2-9
16. Minkovskaya, R.Ya., 2018. Assessment of the State of the Sea Mouths of Rivers in Sevastopol Region. In: I. M. Kabatchenko, ed., 2018. *Proceedings of SOI*. Moscow. Iss. 219, pp. 152–173 (in Russian).
17. Varenik, A.V. and Konovalov, S.K., 2020. Long-Term Changes in the Inorganic Nitrogen Content in the Atmospheric Precipitation of the City of Sevastopol. In: SSC RAS, 2020. *Regularities of Formation and Impact of Marine and Atmospheric Hazardous Phenomena and Disasters on the Coastal Zone of the Russian Federation under the Conditions of Global Climatic and Industrial Challenges ("Dangerous Phenomena – II") in memory of Corresponding Member RAS D.G. Matishov: Proceedings of the International Scientific Conference (Rostov-on-Don, 6–10 July 2020)*. Rostov-on-Don: SSC RAS Publishers, 428 p. (in Russian).
18. Rozhdestvensky, A.V. and Chebotarev, A.I., 1974. *Statistical Methods in Hydrology*. Leningrad: Gidrometeoizdat, 424 p. (in Russian).
19. Orlov, A.I., 2019. The Manifold of Methods for Testing the Homogeneity of Two Independent Samples. In: PGNIU, 2019. [*Statistical Methods of Hypothesis Estimation and Testing: Inter-University Collection of Scientific Papers*]. Perm: Izdatelsky Tsentr PGNIU, pp. 64–83 (in Russian).
20. Panofsky, H.A. and Brier, G.W., 1968. *Some Applications of Statistics to Meteorology*. Pennsylvania State Unversity: University Press, 224 p.

Submitted 30.10.2023; accepted after review 12.12.2023;
revised 27.12.2023; published 25.03.2024

About the author:

Svetlana V. Narivonchik, Senior Engineer, Marine Hydrophysical Institute of RAS (2 Kapitanskaya St., Sevastopol, 299011, Russian Federation), **ORCID ID: 0009-0004-1428-8284**, *Narivonchik_s@mail.ru*

The author has read and approved the final manuscript.

Original article

Thermoprofilemeter-Based Stationary Measuring System on the Oceanographic Platform for Determining Internal Wave Parameters: Testing Results

P. V. Gaisky

Marine Hydrophysical Institute of RAS, Sevastopol, Russia
e-mail: gaysky@inbox.ru

Abstract

An experimental system for monitoring the dynamics of temperature changes in the coastal zone was tested at the oceanographic platform in the village of Katsiveli (Crimea) continuously for more than a year from 2021 to 2022. The created system was based on three distributed temperature sensors (thermoprofilemeters) identical in design and electronics (thermal copolymer), vertically installed on the spatial basis of an equilateral triangle with a side of 18 m. Continuous spatiotemporal data on vertical temperature profiles up to a depth of 19.5 m were obtained. Data correlation of simultaneous measurements of sensors with pronounced dynamics of temperature gradients allowed to calculate, in addition to the amplitude and period of oscillatory processes, the length, velocity and direction of internal wave propagation. Measurement data with pronounced time fronts of temperature changes made it possible to calculate the direction and velocity of transfer of water masses on horizons. Software algorithms for automatic calculation of specified parameters for correlated indicators of spatiotemporal displacement of calculating isotherms have been developed. The results of the experiments proved the possibility of using a system with the specified technical characteristics of thermoprofilemeters installed on a spatial basis limited by the dimensions of the oceanographic platform to measure the parameters of internal waves and temperature variability with pronounced fronts.

Keywords: distributed temperature sensor, thermoprofilemeter, isotherm, heat storage, thermocline, internal waves, temperature field, heat exchange, thermistor chain, oceanographic platform, temperature gradient

Acknowledgements: The research was performed under state assignment on topic no. FNNN-2021-0004.

For citation: Gaisky, P.V., 2024. Thermoprofilemeter-Based Stationary Measuring System on the Oceanographic Platform for Determining Internal Wave Parameters: Testing Results. *Ecological Safety of Coastal and Shelf Zones of Sea*, (1), pp. 98–112.

Стационарная измерительная система на базе термопрофилемеров на океанографической платформе для определения параметров внутренних волн: результаты испытаний

П. В. Гайский

Морской гидрофизический институт РАН, Севастополь, Россия
e-mail: gaysky@inbox.ru

Аннотация
С июня 2021 по август 2022 г. на океанографической платформе в п. Кацивели непрерывно проводились испытания экспериментальной измерительной системы для мониторинга динамики температурных изменений в прибрежной зоне. Система построена на трех идентичных по конструкции и электронным компонентам распределенных датчиках температуры (термопрофилемерах), вертикально установленных на пространственном базисе равностороннего треугольника со стороной 18 м. Получены непрерывные пространственно-временные данные о вертикальных профилях температуры до глубины 19.5 м. Корреляция данных одновременных измерений датчиками при выраженной динамике градиентов температур позволила дополнительно к амплитуде и периоду колебательных процессов рассчитать длину, скорость и направление распространения внутренних волн. Данные измерений с выраженными временными фронтами изменения профилей температур позволили рассчитать направление и скорость переноса водных масс на горизонтах. Разработаны программные алгоритмы автоматического расчета указанных параметров для коррелированных показателей пространственно-временного смещения рассчитанных изотерм. Результаты экспериментов доказали возможность использования предложенной системы на базе термопрофилемеров с заданными техническими характеристиками, установленных на ограниченном габаритами океанографической платформы пространственном базисе, для определения параметров внутренних волн и температурной изменчивости с выраженными фронтами.

Ключевые слова: распределенный датчик температуры, термопрофилемер, изотерма, теплозапас, термоклин, внутренние волны, поле температуры, теплообмен, термокоса, океанографическая платформа, градиент температуры

Благодарности: работа выполнена в рамках государственного задания ФГБУН ФИЦ МГИ по теме FNNN-2021-0004.

Для цитирования: *Гайский П. В.* Стационарная измерительная система на базе термопрофилемеров на океанографической платформе для определения параметров внутренних волн: результаты испытаний // Экологическая безопасность прибрежной и шельфовой зон моря. 2024. № 1. С. 98–112. EDN TSHDME.

Introduction

Monitoring and studies of hydrodynamic processes in the coastal zone with pronounced water temperature gradients are impossible without spatiotemporal reference. Time-continuous measurements of vertical temperature profiles make it possible to observe small-scale variability in water temperature and determine the amplitude and period of subsurface wave processes [1–11]. A measuring system of temperature sensors spatially coordinated in a three-dimensional field is necessary to determine the direction of propagation, length and velocity of internal waves, as well

as the direction and velocity of transfer of water masses accompanied by pronounced temperature fronts. Such sensors should show metrological characteristics identical in accuracy and inertia with a sufficiently high sampling frequency (at least 0.1 Hz). For long-term monitoring, mechanical probing with precision meters or creation of a network of analog point sensors is a complex and expensive solution that cannot ensure synchronous measurements. Therefore, chains of point digital sensors [12, 13] and thermistor chains based on analog sensors [7, 14–19] are often used for these purposes.

The DS18B20 digital sensors used do not always meet these requirements due to high inertia, slow sequential non-synchronous sampling (about 3 s per sensor in a chain) and limited accuracy (maximum digital 12-bit resolution 0.0625 °C and error without additional individual calibration up to 0.5 °C) [20]. Such shortcomings are often compensated by spatiotemporal averaging and smoothing of the measured temperature field which leads to the loss of high-frequency components in the measurements of the process under study. At the same time, it is necessary to increase the spatial basis (the distance among the chains) on the horizon in systems for monitoring the spatial transport of water masses and the propagation of internal waves.

Production of thermistor chains based on analog platinum resistance sensors [14–18] or a chain of thermistors [7, 17] with individual analog-to-digital converters is a labor-intensive and relatively expensive process. However, platinum sensors are characterized by greater metrological measurement accuracy (0.01 °C [14] and ±0.025 °C [17], respectively) and high stability.

In some cases, distributed thermal profilers [21, 22] made on the basis of copper conductors laid according to orthogonal functions continuously along the entire sensor profile can be an alternative. The resolution of each section ranging from a few centimeters to several meters in length is adapted to a specific task. This makes it possible to obtain a continuous smoothed profile with a reconstructed average temperature at each measurement section directly at the hardware level. Visual display of the dynamics of temperature changes in the form of isolines in telemetry mode [1)] without any additional three-dimensional interpolation provides a quick solution to the problems of recording internal waves and determining their parameters. A system of thermoprofilemeters with identical metrological characteristics (inertia and accuracy) makes it possible to determine the temporal displacement in the phases of temperature oscillatory processes (short-period internal waves) and fronts on a smaller spatial basis for installing the meters in a more accurate way. Low overall dimensions of the system allow it to be placed on stationary objects (for example, on an oceanographic platform) avoiding technical difficulties during its installation and

[1)] Gaisky, P.V., 2022. [*Program for Registration and Processing of Thermoprofilemeter Measurement Data "THERMOPROF"*]. Sevastopol: MHI. State Registration no. 2022611315

maintenance (surface waves, drift of buoys, autonomous power supply and data collection) and to monitor small-scale processes in the coastal zone with complex coastline and bottom topography as well as limited spatial localization.

The work aims at developing and testing a small-sized stationary automated system based on distributed thermoprofilemeters in order to determine the spatio-temporal parameters of the distribution in coastal waters of hydrological processes accompanied by changes in temperature gradients and analyzing the results obtained.

Instrumentation

Distributed thermoprofilemeters were created and installed on a stationary basis within the limits of the oceanographic platform in the village of Katsiveli (Crimea) as part of the development and testing of such a small-sized system [21, 22]. Structurally, thermoprofilemeters are copper conductors laid in orthogonal functions along the entire length of a distributed sensor. The number of conductors corresponds to the number of sections. The average temperature in each section of the profile is calculated using matrices of individual calibration coefficients obtained during metrological verification. The protective shell of the sensor part made from the outside in the form of a load-bearing polyamide tube was manufactured to meet the requirements for the same inertia (heat capacity) of the sensors. The metrological characteristics of the measuring channels with an instrumental resolution of 0.0026 °C were also the same. As a result, three 24-meter thermoprofilemeters with spatially distributed sections 1.5 m long, with 16 sensors in each, were produced.

It should be noted that earlier tests of thermoprofilemeters with increased profile resolution (sections of 20 cm in length) carried out on the oceanographic platform demonstrated no significant advantages in recording the primary parameters of the internal waves under study. The inertia of the meters in the liquid was about 30 s due to the protective load-bearing polyamide tube. The measurement error of the temperature averaged over the area is metrologically determined as ±0.1 °C. The sampling period for all 16 sensors (sections of the meter profile) was 0.5 s. Measurement data were received from all three meters simultaneously by the on-board computer linked to a single timer and in telemetry mode were displayed in the form of a gradient field and isotherms.

Fig. 1 shows general location and layout of the system. Since the bottom topography in the area of the platform location is characterized by an increase in depth in the southeast direction, the anchoring depth of the distributed sensors varied from 24 to 28 m (Fig. 2). Based on earlier geography-specific observations [11–13, 21, 22], the most suitable conditions for testing the system corresponded to the season of the formed thermocline and the manifestation of upwelling – downwelling (from May to August).

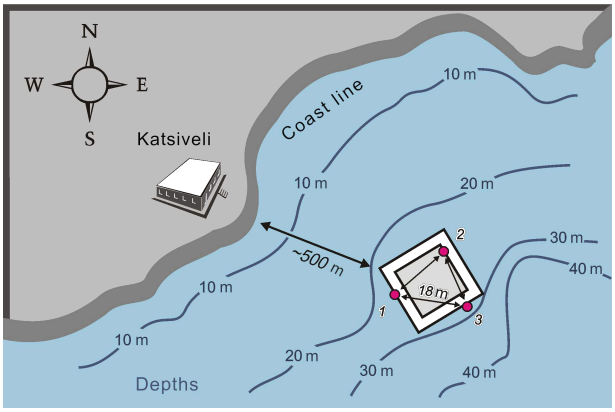

Fig. 1. Location and layout of a system of three thermoprofilemeters at the oceanographic platform. The red dots denote the installed thermoprofilemeters (*1–3*)

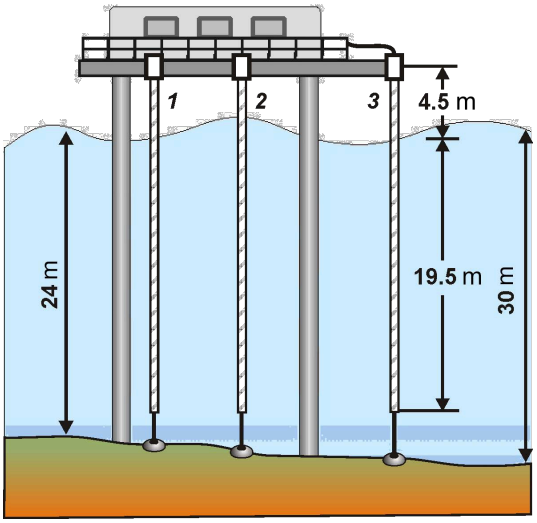

Fig. 2. Depth profile at the installation site of the system and vertical placement of the thermoprofilemeters (*1–3*)

The created system of three thermoprofilemeters was tested for more than a year (from June 2021 to August 2022), which made it possible to analyze the data for two indicated seasonal periods. Almost all recorded significant changes in the depth of the pronounced thermocline were accompanied by wave processes reflected in vertical temperature profiles. Visualization (with a pronounced periodicity of at least

five consecutive frequency components) and possibility of interpretation made it possible to determine about 10 manifestations of short-period internal waves lasting from 1 to 4 hours in one season. Such waves showed their average period of 10–12 minutes and amplitude of 2.5–3 m. Fig. 3 shows the examples of data display on the monitor screen during processing by the program in telemetric measurement mode.

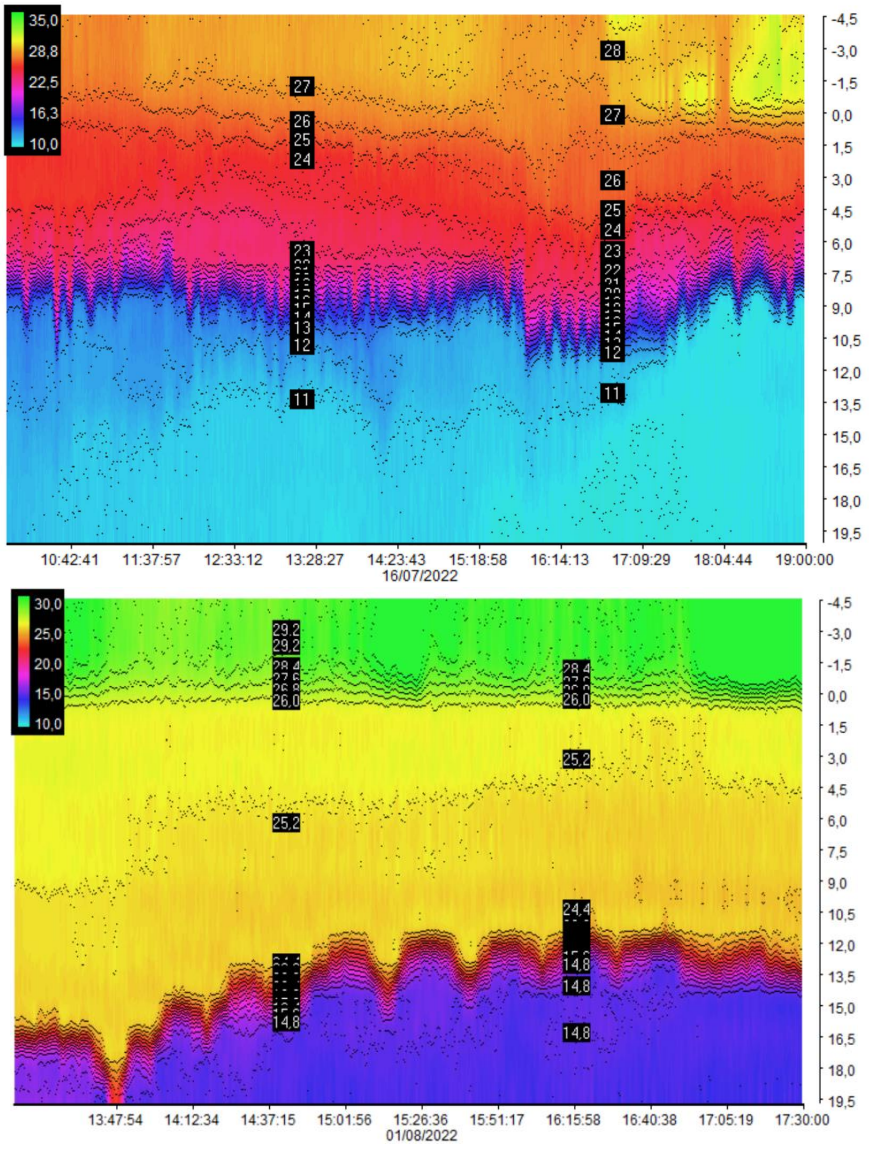

Fig. 3. Examples of a record of short-period internal waves made by one of the thermoprofilemeters

Results

The results of calculations of parameters for observed short-period internal waves are presented as examples of the system operation. This system makes it possible to determine the directions (horizontal and vertical) and velocities of displacement or propagation of internal waves only in the presence of pronounced temperature fronts, based on which we can correlate sensor data and calculate time delays. Coordinate system and geographic location references allow us to further determine the desired dynamic parameters of the observed process.

The calculated spatiotemporal displacements of isotherms in the pycnocline on the temperature profiles obtained by each of the thermoprofilemeters were used as data for synchronous referencing. The calculation of spatial displacements of isotherms was implemented algorithmically in software for each distributed sensor both in telemetry mode and during post-processing [2)]. Algorithms for calculating the direction and velocity of front displacement were implemented in software using trigonometric formulas with updated reference to the spatial orientation and location of the sensors. Direct calculation of these parameters as part of the system tests was carried out in the mode of operator input of primary delays between the sensors (it is enough to enter t_{31} and t_{32} in this case, see Fig. 4) for given geometric parameters.

Fig. 4. Display of the results of data processing by the system on the monitor screen: temperature field with isotherm dynamics and temperature profile gradient – *a*, *d*, *g* (the white rectangle (*a*, *d*) and arrows (*g*) indicate the calculation area); correlated spatial displacements of the selected isotherm in the calculation area at the boundary of the temperature front and internal wave for three thermoprofilemeters (*1*, *2*, *3*) – *b*, *e*, *h*, *k* (the dashed lines mark on the graphs the selected boundaries of the isotherm spatial displacement in the time range for each sensor); results of program calculation of the dynamic characteristics of internal waves (*c*, *f*) based on the obtained time delays (t_{31}, t_{32}, t_{12}) and the velocity and direction of front displacement during upwelling (*j*) and downwelling (*l*)

[2)] Gaisky, P.V., 2022. [*Program for Registration and Processing of Thermoprofilemeter Measurement Data "THERMOPROF"*]. Sevastopol: MHI. State Registration no. 2022611315.

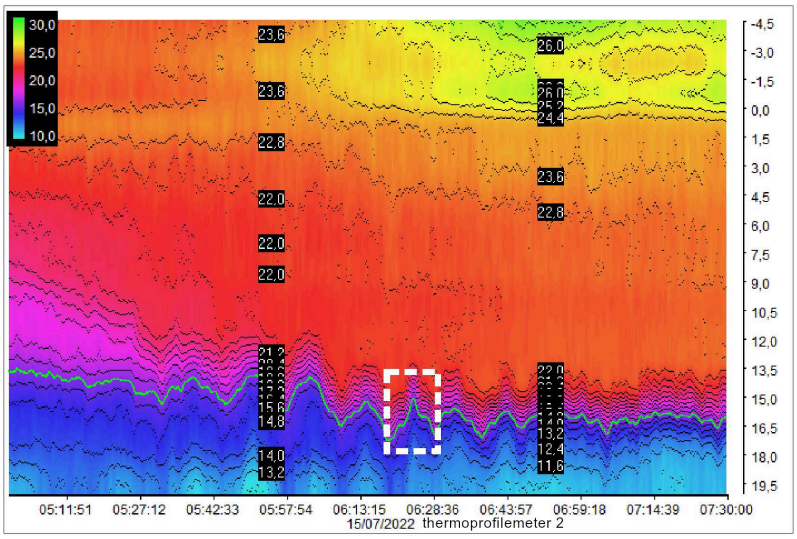
30,0
25,0
20,0
15,0
10,0
05:11:51
05:27:12
05:42:33
05:57:54
06:13:15
06:28:36
06:43:57
06:59:18
07:14:39
07:30:00
15/07/2022 thermoprofilemeter 2

a

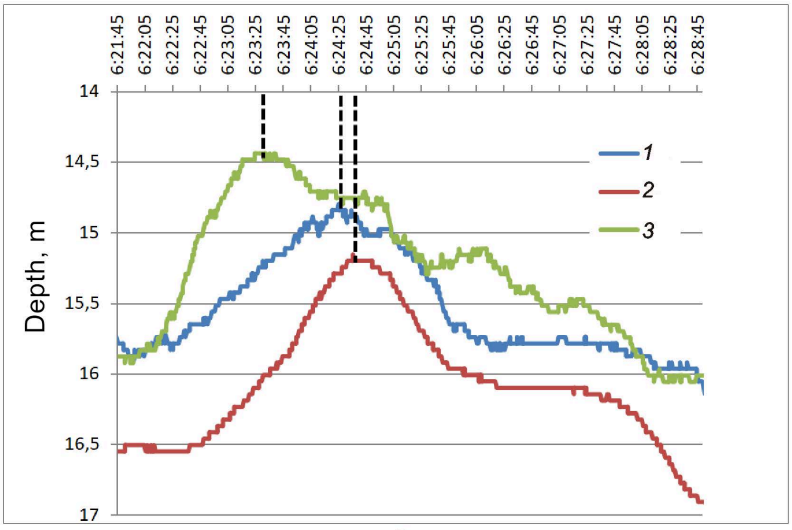
Depth, m
1
2
3

b

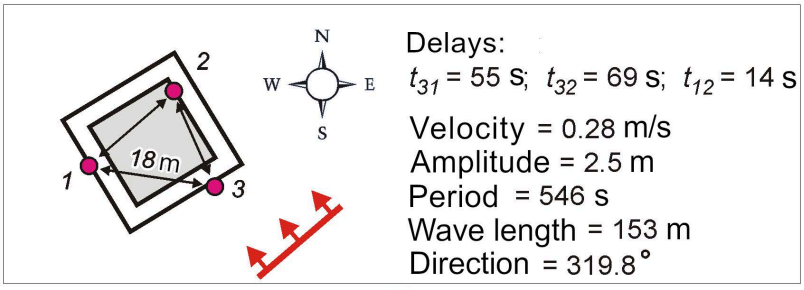
N
W
E
S
1
2
3
18 m
Delays:
t_{31} = 55 s; t_{32} = 69 s; t_{12} = 14 s
Velocity = 0.28 m/s
Amplitude = 2.5 m
Period = 546 s
Wave length = 153 m
Direction = 319.8°

c

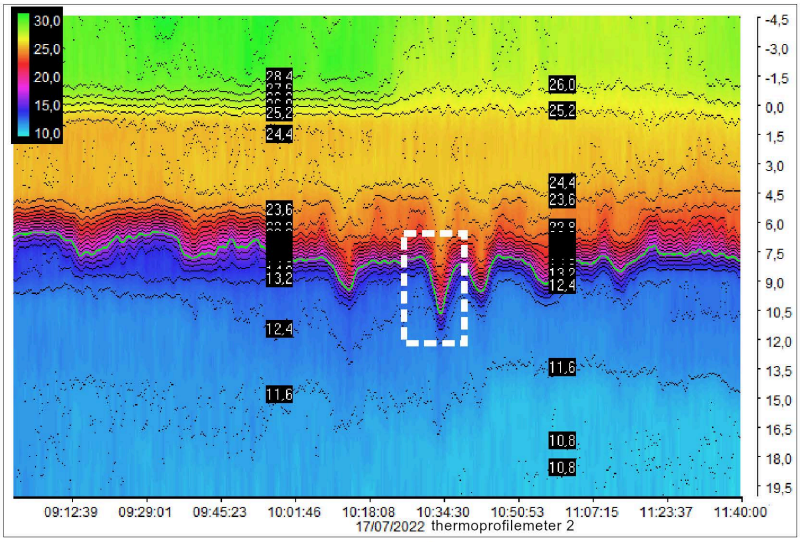

d

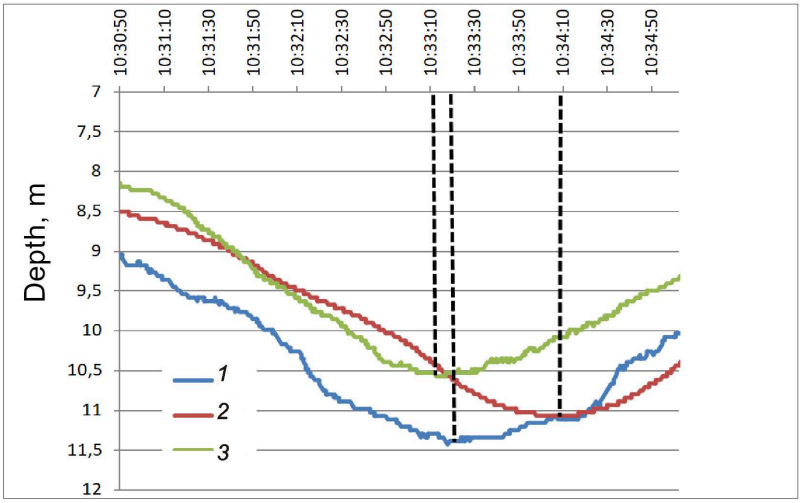

e

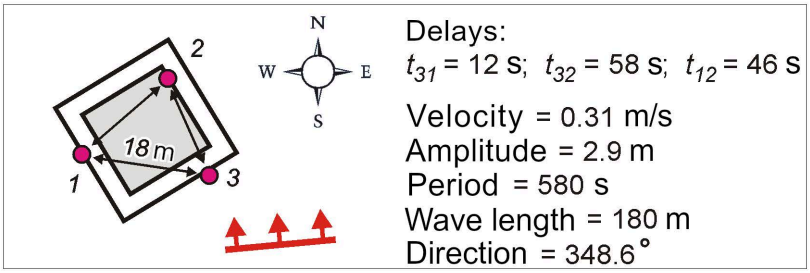

f

Fig. 4. Continued

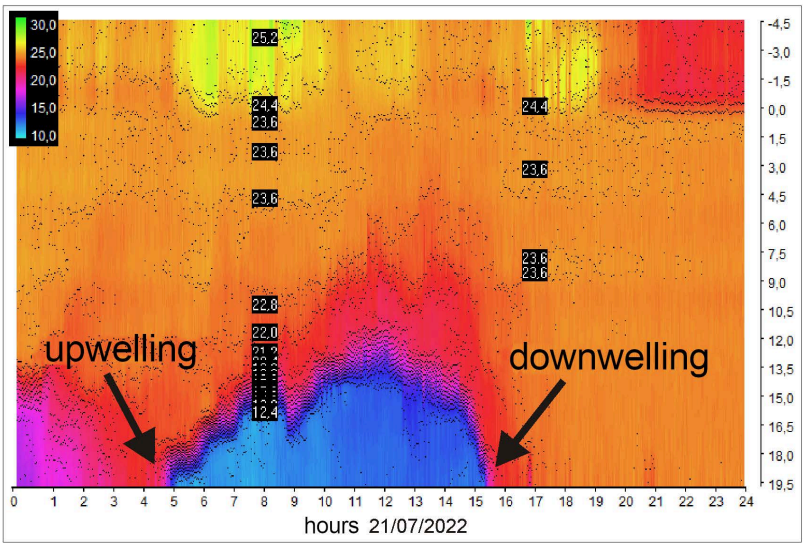

g

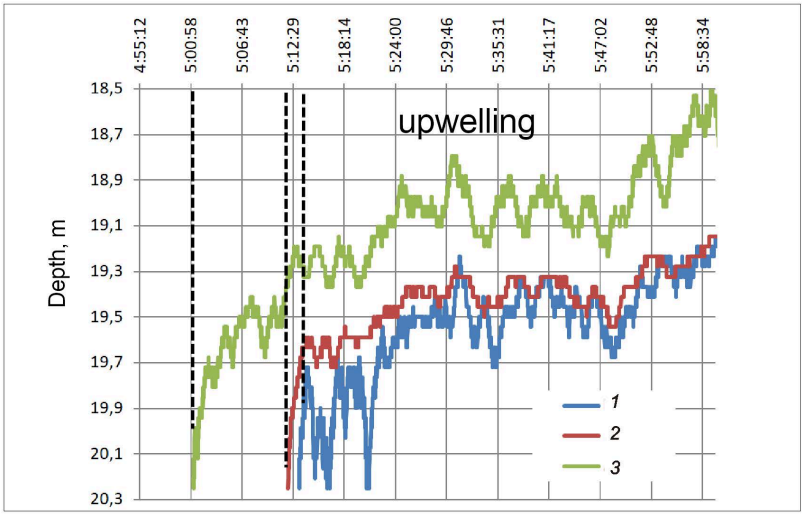

h

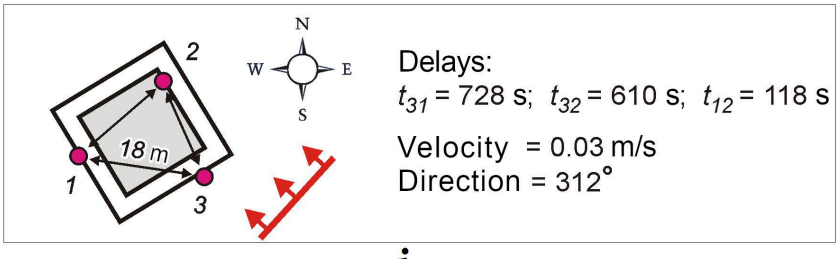

j

Fig. 4. Continued

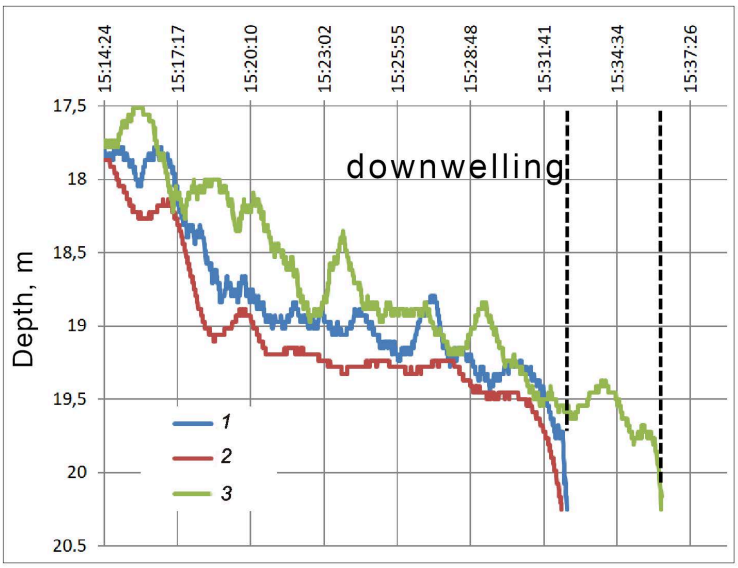

k

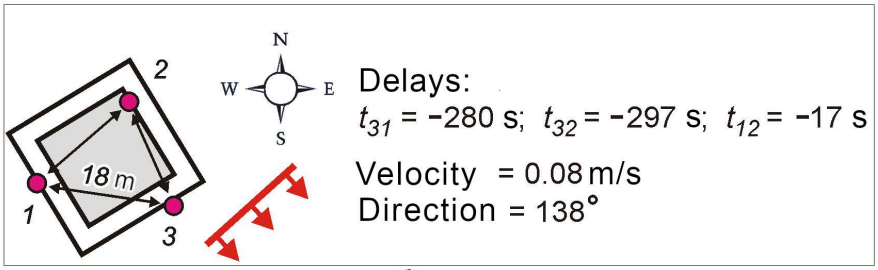

l

Fig. 4. End

Automatic collection of the characteristics of internal waves (amplitude, period, direction, velocity and wavelength) is complicated by a number of factors associated with non-stationary periodicity and complexity of automatic sampling of synchronized fronts of the oscillatory process in telemetric mode. Therefore, at the moment this problem is solved by an operator during visual assessment of events on the monitor screen or during subsequent processing of measurement information.

Figure 4 (*a* – *f*) shows the examples of displaying processing results on the monitor screen (parameters of short-period internal waves at the thermocline boundary). Figure 4 (*g* – *l*) shows calculations for a more time-scale transport of deep cold masses, for which the direction and horizontal velocity were calculated.

It should be noted that during turbulence [23–25] caused by currents and nearby pile structural supports of the platform, the low inertia of the sensors in the system affects negatively the comparison of correlated oscillatory processes associated with the passage of internal waves.

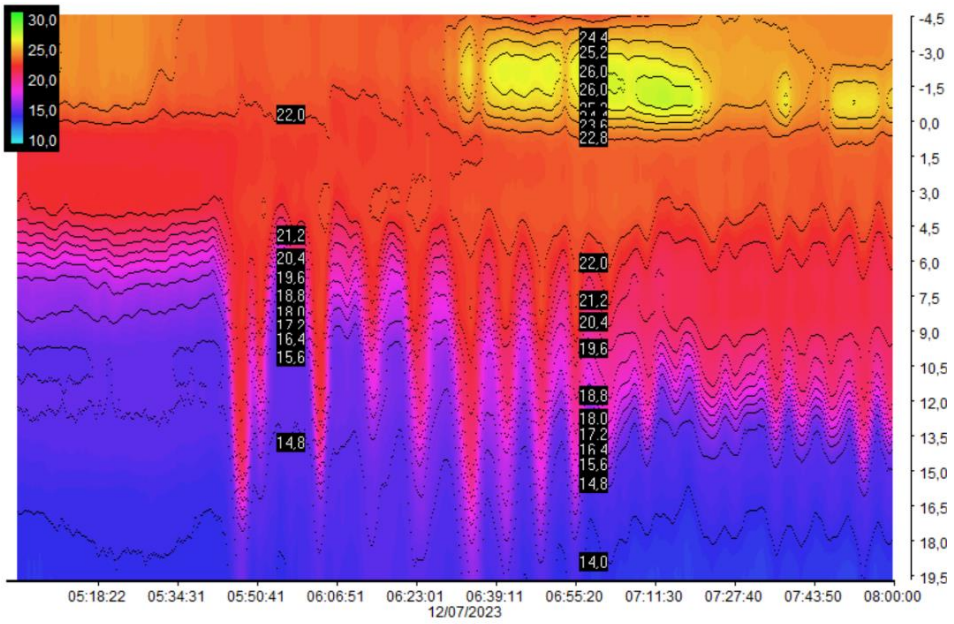

F i g . 5 . Example of a record of intense internal waves with thermoprofilemeters near the oceanographic platform

When testing the system of three thermoprofilemeters, rather rare intense internal waves that had previously been recorded by thermoprofilemeters in the platform area up to three times a year and had had a large amplitude (more than 10 m), a period of about 12 minutes and a pronounced temperature front, were not observed (see Fig. 5).

Conclusion

Tests of the developed system based on distributed thermoprofilemeters showed its performance under conditions of pronounced temperature fronts. The correlation will obviously be clearer in a more laminar environment (relative to the spatial limits of the system installation), which will increase the reliability of automatic software calculations. Influenced by currents, indentation of coastal zone and heterogeneous bottom topography, an increase in the distance among the system sensors can lead to distortions in the synchrony of wave processes in the measured temperature profiles and consequently to difficulties in their comparison (correlation). In this case, installing such a system at a stationary facility is preferable from the point of view of cost and technical support, as well as due to the absence of such factors as drift of buoys and influence of surface waves on the spatial coordinates of the measuring system. Limited spatial localization in a bay or a strait can be ensured for a small-sized system.

The advantages and disadvantages of all types of sensors used to create such systems for determining the parameters of internal waves can be assessed not only by the metrological accuracy of the measuring channels, but also by long-term stability, cost and ease of maintenance. The final conclusion can be made after joint *in situ* tests at monitoring sites and intercalibration.

References

1. Moum, J.N., Farmer, D.M., Smyth, W.D., Armi, L. and Vagle, S., 2003. Structure and Generation of Turbulence at Interfaces Strained by Internal Solitary Waves Propagating Shoreward over the Continental Shelf. *Journal of Physical Oceanography*, 33(10), pp. 2093–2112. https://doi.org/10.1175/1520-0485(2003)033<2093:SAGOTA>2.0.CO;2
2. Navrotsky, V.V., Lyapidevsky, V.Yu., Pavlova, E.P. and Khrapchenkov, F.F., 2010. Internal Waves and Mixing in the Shelf Zone. *Izvestia TINRO*, 162, pp. 324–337 (in Russian).
3. Bondur, V.G., Serebryany, A.N., Zamshin, V.V., Tarasov, L.L. and Khimchenko, E.E., 2019. Intensive Internal Waves with Anomalous Heights in the Black Sea Shelf Area. *Izvestiya, Atmospheric and Oceanic Physics*, 55(1), pp. 99–109. https://doi.org/10.1134/S000143381901002X
4. Navrotsky, V.V., Liapidevskii, V.Yu., Pavlova, E.P. and Khrapchenkov, F.F., 2019. Transformations and Effects of Internal Waves in the Nearshore Region of Sea. *Journal of Oceanological Research*, 47(2), pp. 230–245. https://doi.org/10.29006/1564-2291.JOR-2019.47(2).14 (in Russian).
5. Talipova, T.G., Pelinovsky, E.N., Kurkin, A.A. and Kurkina, O.E., 2014. Modeling the Dynamics of Intense Internal Waves on the Shelf. *Izvestia, Atmospheric and Oceanic Physics*, 50(6), pp. 630–637. https://doi.org/10.1134/S0001433814060164
6. Sabinin, K.D. and Serebryany, A.N., 2007. Hot Spots in the Field of Internal Waves in the Ocean. *Acoustical Physics*, 53(3), pp. 357–380. https://doi.org/10.1134/S1063771007030128
7. Van Haren, H., Groenewegen, R., Laan, M. and Koster, B., 2001. A Fast and Accurate Thermistor String. *Journal of Atmospheric and Oceanic Technology*, 18(2), pp. 256–265. https://doi.org/10.1175/1520-0426(2001)018%3C0256:AFAATS%3E2.0.CO;2
8. Van Haren, H., Groenewegen, R., Laan, M. and Koster, B., 2005. High Sampling Rate Thermistor String Observations at the Slope of Great Meteor Seamount. *Ocean Science*, 1(1), pp. 17–28. https://doi.org/10.5194/os-1-17-2005
9. Liu, A.K., Su, F.-C., Ming.-Kuang., H., Kuo, N.-J. and Ho, C.-R., 2013. Generation and Evolution of Mode-Two Internal Waves in the South China Sea. *Continental Shelf Research*, 59, pp. 18–27. https://doi.org/10.1016/j.csr.2013.02.009
10. Ivanov, V.A., Shul'ga, T.Ya., Bagaev, A.V., Medvedeva, A.V., Plastun, T.V., Verzhevskaya, L.V. and Svishcheva, I.A., 2019. Internal Waves on the Black Sea Shelf near the Heracles Peninsula: Modeling and Observation. *Physical Oceanography*, 26(4), pp. 288–303. https://doi.org/10.22449/1573-160X-2019-4-288-303
11. Serebryany, A.N. and Ivanov, V.A., 2013. Study of Internal Waves in the Black Sea from Oceanography Platform of Marine Hydrophysical Institute. *Fundamental and Applied Hydrophysics*, 6(3), pp. 34–45 (in Russian).
12. Tolstosheev, A.P., Lunev, E.G. and Motyzhev, S.V., 2014. [Analysis of the Results of in situ Experiments with Thermoprofiling Drifting Buoys in the Black Sea and other Areas of the World Ocean]. *Morskoy Gidrofizicheskiy Zhurnal*, (5), pp. 9–32 (in Russian).

13. Tolstosheev, A.P., Motyzhev, S.V. and Lunev, E.G., 2020. Results of Long-Term Monitoring of the Shelf Water Vertical Thermal Structure at the Black Sea Hydrophysical Polygon of RAS. *Physical Oceanography*, 27(1), pp. 69–80. https://doi.org/10.22449/1573-160X-2020-1-69-80
14. Ocherdnik, V.V., Zatsepin, A.G., Kuklev, S.B., Baranov, V.I. and Mashura, V.V., 2020. Examples of Approaches to Studying the Temperature Variability of Black Sea Shelf Waters with a Cluster of Temperature Sensor Chains. *Oceanology*, 60(2), pp. 149–160. https://doi.org/10.1134/S000143702001018X
15. Ocherednik, V.V., Silvestrova, K.P., Myslenkov, S.A. and Mashura, V.V., 2018. [Study of Internal Waves by Data from Three Anchored Thermochains]. In: V. A. Gritsenko, ed., 2018. [*Coastal Zone of Sea: Research, Management, Prospects. Collection of Papers of International Summer School. Kaliningrad, 26–31 August 2018*]. Kaliningrad: BFU im. Kanta, pp. 12–16 (in Russian).
16. Ocherednik, V.V., Baranov, V.I., Zatsepin, A.G. and Kyklev, S.B., 2018. Thermochains of the Southern Branch, Shirshov Institute of Oceanology, Russian Academy of Sciences: Design, Methods, and Results of Metrological Investigations of Sensors. *Oceanology*, 58(5), pp. 661–671. https://doi.org/10.1134/S0001437018050090
17. Ocherednik, V.V., Zatsepin, A.G., Kuklev, S.B., Baranov, V.I. and Mashura, V.V., 2020. Examples of Approaches to Studying the Temperature Variability of Black Sea Shelf Waters with a Cluster of Temperature Sensor Chains. *Oceanology*, 60(2), pp. 149–160. https://doi.org/10.1134/S000143702001018X
18. Ocherednik, V.V. and Zatsepin, A.G., 2023. Packages of Short-Period Internal Waves on the Black Sea Shelf Based on the Measurement Data of the Thermoresistor Chains Cluster. *Physical Oceanography*, 30(5), pp. 612–631.
19. Silvestrova, K., Myslenkov, S., Puzina, O., Mizyuk, A. and Bykhalova, O., 2023. Water Structure in the Utrish Nature Reserve (Black Sea) during 2020–2021 According to Thermistor Chain Data. *Journal of Marine Science and Engineering*, 11(4), 887. https://doi.org/10.3390/jmse11040887
20. Suchova, L.I., Hussein, H.M., Yakunin, M.A. and Yakunin, A.G., 2015. Study of Long-Term Stability Parameters of Thermal Sensors DS18B20. *Proceedings of TUSUR University*, (1), pp. 42–46 (in Russian).
21. Gaisky, V.A. and Gaisky, P.V., 2001. Distributed Thermoprofilometers and their Capabilities in Oceanographic Investigations. *Physical Oceanography*, 11(6), pp. 543–577. https://doi.org/10.1007/BF02509846
22. Gayskiy, V.A. and Gayskiy, P.V., 2018. *Use of Distributed Sensors for Sea Temperature Measurements*. Sevastopol: IPTS, 222 p. https://doi.org/10.33075/978-5-6040795-4-6 (in Russian).
23. Slepyshev, A.A., Alieva, A.N. and Laktionova, N.V., 2011. Nonlinear Effects in the Process of Propagation of Internal Waves in the Presence of Turbulence. *Physical Oceanography*, 21(2), pp. 85–97. https://doi.org/10.1007/s11110-011-9106-6
24. Samodurov, A.S., Chukharev, A.M., Kazakov, D.A., Pavlov, M.I. and Korzhuev, V.A., 2023. Vertical Turbulent Exchange in the Black Sea: Experimental Studies and Modeling. *Physical Oceanography*, 30(6), pp. 689–713.
25. Biliunas, M.V. and Dotsenko, S.F., 2012. Free Internal Waves in an Inhomogeneous Current with Vertical Shear of Velocity. *Morskoy Gidrofizicheskiy Zhurnal*, (1), pp. 3–16 (in Russian).

Submitted 29.07.2023; accepted after review 11.12.2023;
revised 27.12.2023; published 25.03.2024

About the author:

Pavel V. Gaisky, Leading Research Associate, Head of Innovation Marine Instrument Engineering Laboratory of SCU, Marine Hydrophysical Institute of RAS (2 Kapitanskaya St., Sevastopol, 299011, Russian Federation), Ph.D. (Tech.), **Scopus Author ID: 7801588003**, **ORCID ID: 0000-0003-3110-848X**, **ResearcherID: HQZ-3112-2023**, *gaysky@inbox.ru*

The author has read and approved the final manuscript.

Original article

The Content of Hydrocarbons and Indicator Groups of Bacteria in the Marine Environment of Laspi Bay (Southern Coast of Crimea)

E. A. Tikhonova, O. V. Soloveva, Yu. S. Tkachenko *, N. V. Burdiyan, Yu. V. Doroshenko, E. V. Guseva, S. V. Alyomov

A. O. Kovalevsky Institute of Biology of the Southern Seas of RAS, Sevastopol, Russia
** e-mail: yulechkatkachenko.90@mail.ru*

Abstract
The paper assesses the quality of the marine environment of Laspi Bay near the Batiliman Stow according to main chemical and microbiological parameters under various recreational impacts on the water area. The material for the study was water and fouling samples taken in May, July and October 2023. The qualitative and quantitative composition of hydrocarbons was determined by gas chromatography on a Crystal 5000.2 chromatograph with a flame ionization detector in the Scientific and Educational Center for Collective Use «Spectrometry and Chromatography» of A. O. Kovalevsky Institute of Biology of the Southern Seas of RAS. Diagnostic markers of the origin of hydrocarbons were used to identify possible sources of organic substances. The abundance of bacteria groups (saprophytic heterotrophic, hydrocarbon-oxidizing, lipolytic and phenol-oxidizing) was determined by the method of tenfold dilutions using elective nutrient media. From May to October 2023, the concentration of hydrocarbons in the coastal waters of the Batiliman Stow was 0.013–0.304 mg·L^{-1}. The composition of n-alkanes indicated the absence of oil pollution in the studied water area. The exceedance of the maximum permissible concentration for hydrocarbons, noted in July at one of the stations, is of natural origin and is associated with an active intake of allochthonous compounds. The quantitative assessment of the mentioned bacteria groups in the water and microperiphyton of macrofouling indicates an increase in the abundance of indicator groups of bacteria in all samples taken in July. Nevertheless, the results of the hydrocarbon content study and the quantitative assessment of the main microbiological indicators in the water and microperiphyton of macrofouling suggest that there are active bacterial self-purification processes in the water area of the Batiliman Stow. According to microbiological indicators, the studied area can be classified as conditionally clean.

Keywords: coastal water area, recreational load, seawater, markers, periphyton, heterotrophic bacteria, hydrocarbon-oxidizing bacteria, lipolytic bacteria, phenol-oxidizing bacteria, macrophytes, Laspi Bay, anthropogenic pollution, petroleum hydrocarbons

Acknowledgments: The work was carried out under IBSS state research assignment “Study of biogeochemical patterns of radioecological and chemoecological processes in the ecosystems of water bodies of the Sea of Azov–Black Sea Basin in comparison with other areas of the World Ocean and individual aquatic ecosystems of their drainage basins to ensure sustainable development in the southern seas of Russia” (no. 1023032000047-8-1.6.19).

For citation: Tikhonova, E.A., Soloveva, O.V., Tkachenko, Yu.S., Burdiyan, N.V., Doroshenko, Yu.V., Guseva, E.V. and Alyomov, S.V., 2024. The Content of Hydrocarbons and Indicator Groups of Bacteria in the Marine Environment of Laspi Bay (Southern Coast of Crimea). *Ecological Safety of Coastal and Shelf Zones of Sea*, (1), pp. 113–129.

Содержание углеводородов и индикаторных групп бактерий в морской среде бухты Ласпи (Южный берег Крыма)

Е. А. Тихонова, О. В. Соловьёва, Ю. С. Ткаченко *, Н. В. Бурдиян, Ю. В. Дорошенко, Е. В. Гусева, С. В. Алёмов

ФГБУН ФИЦ Институт биологии южных морей имени А. О. Ковалевского РАН, Севастополь, Россия

* *e-mail: yulechkatkachenko.90@mail.ru*

Аннотация

Оценено качество морской среды бухты Ласпи в районе урочища Батилиман по основным химико-микробиологическим параметрам в периоды различной рекреационной нагрузки на акваторию. Материалом для исследования послужили пробы воды и обрастаний, отобранные в мае, июле и октябре 2023 г. Качественный и количественный состав углеводородов определялся на базе НОЦКП «Спектрометрия и хроматография» ФИЦ ИнБЮМ методом газовой хроматографии на хроматографе «Кристалл 5000.2» с пламенно-ионизационным детектором. Для идентификации вероятных источников поступления органических веществ использовали диагностические маркеры происхождения углеводородов. Численность групп бактерий (сапрофитных гетеротрофных, углеводородокисляющих, липолитических и фенолокисляющих) определяли методом предельных десятикратных разведений с использованием элективных питательных сред. Концентрация углеводородов в прибрежных водах урочища Батилиман с мая по октябрь 2023 г. составляла 0.013–0.304 мг·л$^{-1}$. Состав н-алканов указывал на отсутствие нефтяного загрязнения в исследуемой акватории. Превышение ПДК для углеводородов, отмеченное в июле на одной из станций, носит природный характер и связано с активным поступлением аллохтонных соединений. Количественная оценка обозначенных групп бактерий в воде и микроперифитоне макрообрастаний указывает на возрастание численности индикаторных групп бактерий во всех пробах, отобранных в июле. Тем не менее результаты исследования углеводородного фона и количественной оценки основных микробиологических показателей в воде и микроперифитоне макрообрастаний указывают на то, в акватории урочища Батилиман активно происходят процессы бактериального самоочищения. По микробиологическим показателям исследуемый участок можно отнести к условно-чистым акваториям.

Ключевые слова: прибрежная зона, рекреационная нагрузка, морская вода, маркеры, перифитон, гетеротрофные бактерии, углеводородокисляющие бактерии, липолитические бактерии, фенолокисляющие бактерии, макрофиты, бухта Ласпи, антропогенное загрязнение, нефтяные углеводороды

Благодарности: работа выполнена в рамках государственного задания ФИЦ ИнБЮМ по теме «Изучение биогеохимических закономерностей радиоэкологических и хемоэкологических процессов в экосистемах водоемов Азово-Черноморского бассейна в сравнении с другими акваториями Мирового океана и отдельными водными экосистемами их водосборных бассейнов для обеспечения устойчивого развития на южных морях России» (номер гос. регистрации 1023032000047-8-1.6.19).

Для цитирования: Содержание углеводородов и индикаторных групп бактерий в морской среде бухты Ласпи (Южный берег Крыма) / Е. А. Тихонова [и др.] // Экологическая безопасность прибрежной и шельфовой зон моря. 2024. № 1. С. 113–129. EDN SIPAOH.

Introduction

The coastline of the Batiliman Stow (a coastal-aquatic complex between Cape Sarych and Laspi Bay), from where the mountains of the Southern coast of Crimea begin, stretches from the base of Mount Kush-Kaya to Laspi Bay. The area is characterised by intense water exchange with the open sea and by high aeration. Runup and surge phenomena typical of the Southern coast of Crimea result in water salinity fluctuating from 17.70 to 18.47 [1].

From the water's edge to shallow depths (10 m) the bottom is represented by boulders (boulder bench) (Fig. 1) with rare areas of sandy bottom (Fig. 2). The granulometric composition of bottom sediments and peculiarities of morphodynamic conditions of the environment (drift of fine fractions to shallow zones) determine the absence of organic carbon accumulation within this coastal area [2].

This is correlated with the reports [3] on the low number of microbial population in the loose bottom sediments of nearby Laspi Bay where the number of saprophytic heterotrophic bacteria averages 2500 cells·g^{-1} and the number of hydrocarbon-oxidising bacteria does not exceed 2 cells·g^{-1}. Of the macrophytes, *Cystoseira crinita* (Dyby, 1830) and *Ceramium diaphanum* (Roth, 1806) dominate year-round in terms of occurrence, while *C. crinita* and *C. barbata* (C. Agardh, 1820) dominate in terms of phytomass [4]. *Cystoseira spp*. is the main component of coastal phytocenosis and one of the main sources of organic matter [5]. Besides, *Cystoseira spp*. is considered to be the most suitable object of algomonitoring in assessing the environmental quality of marine coastal water areas, including the water area of Batiliman Stow [6].

The Batiliman Stow bordering the sea from the west of Cape Aya is a state natural landscape reserve of regional significance [1)] and includes 208 ha of the Black Sea water area. The territory up to the next protected object, hydrological natural monument Coastal Aquatic Complex at Cape Sarych, has no nature protection status, although works in this regard are being done. The authors of work [7] proposed

[1)] Government of the City of Sevastopol, 2016. *On Amendments to the Resolution of the Government of the City of Sevastopol no. 409-ПП "On Approval of the Regulations on the State Natural Landscape Reserve of Regional Significance Cape Aya" as of 29 April 2016.* Resolution of the Government of the City of Sevastopol no. 178-ПП as of 25 April 2022. Sevastopol: Government of the City of Sevastopol (in Russian).

to create a national park Yuzhnoberezhny from Balaklava Bay to Cape Sarych including the adjacent water area and protected areas of regional significance.

This area is highly appealing for tourists, but due to its small recreational capacity there is a danger of negative impact of mass unregulated visitation on the state of the water area ecosystem. Over the last decades, the ecological state of the concerned water area has deteriorated. This is due to the increase in the flow of visitors and development of the coastal zone, as well as the placement of mussel farms nearby (with an output of up to 83 t (per dry weight) of biosediments per year, including 3 t of protein and 1 t each of carbohydrates and lipids [8]). Recent studies have shown that the number of polychaete species has decreased from 64 (1983) to 45 (2019) [9], the macrophytobenthos stock of the Black Sea environment-forming species have decreased by about 1.5 times, whereas some bottom areas have lost vegetation at all [10]. According to the authors of work [11], in 2017–2018, the content of petroleum hydrocarbons (PHC) in the water of Laspi Bay was close to the maximum permissible levels. At the same time, in the summer of 2018, the maximum permissible concentration (MPC) was exceeded 3–4 times. The PHC content in Laspi Bay was higher than their average content in Sevastopol bays, and in 2016 the frequency of recorded cases of exceeding MPC in the bottom horizon of the water area of Laspi Bay was 25% [12, 13]. Thus, the authors indicate that the study area, previously classified as reference clean, is under a significant anthropogenic impact. Probably, the obtained results are related to the recent active development of the coastline of Laspi Bay [11].

Of note, this part of the coast is often affected by landslides, mudflows and coastal abrasion [14]. Development of this area only worsens the situation.

Preservation of the Batiliman Stow coastal-aquatic complex requires an integrated approach to the study of the coastal water area to calculate the current level of anthropogenic pressure and the stability of the complex against it. This approach will also allow proposing measures to minimise the negative effects of increasing recreational load without affecting the established cycle of matter and energy as well as aesthetics of this unique place.

Within an integrated approach to the study of the ecological state of the Batiliman beach water area, there has been little research of the hydrocarbon (HC) content in seawater and characteristics of its bacterial population, which is the first link in the process of biological self-purification of the marine environment.

The work aims to assess the content of HCs and indicator groups of bacteria in the marine environment of Laspi Bay.

The objectives of the study include determination of:

– qualitative and quantitative composition of HCs in the coastal water area of Laspi Bay;

– the number of saprophytic heterotrophic bacteria – the main destructors of readily available organic compounds in water and in microperiphyton of macrofouling;

– abundance of indicator groups of bacteria – oil, phenol and fat destructors in water and in microperiphyton of macrofouling.

Material and methods

Water samples for HC analysis were taken in May, July and October 2023 at two stations. Station *1* – biostation, low-exploited area with a low anthropogenic load. Station *2* – Tavrida Beach, an area with a high anthropogenic load in summer. Both at Station *1* and Station *2*, water was sampled near the water edge (Fig. 1).

Water samples were taken in glass-stoppered glass bottles with a capacity of 1 dm^3, pre-washed with chromium mixture, tap and distilled water and rinsed with hexane. Before sampling, the bottles were pre-washed with n-hexane and rinsed with the sampled water.

Sample preparation was carried out according to the procedure [2)]. A water sample (250 mL) acidified with sulfuric acid (1:1) (1.5 mL) was extracted twice with n-hexane (25 mL each). The hexane extract was passed through a glass column filled with aluminium oxide and concentrated to a volume of 1 mL at room temperature in a fume hood.

The qualitative and quantitative composition of HCs was determined at the Scientific and Educational Center for Collective Use "Spectrometry and Chromatography" of IBSS using a Crystal 5000.2 gas chromatograph with a flame ionization detector (FID).

An aliquot of the concentrated extract was injected with a microsyringe into the gas chromatograph evaporator heated to 250 °C. HCs were separated

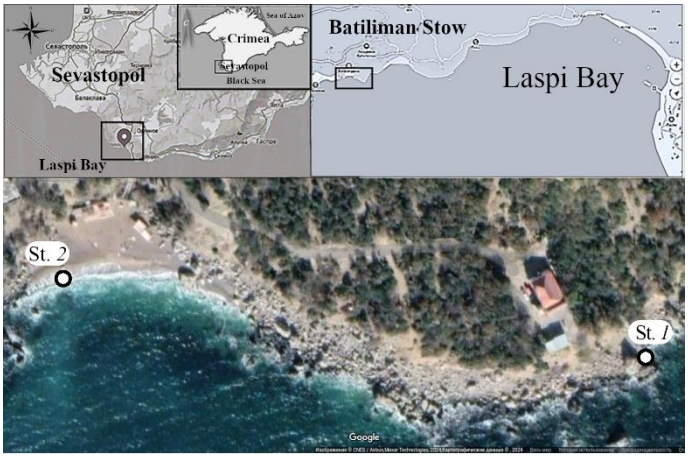

Fig. 1. The map of seawater and macrofouling sampling in the water area of the Batiliman Stow, 2023. Google Maps image (available at https://www.google.ru/maps)

[2)] Drugov, Yu.S. and Rodin, A.A., 2020. [*Ecological Analyses in Oil and Petroleum Product Spills. A Practical Guide*]. Moscow: Laboratoriya Znaniy, 270 p. (in Russian).

on a TR-1MS capillary column 30 m long, 0.32 mm in diameter and with the stationary phase film thickness of 0.25 μm (Termo Scientific). The column temperature was programmed from 70 to 280 °C (rate of temperature rise: 8 °C·min^{-1}). The carrier gas (nitrogen) flow in the column was 2.5 mL·min^{-1} without flow splitting. The detector temperature was 320 °C.

Quantitation of the total HC content was performed by absolute calibration of the FID with a standard mixture of HCs (C_{10}–C_{40}) ranging 0.01–0.5 mg·L^{-1}. A standard sample of ASTMD2887 Reference Gas Oil standard (SUPELCO, USA) was used as a HC mixture. The total HC content was determined by the sum of the areas of eluted n-alkanes peaks and the unresolved complex mixture (UCM). The results were processed with the Chromatec Analytical 3.0 software (the absolute calibration and percentage normalization method).

The following diagnostic indices were used to identify HC genesis: terrigenous/aquatic ratio (TAR) [15], average chain length (ACL) [16], and low-molecular weight to high-molecular weight homologues ratio (LWH/HWH) [17]. The P_{aq} index [18] (aquatic to terrestrial plant index) determines the type of vegetation prevailing in the organic matter formation. Carbon Preference Indices CPI_1 [19], calculated for lighter n-alkanes, and CPI_2 [16], calculated for the high-molecular weight part of the spectrum, are used to identify the petroleum and biogenic origin of HCs. The HC genesis markers were determined according to the ratios presented in Table 1.

Seawater samples for microbiological analysis were collected in sterile 50 cm^3 tubes and fouling samples were collected in sterile jars. In this study, the macrofouling community was assessed from which microperiphyton was then washed out

Table 1. Main diagnostic indices for identification of the hydrocarbon genesis

Index	Formula
TAR	$\sum(C_{27} + C_{29} + C_{31})/\sum(C_{15} + C_{17} + C_{19})$
LWH/HWH	$\sum(C_{13}–C_{21})/\sum(C_{22}–C_{37})$
ACL	$(27C_{27} + 29C_{29} + 31C_{31} + 33C_{33} + 35C_{35} + 37C_{37})/(C_{27} + C_{29} + C_{31} + C_{33} + C_{35} + C_{37})$
CPI_1	$^1/_2\ \{(C_{15} + C_{17} + C_{19} + C_{21})/(C_{14} + C_{16} + C_{18} + C_{20}) + (C_{15} + C_{17} + C_{19} + C_{21})/(C_{16} + C_{18} + C_{20} + C_{22})\}$
CPI_2	$^1/_2\{(C_{25} + C_{27} + C_{29} + C_{31} + C_{33} + C_{35})/(C_{24} + C_{26} + C_{28} + C_{30} + C_{32} + C_{34}) + (C_{25} + C_{27} + C_{29} + C_{31} + C_{33} + C_{35})/(C_{26} + C_{28} + C_{30} + C_{32} + C_{34} + C_{36})\}$
P_{aq}	$(C_{23} + C_{25})/(C_{23} + C_{25} + C_{29} + C_{31})$

to determine bacterial abundance. In all sampling periods, macrofouling was represented exclusively by Cystosira. Its abundance decreased naturally from May to October, and its biomass was slightly higher in all sampling periods at St. *1*. The abundance of saprophytic heterotrophic (HB), hydrocarbon-oxidising (HOB), lipolytic (LB) and phenol-oxidising (POB) bacterial groups was determined in each sample. The abundance of these bacterial groups was determined by the method of tenfold dilutions using selective nutrient media. For HBs, a peptone medium was used [20]. HOBs and LBs were cultured on a Voroshilova–Dianova medium [21], to which sterile oil or vegetable fat (1% of the volume) was added as the only source of carbon and energy. For phenol-oxidising bacteria, a modified Kalabina–Rogovskaya medium was used [22]. When preparing the media, the salinity of seawater was taken into account. The most probable number of microorganisms per unit volume was calculated using McCready's table (in triplicate) based on the method of variation statistics [3)].

Results and discussion

The total HC content in water at the studied stations from May to October 2023 ranged from 0.013 to 0.304 mg·L^{-1} (Fig. 2). In July, at St. *1*, the exceedance of MPC for fishery water bodies (0.05 mg/L) [4)] by 6 times was recorded (Fig. 2), at St. *2* during the study period, the value of HC concentration was rather low and did not exceed the MPC.

Comparing the indicators of the low-exploited coastal area and the beach, it is difficult to speak about the increase of HC content on the beach in summer, when the anthropogenic load on the coast increases significantly. Probably, other factors play the leading role in formation of hydrocarbon content in the coastal waters of this area.

The study of the individual composition of n-alkanes, as well as calculation of markers characterising the sources of organic substances origin in water, allow more reliable identification of HC input sources.

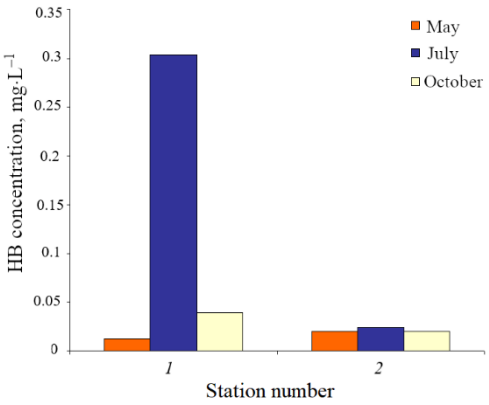

Fig. 2. Hydrocarbon concentrations in the coastal waters of the Batiliman Stow, May–October 2023

[3)] Netrusov, A.I., ed., 2005. [*Practical Course on Microbiology*]. Moscow: Akademiya, 608 p. (in Russian).

[4)] Ministry of Agriculture of Russia, 2016. *On the Approval of Water Quality Standards for Water Bodies of Commercial Fishing Importance, Including Standards for Maximum Permissible Concentrations of Harmful Substances in the Waters of Water Bodies of Commercial Fishing Importance*: Order of the Ministry of Agriculture of Russia dated December 13, 2016, No. 552. Moscow: Ministry of Agriculture of Russia (in Russian).

In water samples collected from May to October 2023, n-alkanes in the range n-C_{17}–C_{31} were identified (Fig. 3), the n-alkane C_{31} was detected only once at St. *1* in July (Fig. 3, *b*). The homologues of C_{29} and C_{30} were not detected in May at both stations (Fig. 3, *a*), the other n-alkanes were represented everywhere.

The distribution of n-alkanes obtained in May at both stations was unimodal. Surface water samples collected in May 2023 were dominated by low-molecular weight homologues (Fig. 3, *a*), in particular heptadecane (n-C_{17}), which is the main alkane produced by phyto- and zooplankton [23, 24], and alkane n-C_{19}, also of phytoplanktonic genesis. The C_{18} and C_{20} peaks were well pronounced. They are associated with the development of bacterial community [25]. Markers *TAR* and CPI_1 (Table 2) show the predominance of autochthonous matter in water, formed as a result of microbiological degradation of organic matter [26].

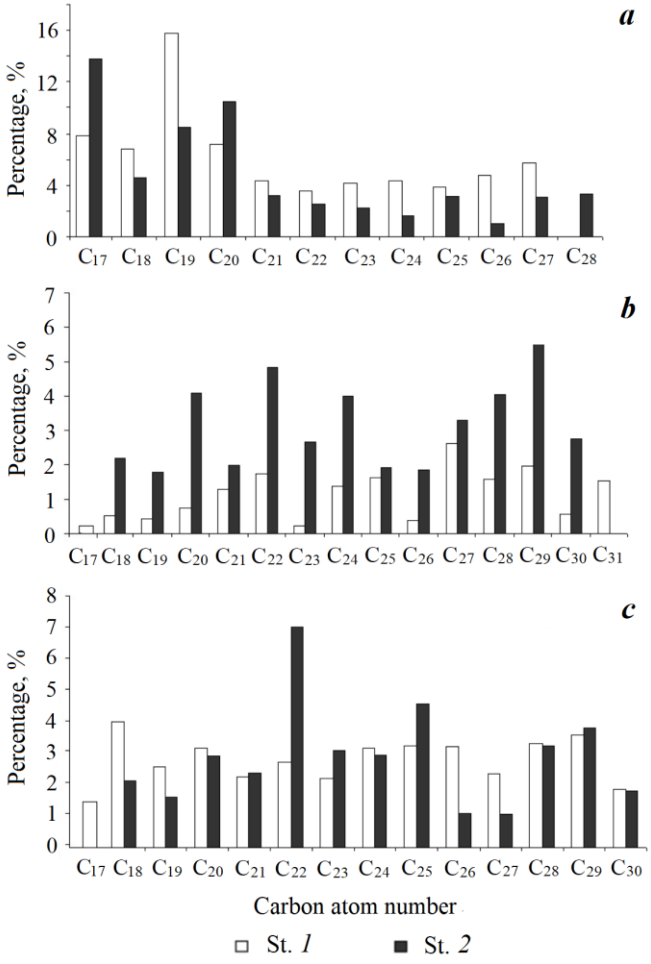

F i g . 3 . Distribution of n-alkanes in the coastal waters of the Batiliman Stow: May (*a*), July (*b*), October (*c*), 2023

Table 2. Content and composition of n-alkanes (markers) in the water of the coastal water area of the Batiliman Stow, May–October 2023

Station number	D	C	LWH/ HWH	P_{aq}	TAR	ACL	CPI_1	CPI_2
				May				
1	C_{17}–C_{27}	0.013	1.59	1.00	0.23	26.17	1.78	1.50
2	C_{17}–C_{28}	0.020	2.66	1.00	0.12	26.00	1.79	1.23
				July				
1	C_{17}–C_{31}	0.304	0.21	0.34	13.57	28.00	1.08	2.50
2	C_{18}–C_{30}	0.024	0.34	0.52	4.50	27.40	0.48	0.92
				October				
1	C_{17}–C_{30}	0.040	0.65	0.65	1.27	27.00	0.73	0.93
2	C_{18}–C_{30}	0.020	0.34	0.65	3.33	26.90	0.60	1.32

Note: D – the range of identified n-alkanes; C – total concentration of identified n-alkanes, mg·L^{-1}.

Thus, the n-alkanes in the water samples collected in May 2023 are predominantly autochthonous and are associated with phytoplankton and bacterial production. The above season is characterised by active phytoplankton development [27].

In July, a relatively uniform distribution of n-alkanes was recorded at St. *1*, where the MPC exceedance was observed. At St. *2*, the distribution differed, showing signs of bimodality (Fig. 3, *b*): the first peak (even-numbered n-alkanes in the range C_{18}–C_{24}) may be associated with the work of the bacterial community, whereas the second peak (C_{27}–C_{30}) is usually associated with higher plants of both aquatic and terrestrial origin [25].

At St. *1*, the n-C_{17} homologue was identified in small amounts, while at St. *2* it was not detected at all (Fig. 3, *b*). The *TAR* index at both stations was significantly greater than unity (Table 2), indicating the predominance of allochthonous matter coming from land.

Though at St. *1* in July 2023, the exceedance of MPC by 6 times was recorded, the CPI_2 index value was 2.5 (Table 2), indicating the biogenic origin of organic matter. Moreover, the C_{17}/C_{25} ratio was 0.08 (Table 2), indicating the predominance of allochthonous homologues [28]. The *TAR* index value significantly exceeded unity and was 13.57 (Table 2), which also shows the predominance of allochthonous matter in the water area.

Thus, despite the relatively uniform distribution of n-alkanes, which may signify fresh oil pollution, markers of the latter were absent. Diagnostic indices clearly indicate the predominance of biogenic allochthonous matter. It can be concluded that no oil pollution was detected in the studied samples, and the increased values of HC concentrations were due to natural processes.

In surface water samples collected in October 2023, the distribution of n-alkanes was relatively monotonous (Fig. 3, *c*). The n-C_{22} homologue was dominant at St. *2*; together with the CPI value (Table 2), this indicates the presence of HC microbial degradation products in open surface water [25, 29]. In the high-molecular weight part of the spectrum, the peak associated with the n-alkane C_{25}, which is of allochthonous origin, was pronounced for St. *2*. The homologue C_{17}, which is a marker of phyto- and zooplankton, was absent at St. *2* (Fig. 3, *c*). The values of TAR and LWH/HWH indices (Table 2) at the studied stations indicate the dominance of allochthonous matter coming from land. No signs of oil pollution were detected, as indicated by the CPI_2 marker value (Table 2).

The ACL marker is used to reveal changes in the ecosystem. The marker remains stable for a long time and decreases abruptly in case of oil pollution [30]. High values of the ACL marker indicate the predominant contribution of herbaceous vegetation to HC formation, while low ACL values are characteristic of HCs of wood origin. This index ranged from 26 to 28 (mean 26.9 ± 0.7) (Table 2) at both stations, which indicates the absence of fresh oil inputs and reflects approximately the same contribution of woody and herbaceous plants to the formation of organic matter of surface open waters in the water area. The P_{aq} indicator [18] (Table 2) allows determining the type of vegetation prevailing in the process of organic matter formation: terrigenous or aquatic [18]. The indicator shows that in May, HCs of aquatic origin prevailed, whereas in July, terrigenous matter dominated at St. *1*. The proportions of autochthonous and allochthonous matters were approximately equal at St. *2*. In October, a slight predominance of autochthonous compounds was noted at both stations.

From the analysis results of the water samples taken in the water area of the Batiliman Stow from May to October 2023, including during the high recreational season, it was not possible to establish oil pollution of the bay waters. The main sources of formation of hydrocarbon background of the water area in May were autochthonous processes associated with the production of phytoplankton and bacterial destruction of organic matter. In subsequent periods, the importance of phytoplankton production decreased, bacterial processes and the input of allochthonous compounds came to the foreground. The exceedance of sanitary norm values (MPC = 0.05 mg·L^{-1}), observed in July (0.304 mg·L^{-1}) at one of the stations, is of natural character and associated with active input of allochthonous compounds.

An important indicator of the marine environment quality is the state of the bacterial community, for which organic matter, including HCs, entering

the water area is a nutritious substrate. Our results on the origin of HCs indicate active participation of bacteria in the synthesis and transformation of HCs.

The results of the performed microbiological studies show that the maximum HB abundance ($2.5 \cdot 10^3$ cells·mL^{-1}) in water was observed once in the May sample of St. *1* (Fig. 4, *a*), while in the other samples of St. *1*, the number of HBs varied from 95 to 950 cells·mL^{-1}. In the beach water area (St. *2*), HB abundance ranged from 150 to 950 cells·mL^{-1} (Fig. 4, *a*). In May and July, the HB abundance at both stations exceeded the HB values in October samples, which is probably related to the phytoplankton blooms, typical of spring [31], and the increase in water temperature in summer. The HB abundance in water of the studied sites is similar to the data [32] obtained earlier in the conditionally clean water area.

At St. *1*, HOBs were detected in all samples. The maximum (95 cells·mL^{-1}) was observed in the July sample, while in the remaining samples, the abundance of HOBs did not exceed 10 cells·mL^{-1} (Fig. 4, *b*). In the May sample of St. *2*, no HOBs were detected, and in October they were represented by single cells in a millilitre of seawater (Fig. 4, *b*). The HOB maximum at St. *2* was identified in July (95 cells·mL^{-1}). The HOB share of the HB abundance in water samples at St. *1* did not exceed one per cent in May, and in July and October it was 10%. At St. *2* , the HOB share of the HB abundance was 10% in July and it decreased to 1.6% in the October sample. In clean waters, hydrocarbon-oxidising microorganisms are considered to account for up to 7% of saprophytic heterotrophic microflora [33].

No lipolytic bacteria were cultured in the May sample of St. *1* (Fig. 4, *c*). The maximum LB abundance was observed in July (200 cells·mL^{-1}), and in October, the LB value was an order of magnitude less. The LB abundance in the water of St. *2* ranged from 2 to 150 cells·mL^{-1} (Fig. 4, *c*). The LB maximum was determined in July, as at St. *1*.

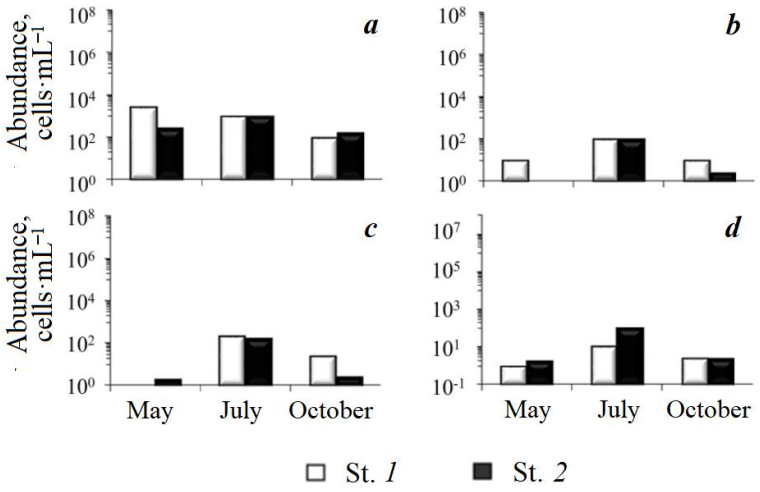

F i g . 4 . Dynamics of the abundance (cells·mL^{-1}) of heterotrophic (*a*), hydrocarbon-oxidizing (*b*), lipolytic (*c*), phenol-oxidizing (*d*) bacteria in the water

POBs at St. *1* were detected in all samples (Fig. 4, *d*). The maximum (10 cells·mL^{-1}) was detected at station *1* in July, while in the other samples of St. *1*, this group of bacteria was represented by single cells per millilitre of seawater. At St. *2*, POBs were also detected in all samples (Fig. 4, *d*). The maximum (95 cells·mL^{-1}) was detected at St. *2* in July. In other samples, the POB abundance was under 10 cells·mL^{-1}.

The obtained results (Fig. 5, *a*) for the assessment of HB abundance in the macrofouling microperiphyton showed that at St. *1* the maximum HB abundance ($2.5 \cdot 10^6$ cells·g^{-1}), indicating a sufficient amount of highly digestible organic matter, was observed in the May sample. In subsequent determinations, the HB abundance was $9.5 \cdot 10^3$ cells·g^{-1}. At St. *2*, the HB abundance in the May and October samples ranged from $2.5 \cdot 10^4$ – $4.5 \cdot 10^4$ cells·g^{-1}, with the abundance value of HBs decreasing by an order of magnitude in July. The highest HB abundance at St. *2*, as at St. *1*, was determined in the May sample ($4.5 \cdot 10^4$ cells·g^{-1}).

HOBs were cultured from all fouling samples from the mentioned stations (Fig. 5, *b*). At both stations, the HOB abundance varied from 95 to $2.5 \cdot 10^2$ cells·g^{-1}. However, at St. *1*, the lowest (95 cells·g^{-1}) HOB value was recorded in the May sample, while in the other samples of St. *1*, the HOB abundance ranged from $1.5 \cdot 10^2$ to $2.5 \cdot 10^2$ cells·g^{-1}. In the beach fouling (St. *2*), the maximum ($2.5 \cdot 10^2$ cells·g^{-1}) was obtained in July and the minimum (95 cells·g^{-1}) was recorded in October. The HOB share of HB in July samples of St. *1* was 1.6%, and in July samples of St. *1* and *2* it was 2.6 %. In other months the HOB share at both stations was under 1%. The quantitative indicators of HOB obtained in the water area of the Batiliman Stow are much lower than those obtained in the microperiphyton of breakwaters of the Sevastopol water area, which are under a significant anthropogenic load [34].

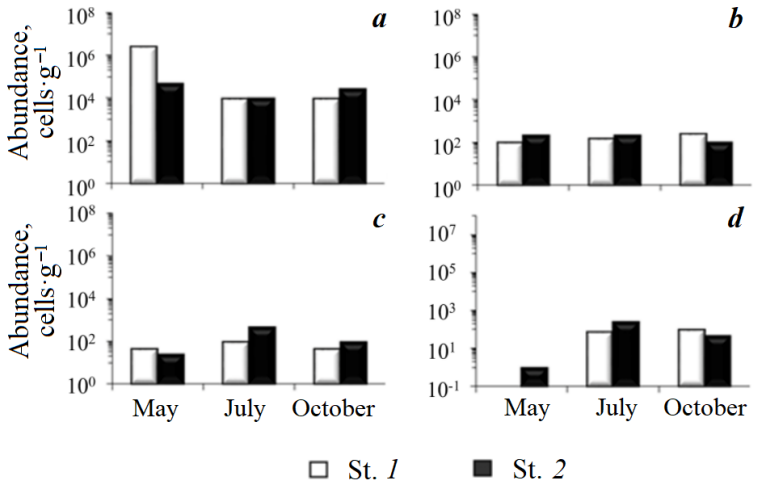

Fig. 5. Dynamics of the abundance (cells·g^{-1}) of heterotrophic (*a*), hydrocarbon-oxidizing (*b*), lipolytic (*c*), phenol-oxidizing (*d*) bacteria in the fouling

LBs were detected in 100% of fouling samples from St. *1* and *2* (Fig. 5, *c*). At St. *1*, the abundance of LBs ranged from 45 to 95 cells·g^{-1}, while at St. *2*, the range of LB abundance was 25–450 cells·g^{-1}. The highest LB abundance values at both stations were obtained at the height of the holiday season. The minimum LB abundance (25 cells·g^{-1}) was determined in the May sample at St. *2*. In the other samples at St. *1* and *2*, the abundance of LBs varied from 45 to 95 cells·g^{-1}.

POBs at St. *1* were not cultured in the May sample, the results of follow-up observations at St. *1* showed an increase in the POB abundance in July and October samples, 75 and 95 cells·g^{-1}, respectively (Fig. 5, *d*). At St. *2*, the POB abundance ranged from 1 to 250 cells·g^{-1} (Fig. 5, *d*). The maximum (250 cells·g^{-1}) at St. *2* was recorded in the July sample, the minimum in May, and in October the POB abundance in beach fouling decreased to 45 cells·g^{-1}.

The data analysis showed that the absence of a pronounced abundance peak of saprophytic heterotrophic bacteria (Fig. 4, *a*) and the observed increase in the hydrocarbon content in July at St. *1* (Fig. 2), given the composition of n-alkanes, can be related to the entry of high-molecular weight allochthonous compounds, which are less susceptible to bacterial degradation [35]. The input of allochthonous material can be related to precipitation occurred the day before (21–23 July 2023) (available at: https://goodmeteo.ru/pogoda-batiliman-orlinoe-sevastopol/23-7/) and the peculiarities of the station location (possibility of mudflows). The HOB share of the HB abundance in fouling at both stations was rather low and did not exceed 2.6%, which corresponds to the values for clean water areas [5)]. The obtained quantitative characteristics of POBs and LBs in the fouling of the Batiliman Stow water area at the investigated sites were much lower than similar indicators of Golubaya Bay Beach (Sevastopol water area), at the same time the POB content was much higher than that in the periphyton of Golubaya Bay Beach [32]. The increase in the abundance of indicator groups of bacteria (HOBs, LBs and POBs) at St. *1* and *2* in July both in the water samples and in the microperiphyton is a response of the microbial community to seasonal changes in the ecosystem, including an increase in the anthropogenic load on the water area of the Southern Coast of Crimea.

Conclusions

From May to October 2023, the HC concentration in the coastal waters of Batiliman Stow was 0.013–0.304 mg/L. The composition and content of HCs in the coastal waters of the Batiliman Stow are caused by natural processes. Oil pollution was not recorded.

Quantitative assessment of the indicated groups of bacteria in water and microperiphyton of macrofouling and the obtained results of hydrocarbon content study indicate that, despite a significant anthropogenic load in summer, there are active bacterial self-purification processes in the water area of the Batiliman Stow. Based on the microbiological indicators, the studied area can be classified as conditionally clean.

[5)] Mishustina, I.E., Shcheglova, I.K. and Mitskevich, I.N., 1985. [*Marine Microbiology*]. Vladivostok: DVGU, 184 p. (in Russian).

Taking into account the increasing anthropogenic load on this part of the coast, associated with the construction of tourist facilities, the results of baseline studies can be used further for comparative analysis of the state of the waters of the Batiliman Stow during environmental monitoring or environmental assessment in emergencies.

REFERENCES

1. Kuftarkova, E.A., Kovrigina, N.P. and Bobko, N.I., 1990. Estimation of Hydrochemical Conditions of the Laspi Bay, the Region of Mussel Cultivation. In: IBSS, 1990. *Ekologiya Morya.* Kiev: Naukova Dumka. Iss. 36, pp. 1–7 (in Russian).
2. Orekhova, N.A. and Ovsyany, E.I., 2020. Organic Carbon and Particle-Size Distribution in the Littoral Bottom Sediments of the Laspi Bay (the Black Sea). *Physical Oceanography*, 27(3), pp. 266–277. doi:10.22449/1573-160X-2020-3-266-277
3. Skuratovskaya, E. and Doroshenko, Yu., 2022. Complex Application of Microbiological Characteristics in Bottom Sediments and Biochemical Parameters of Mussel *Mytilus galloprovincialis* (Lam.) for Assessing the Ecological State of Marine Coastal Areas. *Pollution*, 8(3), pp. 1038–1048. doi:10.22059/poll.2022.337948.1341
4. Evstigneeva, I.K. and Tankovskaya, I.N., 2018. Macrophytobenthos of the Batiliman Seashore Region (Black Sea, Cape Ajja Reserve). *Bulletin of Tver State University. Series: Biology and Ecology*, (4), pp. 100–117. doi:10.26456/vtbio31 (in Russian).
5. Podkorytova, A.V. and Vafina, L.Kh., 2013. Chemical Composition of Brown Algae from the Black Sea: Genus Cystoseira, Perspectives for Their Use. In: M. K. Glubokovsky, ed., 2013. *Trudy VNIRO*. Moscow: VNIRO. Vol. 150, pp. 100–107 (in Russian).
6. Kravtsova, A.V., Milchakova, N.A. and Frontasyeva, M.V., 2014. The Features of Trace Elements Accumulation by Macroalgae Cystoseira in the Coastal Zone of Marine Protected Areas of the Crimea (the Black Sea). In: TNU, 2014. *Optimization and Protection of Ecosystems*. Simferopol: TNU. Iss. 10, pp. 146–158 (in Russian).
7. Milchakova, N.A., Bondareva, L.V., Aleksandrov, V.V., Chernysheva, E.B. and Ryabogina, V.G., 2019. Prospects for Forming Specially Protected Natural Territories of Federal Significance in Sevastopol City. In: KFU, 2019. *The Nature Reserves –2019. Biological and Landscape Diversity, Conservation and Management. The Abstracts of the IX Pan-Russian Scientific-Practical Conference (Simferopol, 2019 October 9–11).* Simferopol: PP "ARIAL", pp. 68–74 (in Russian).
8. Nekhoroshev, M.V., Uss, Yu.A. and Shalyapin, V.K., 1990. Chemical Composition of Biodeposits and the Rate of Their Extraction by Cultivated Mussels. In: IBSS, 1990. *Ekologiya Morya.* Kiev: Naukova Dumka. Iss. 36, pp. 37–41 (in Russian).
9. Kopiy, V.G., 2013. Taxocene of Polychaeta of the Laspi Bay Water Area (the Crimea, Black Sea). *Vestnik of MSTU*, 26(1), pp. 69–77. doi:10.21443/1560-9278-2023-26-1-69-77 (in Russian).
10. Mironova, N.V. and Pankeeva, T.V., 2018. Long Time Changes of Spatial Distribution of Phytomasses Stock of Seaweeds in the Laspi bay (the Black Sea). *Ekosistemy*, (16), pp. 33–46 (in Russian).
11. Tikhonova, E.A., Soloveva, O.V., Mironov, O.A. and Burdiyan, N.V., 2020. Sanitary and Biological Characteristics of the Laspi Reserve Coastal Waters (the Black Sea). *Ecological Safety of Coastal and Shelf Zones of Sea*, (3), pp. 95–106. doi:10.22449/2413-5577-2020-3-95-106 (in Russian).

12. Soloveva, O.V., Tikhonova, E.A. and Mironov, O.A., 2017. The Concentrations of Oil Hydrocarbons in Coastal Waters of Crimea. *Scientific Notes of V.I. Vernadsky Crimean Federal University. Biology. Chemistry*, 3(3), pp. 147–155 (in Russian).
13. Soloveva, O.V., Tikhonova, E.A., Mironov, O.A. and Zakharchenko, D.A., 2018. Monitoring of Oil Hydrocarbons Concentrations in the Coastal Waters of the Crimea. *Water: Chemistry and Ecology*, (4–6), pp. 19–24 (in Russian).
14. Novikov, A.A., Kashirina, E.S. and Belokon, V.V., 2014. [Geological and Geomorphological Hazardous Processes as Threat Factors for Protected Areas of Sevastopol]. In: MHI, 2014. *Ekologicheskaya Bezopasnost' Pribrezhnoy i Shel'fovoy Zon i Kompleksnoe Ispol'zovanie Resursov Shel'fa* [Ecological Safety of Coastal and Shelf Zones and Comprehensive Use of Shelf Resources]. Sevastopol: ECOSI-Gidrofizika. Iss. 29, pp. 61–69 (in Russian).
15. Meyers, P.A., 1997. Organic Geochemical Proxies of Palaeoceanographic, Paleolimnologic, and Paleoclimatic Processes. *Organic Geochemistry,* 27(5–6), pp. 213–250. doi:10.1016/S0146-6380(97)00049-1
16. Zhang, S., Li, S., Dong, H., Zhao, Q., Lu, X. and Shi, J., 2014. An Analysis of Organic Matter Sources for Surface Sediments in the Central South Yellow Sea, China: Evidence Based on Macroelements and N-Alkanes. *Marine Pollution Bulletin*, 88(1–2), pp. 389–397. doi:10.1016/j.marpolbul.2014.07.064
17. Blumer, M., Guillard, R.R.L. and Chase, T., 1971. Hydrocarbons of Marine Phytoplankton. *Marine Biology,* 8(3), pp. 183–189. doi:10.1007/BF00355214
18. Ficken, K.J., Li, B., Swain, D.L. and Eglinton, G., 2000. An N-Alkane Proxy for the Sedimentary Input of Submerged/Floating Freshwater Aquatic Macrophytes. *Organic Geochemistry*, 31(7–8), pp. 745–749. doi:10.1016/S0146-6380(00)00081-4
19. L(U), X. and Zhai, S., 2008. The Distribution and Environmental Significance of n-Alkanes in the Changjiang River Estuary Sediment. *Acta Scientiae Circumstantiae*, 28(6), pp. 1221–1226.
20. Mironov, O.G., ed., 1988. [*Biological Aspects of Oil Pollution of the Marine Environment*]. Kiev: Naukova Dumka, 247 p. (in Russian).
21. Voroshilova, A.A. and Dianova, E.V., 1952. [Oil-Oxidizing Bacteria – Performance Indices of Oil Biological Oxidation under Natural Conditions]. *Mikrobiologiya*, 21(4), pp. 408–415 (in Russian).
22. Ermolaev, K.K. and Mironov, O.G., 1975. The Role of Phenol Decomposing Microorganisms in Detoxication of Phenol in the Black Sea. *Mikrobiologiya*, 44(5), pp. 928–932 (in Russian).
23. Tashlikova, N.A., Kuklin, A.P. and Bazarova, B.B., 2009. Primary Production of Phytoplancton, Epiphytic Seaweed and the Higher Water Plants in the Channels of the Selenga River Delta. *The Bulletin of KrasGAU*, (9), pp. 106–112 (in Russian).
24. Yáñez-Arancibia, A. and Day, J., 1982. Ecological Characterization of Terminos Lagoon, a Tropical Lagoon-Estuarine System in the Southern Gulf of Mexico. *Oceanologica Acta*, 5(4), pp. 431–440.
25. Nemirovskaya, I.A., 2013. *Oil in the Ocean (Pollution and Natural Flow)*. Moscow: Nauchny Mir, 432 p. (in Russian).
26. Nishimura, M. and Baker, E.W., 1986. Possible Origin of N-Alkanes with a Remarkable Even-to-Odd Predominance in Recent Marine Sediments. *Geochimica et Cosmochimica Acta*, 50(2), pp. 299–305. doi:10.1016/0016-7037(86)90178-X

27. Vostokov, S.V., Lobkovskiy, L.I., Vostokova, A.S. and Solov'ev, D.M., 2019. Seasonal and Interannual Variability of Phytoplankton in the Balck Sea on the Basis of Remote Sensing Data and In Situ Measurements of Chlorophyll-A. *Doklady Earth Sciences*, 485(1), pp. 293–297. doi:10.1134/S1028334X19030097

28. Nemirovskaya, I.A., 2021. Distribution and Origin of Hydrocarbons on a Transarctic Transect. *Oceanology*, 61(2), pp. 183–192. doi:10.1134/S0001437021020144

29. Bieger, T., Abrajano, T.A. and Hellou, J., 1997. Generation of Biogenic Hydrocarbons During a Spring Bloom in Newfoundland Coastal (NW Atlantic) Waters. *Organic Geochemistry*, 26(3–4), pp. 207–218. doi:10.1016/S0146-6380(96)00159-3

30. Huang, X., Meyers, P.A., Wu, W., Jia, C. and Xie, S., 2011. Signicance of Long Chain *Iso* and *Anteiso* Monomethyl Alkanes in the Lamiaceae (Mint Family). *Organic Geochemistry*, 42(2), pp. 156–165. doi:10.1016/j.orggeochem.2010.11.008

31. Finenko, Z.Z., Mansurova, I.M. and Suslin, V.V., 2022. Temporal Dynamics of Phytoplankton Biomass in the Surface Layer of the Black Sea According to Satellite Observations. *Oceanology*, 62(3), pp. 358–368. doi:10.1134/S0001437022030043

32. Doroshenko, Yu.V., 2018. The Estimation of the State of Golubaya Bay on Microbiological Criteria During the Summer. *Russian Journal of Biological Physics and Chemistry*, 3(4), pp. 892–896 (in Russian).

33. Studenikina, E.I., Tolokonnikova, L.I. and Volovik, S.P., 2002. [*Microbiological Processes in the Sea of Azov under Anthropogenic Influence*]. Moscow: FGUP "NatsRybResursy", 168 p. (in Russian).

34. Doroshenko, Yu.V., 2022. Microbiological Characteristics of the Hydraulic Structures of Some Sevastopol Bays. *Russian Journal of Biological Physics and Chemistry*, 7(4), pp. 645–649. doi:10.29039/rusjbpc.2022.0576 (in Russian).

35. Corner, E.D.S., 1979. Pollution Studies with Marine Plankton: Part 1. Petroleum Hydrocarbons and Related Compounds. *Advances in Marine Biology*, 15, pp. 289–380. doi:10.1016/S0065-2881(08)60407-1

Submitted 30.11.2023; accepted after review 10.12.2023;
revised 27.12.2023; published 25.03.2024

About the authors:

Elena A. Tikhonova, Leading Research Associate, A. O. Kovalevsky Institute of Biology of the Southern Seas of RAS (2 Nakhimova Ave, Sevastopol, 299011, Russian Federation), PhD (Biol.), **ORCID ID: 0000-0002-9137-087X, Scopus Author ID: 57208495804, ResearcherID: X-8524-2019**, *tihonoval@mail.ru*

Olga V. Soloveva, Leading Research Associate, A. O. Kovalevsky Institute of Biology of the Southern Seas of RAS (2 Nakhimova Ave, Sevastopol, 299011, Russian Federation), PhD (Biol.), **ORCID ID: 0000-0002-1283-4593, Scopus Author ID: 57208499211, ResearcherID: X-4793-2019**, *kozl_ya_oly@mail.ru*

Nataliya V. Burdiyan, Senior Research Associate, A. O. Kovalevsky Institute of Biology of the Southern Seas of RAS (2 Nakhimova Ave., Sevastopol, 299011, Russian Federation), PhD (Biol.), **ORCID ID: 0000-0001-8030-1556, Scopus Author ID: 57208497483, ResearcherID: AAD-1704-2022,** *burdiyan@mail.ru*

Yulia S. Tkachenko, Junior Research Associate, A. O. Kovalevsky Institute of Biology of the Southern Seas of RAS (2 Nakhimova Ave, Sevastopol, 299011, Russian Federation), **ORCID ID: 0009-0001-1752-1043**, **Scopus Author ID: 1220495;** *yulechkatkachenko.90@mail.ru*

Yulia V. Doroshenko, Research Associate, A.O. Kovalevsky Institute of Biology of the Southern Seas of RAS (2 Nakhimova Ave., Sevastopol, 299011, Russian Federation), PhD (Biol.), **ORCID ID: 0000-0003-0498-3369; Scopus Author ID: 57211643141, ResearcherID: AAD-1706-2022,** *julia_doroshenko@mail.ru*

Elena V. Guseva, Junior Research Associate, A.O. Kovalevsky Institute of Biology of the Southern Seas of RAS (2 Nakhimova Ave., Sevastopol, 299011, Russian Federation), **Scopus Author ID: 57208488324;** *guseva_ev@ibss-ras.ru*

Sergey V. Alyomov, Leading Research Associate, A. O. Kovalevsky Institute of Biology of the Southern Seas of RAS (2 Nakhimova Ave., Sevastopol, 299011, Russian Federation), PhD (Biol.), **ORCID ID: 0000-0002-3374-0027, Scopus Author ID: 24070027300,** *alyomov_sv@ibss-ras.ru*

Contribution of the authors:

Elena A. Tikhonova – statement of aims and objectives of the complex study, water and fouling sampling, manuscript writing

Olga V. Soloveva – analysis of the results obtained on the hydrocarbon composition of water, results discussion, manuscript writing

Yulia S. Tkachenko – preparation of water samples, determination of qualitative and quantitative composition of hydrocarbons in the water, writing and presentation of the article

Nataliya V. Burdiyan – statement of the objectives of the microbiological study, analysis of the results obtained in the microbiological study, results discussion, manuscript writing, microbiological works to determine the abundance of indicator groups of bacteria in the periphyton

Yulia V. Doroshenko – analysis of the obtained results on microbiological research, results discussion, manuscript writing, microbiological works to determine the abundance of indicator groups of bacteria in the water

Elena V. Guseva – study rationale, preparation of the literature review, fouling sampling, construction of graphical materials

Sergey V. Alyomov – sampling, description of the macrofouling community and its changes during different sampling periods

All the authors have read and approved the final manuscript.